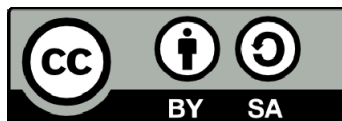




UNIVERSITAT DE
BARCELONA

Outer membrane: a key obstacle for new antimicrobial agents

Marta Jorba Pedrosa



Aquesta tesi doctoral està subjecta a la llicència **Reconeixement- Compartitqual 4.0. Espanya de Creative Commons**.

Esta tesis doctoral está sujeta a la licencia **Reconocimiento - Compartitqual 4.0. España de Creative Commons**.

This doctoral thesis is licensed under the **Creative Commons Attribution-ShareAlike 4.0. Spain License**.



UNIVERSITAT DE
BARCELONA

Outer membrane: a key obstacle for new antimicrobial agents

Thesis submitted by **Marta Jorba Pedrosa** in fulfilment
of the requirements for the degree of PhD by the
University of Barcelona

Supervised by Prof. Miquel Viñas Ciordia
Doctorate in Translational Medicine and Research
Faculty of Medicine and Health Sciences
Department of Pathology and Experimental Therapeutics
Laboratory of Molecular Microbiology and Antimicrobials

Universitat de Barcelona
L'Hospitalet de Llobregat – June 2021

Miquel Viñas Ciordia, Catedràtic de Microbiologia del Departament de Patologia i Terapèutica Experimental de la Facultat de Medicina i Ciències de la Salut de la Universitat de Barcelona,

CERTIFICA,

Que la Tesi Doctoral presentada per Marta Jorba Pedrosa i titulada "Outer membrane: a key obstacle for new antimicrobial agents" ha estat desenvolupada per l'autora sota la nostra supervisió en el laboratori de Microbiologia Molecular i Antimicrobians del Campus de Bellvitge.

Que la recerca desenvolupada i el manuscrit presentat compleixen els requisits formals i conceptuals per a que pugui ser defensada davant del tribunal corresponent.

I per a que consti signo el present document a l'Hospitalet de Llobregat, el dia 2 de juny de 2021

Prof. Dr. Miquel Viñas Ciordia

Title: Outer membrane: a key obstacle for new antimicrobial agents

Author: Marta Jorba Pedrosa

Setting: Laboratory of Molecular Microbiology and Antimicrobials. Dept. Pathology and Experimental Therapeutics. Faculty of Medicine and Health Sciences. University of Barcelona

Supervisor: Prof. Miquel Viñas Ciordia (Full Professor Dept. Pathology and Experimental Therapeutics. University of Barcelona)

Thesis submitted in fulfilment of the requirements for the degree of PhD by the University of Barcelona

Signed: Marta Jorba Pedrosa

L'Hospitalet de Llobregat, 2 June 2021

Mistakes are the portals of discovery.

James Joyce

Nothing great was ever achieved without enthusiasm.

Ralph Waldo Emerson

ACKNOWLEDGMENTS

La realització d'aquesta Tesis Doctoral ha estat possible gràcies a un contracte de recerca realitzat pel grup liderat per el Prof. Dr. Miquel Viñas (Setembre 2019- juliol 2021) a la unitat de microbiologia del Departament de Patologia i Terapèutica Experimental de la Universitat de Barcelona mitjançant el projecte:

Fundació Marató de TV3 (201C/2018): Trencant les fronteres de la resistència als antimicrobians; cercant nous antimicrobians contra bacteris multiresistents: un treball sobre pèptids policatiònics i nanopartícules lipídiques (**BARNAPA**).

A l'acabar aquesta etapa miro enrere i me n'adono que tot aquest procés no hauria sigut possible sense l'ajuda, suport, companyia,... de moltíssimes persones a les que estic immensament agraïda.

Al Dr. Miquel Viñas, el meu director. Per donar-me l'oportunitat d'endinsar-me en el món de la microbiologia en el teu laboratori. Per la teva saviesa, bondat i sentit de l'humor.

La primera cosa que em vas dir quan et vaig conèixer va ser que el que més valoraves del laboratori era el bon rollo. I al llarg dels anys n'has aconseguit tant, que em vaig enganxar des dels primers dies.

A la Dra. Teresa Vinuesa per contagiar-nos a tots de la teva vitalitat i energia i sempre preocupar-te per nosaltres.

A la Dra. Ester Fusté per les llargues converses i tota l'ajuda. Al Dr. Josep M^a Sierra, per estar sempre disposat a resoldre els dubtes. A la Dra. Lupe Jiménez, per les tardes de xerrades solucionant-ho tot i per la teva ajuda i bondat. A la Dra. Blanca Martínez per haver sigut la millor mestra i haver-me ensenyat les bases del laboratori de micro.

A la Dra. Helena Martín, la Dra. Judit Tulla i al Prof. Fernando Albericio, per la vostra col·laboració i ajuda en tot moment.

A la Marina Pedrola, la Dra. Ouldouz Ghashghaei i al Prof. Rodolfo Lavilla. Per estar sempre disposats a ajudar i per la vostra motivació sense límits, treballar amb vosaltres ha estat un plaer. Al Prof Javier Luque per la seva col·laboració amb el model de Docking.

A l'Esther, el Benja i la Bea dels serveis Científicotècnics. Pel vostre suport en els experiments i la vostra comprensió i paciència amb els infinits canvis de filtres!

Al personal del Servei de Microbiologia de l'Hospital de Bellvitge per cedir-nos les soques clíniques de Trimethoprim-R i al personal del laboratori de Microbiologia de la facultat de Biologia de la Universitat de Barcelona per proporcionar-nos les soques de *Salmonella*.

A la Sonia, per fer-nos de mami. A l'Elena P. per venir sempre a portar bon rollo. A l'Alex pels bons moments.

Als meus companys o més ben dit AMICS del "Lab Non-Stop". Sou tots impressionants i us diria mil coses boniques, però hem d'anar per feina! A l'Eulàlia que ho il·lumina tot amb la seva presència, l'Héctor el nostre savi sense límits, el Pablo mi compañero del lado oscuro i de las charlas sin fin, la Montxi pastissera i persona preciosa, l'Anna sempre amb bons consells, i les meves petites Idoia i Estela que vau ser les millors alumnes que es pot desitjar! Per últim a les de la resistència final; la Rocío confident i boníssima persona, l'Eva juntes en totes les etapes i sempre disposada a ajudar i a buscar un moment per desfogar-nos i l'Isa que sempre fa un acudit per fer-te somriure en els pitjors moments. Si em vaig embrancar en aquesta tesi va ser per vosaltres, perquè em fascinava la idea de poder venir a treballar cada dia al vostre costat. No em podia ni imaginar, però, totes les aventures que ens esperaven junts! Tots vosaltres i totes les experiències viscudes son una de les coses més boniques que m'enduc d'aquesta etapa. Moltes gràcies!

Als petits Eric, Fiorela, Paula, Marc i Felipe, que m'heu fet passar molts bons moments en aquesta última etapa. A seguir sent feliços fent ciència!

A la meva mare, el meu pare i el meu germà. Per haver sigut valents en la pitjor època de la nostra vida. Per tot el que heu fet per mi, sempre.

A l'àvia, que es va apagar durant el camí però que brillarà per sempre.

A l'Àngels per haver-me donat confiança i un suport tant gran amb l'escriptura. Al Jaume per ser el fan nº 1 dels meus articles i de la meva tesi. Als dos per ser-hi en els moments més durs.

Al Joan Ramon. Perquè no em podria imaginar un millor company de vida. T'agraeixo que m'hagis impulsat a no conformar-me i a lluitar pel que em mereixo en cada moment. Per acompanyar-me sempre.

A la família de Viladrau. Per ser un suport sempre, per tota la vostra ajuda i estima. Als petits Arlet i Sergi per portar llum i alegria a les nostres vides.

A totes les amigues i amics. Per haver-me donat bons moments de desconexió i per haver-me fet veure que tot i que en algunes ocasions no hi he pogut ser, us tindrè sempre. En especial a l'Olímpia, l'autora de la portada, que sempre m'acompanya il·lustrant els moments importants!

A mi Julita, super mujer y super trabajadora. La major acompanyante de tesis des de la distancia. Eres una persona preciosa y, ya sabes, eres la siguiente!

CONTENTS

| | |
|--|-------|
| ACKNOWLEDGMENTS..... | ix |
| ACRONYMS AND ABBREVIATIONS | xxi |
| SCIENTIFIC PRODUCTION | xxv |
| ABSTRACT | xxxi |
| RESUMEN | xxvii |
| 1. INTRODUCTION | 1 |
| 1.1. Bacterial cell envelope structure: overview | 3 |
| 1.1.1. Gram-positive bacterial wall..... | 5 |
| 1.1.2. Gram-negative bacterial wall..... | 5 |
| 1.2. Antimicrobials' overview | 10 |
| 1.2.1. Antibiotics mechanisms of action..... | 10 |
| 1.2.2. Antibiotics history | 12 |
| 1.2.3. Bacteriocins..... | 17 |
| 1.2.3.1. Microcins..... | 18 |
| 1.2.4. The antifolates | 25 |
| 1.2.4.1. Trimethoprim | 27 |
| 1.2.4.2. Sulphonamides: Sulfamethoxazole | 31 |

| | |
|---|----|
| 1.2.5. Colistin | 33 |
| 1.3. Antimicrobial resistance | 35 |
| 1.3.1. Mechanisms of antimicrobial resistance | 39 |
| 1.4. Present and future perspectives of antibiotics | 41 |
| 1.4.1. Strategies to fight MDR bacteria..... | 43 |
| a) Natural products antibiotic discovery..... | 43 |
| b) Synthesis of new molecules..... | 44 |
| c) Combination of already known compounds..... | 44 |
| d) Alternative therapies..... | 45 |
| e) Improvement of already known compounds..... | 45 |
| 2. HYPOTHESIS AND OBJECTIVES..... | 47 |
| 2.1. Hypothesis..... | 49 |
| 2.2. Justification of the study and objectives..... | 50 |
| 3. Results | 53 |
| 3.1. ARTICLE 1..... | 55 |
| 3.2. ARTICLE 2..... | 73 |
| 3.3. ARTICLE 3..... | 93 |

| | |
|-------------------------|--------|
| 4. DISCUSSION..... | 111 |
| 5. CONCLUSIONS | 127 |
| 6. REFERENCES..... | 133 |
| 7. ANNEXES..... | I |
| 7.1. ANNEX I..... | III |
| 7.1.1. ARTICLE I | VII |
| 7.1.2. ARTICLE II | XXI |
| 7.2. ANNEX II..... | XXIX |
| 7.2.2. ARTICLE III..... | XXXIII |

ACRONYMS AND ABBREVIATIONS

A

ABC: ATP Binding Cassete

AMP: Antimicrobial Peptide

AMR: Antimicrobial Resistance

ATCC: American Tissue Culture
Collection

ATP: Adenosine Triphosphate

B

BGC: Biosynthetic gene cluster

C

CAP: Covalently attached protein

CRAB: Carbapenem resistant *A. baumannii*

CRKN: Carbapenem resistant *K. pneumoniae*

D

DHFR: Dihydrofolate Reductase

DHFS: Dihydrofolate Synthetase

DHPS: Dihydropteroate Synthetase

E

et al.: et alii

e.g.: Exempli gratia

F

FDA: Food and drug administration

G

GBBR: Groebke-Blackburn-
Bienaymé reaction

I

IM: Inner membrane

IMP: Integral membrane protein

L

LP: lipoprotein

LPS: Lipopolysaccharide

LTA: Lipoteichoic acid

M

MATE: Multidrug and toxin

extrusion family

MccJ25: Microcin J25

MDR: Multidrug Resistant

MFS: Major facilitator superfamily

MRSA: Methicillin resistant *S. aureus*

MTX: Methotrexate

Outer membrane: a key obstacle for new antimicrobial agents

N

NADPH: Nicotinamide Adenine
Dinucleotide Phosphate

NTP: Nucleoside Triphosphate

O

OM: Outer membrane

OMP: Outer membrane protein

P

PACE: proteobacterial antimicrobial
compound efflux family

PDR: Pan-drug Resistant

PG: Peptidoglycan

R

RNA: Ribonucleic Acid

RNAP: RNA Polymerase

RND: resistance- nodulation-cell

division superfamily

ROS: Reactive Oxygen Species

S

SAR: Structure Activity
Relationship

SMR: Small multidrug resistance
family

SMX: Sulfamethoxazole

T

TMP: Trimethoprim

U

UTIs: Urinary tract infections

X

XDR: Extensively Drug Resistant

W

WGS: Whole genome sequencing

WHO: World Health Organization

WTA: Wall teichoic acid

SCIENTIFIC PRODUCTION

This Thesis has been done in article compendium format. The four years period employed in this PhD thesis has allowed the participation in the research which production is presented in the following list:

Publications in international peer-reviewed journals forming part of this thesis:

1. Martin-Gómez H, **Jorba M**, Albericio F, Viñas M, Tulla-Puche J. Chemical modification of microcin j25 reveals new insights on the stereospecific requirements for antimicrobial activity. *Int J Mol Sci.* 2019;20(20). The **Impact factor** according to 2019 Journal Citation Reports in Biochemistry and Molecular biology is **4.556 (Q1)**.
2. Pedrola M*, **Jorba M***, Jardas E, Jordi F, Ghashghaei O, Viñas M, Lavilla R. Multicomponent Reactions Upon the Known Drug Trimethoprim as a Source of Novel Antimicrobial Agents. *Front Chem.* 2019;7(July):1–9. The **Impact factor** according to 2019 Journal Citation Reports in Chemistry Multidisciplinary is **3.693 (Q2)**.
3. **Jorba M**, Pedrola M, Ghashghaei O, Herráez R, Campos-Vicens L, Luque FJ, Lavilla R, Viñas M. New trimethoprim-like molecules: bacteriological evaluation and insights into their action. *Antibiotics.* 2021; 10(6):709. The **Impact factor** according to 2019 Journal Citation Reports in Infectious diseases is **3,893 (Q1)**.

Publications in international peer-reviewed journals from complementary experimental collaborations:

1. Sans-Serramitjana, E., **Jorba, M.**, Fusté, E., Pedraz J.L., Vinuesa, T. & Viñas, M. Free and Nanoencapsulated Tobramycin: Effects on Planktonic and Biofilm Forms of *Pseudomonas*. *Microorganisms* 5, 35 (2017). The **Impact factor** according to 2018 Journal Citation Reports in Microbiology is **4,167 (Q2)**.
2. Sans-Serramitjana, E., **Jorba, M.**, Pedraz, J. L., Vinuesa, T. & Viñas, M. Determination of the spatiotemporal dependence of *Pseudomonas aeruginosa* biofilm viability after treatment with NLC-colistin. *Int. J. Nanomedicine* 12, 4409–4413 (2017). The **Impact factor** according to 2017 Journal Citation Reports in Pharmacology and Pharmacy is **4,370 (Q1)**.
3. Sánchez-Garcés, M. A., **Jorba, M.**, Ciurana, J., Viñas, M. & Vinuesa, T. Is the re-use of sterilized implant abutments safe enough? (Implant abutment safety). *Med. Oral Patol. Oral y Cir. Bucal* 24, e583–e587 (2019). The **Impact factor** according to 2019 Journal Citation Reports in Dentistry Oral Surgery and Medicine is **1.284 (Q3)**.

Congress participations

1. Sans-Serramitjana E, Fusté E, Martínez-Garriga B, Merlos A, **Jorba M**, Vinuesa T, Viñas M. Poster presentation: Nano-Encapsulated colistin sulphate to fight *Pseudomonas aeruginosa* infections. IMI Translocation meeting 2016. Novel approaches to fight bacteria. 10-14 July 2016. Bremen, Germany.
2. Mur A, Herráez R, Armengol E, **Jorba M**, Viñas M, Vinuesa T. Poster participation: Different prodigiosin Extraction Methods and its antimicrobial properties. XXIV Congreso Latinoamericano de Parasitología (FLAP 2017). 10-14 December 2017. Santiago de Chile, Chile.
3. Lavilla, R.; Pedrola, M.; Ghashghaei, O.; Jardas, E.; Jardí, F.; **Jorba, M.**; Viñas, M. Congress participation: Multicomponent Reaction-Based Trimethoprim Analogues as Potential Antibiotics for Resistant Bacteria. 2nd Molecules Medicinal Chemistry Symposium (MMCS): Facing Novel Challenges in Drug Discovery. 15–17 May 2019. Barcelona, Spain.
4. **M. Jorba**, H. Martín-Gómez, F. Albericio, M. Viñas, J. Tulla-Puche. Poster presentation: Alteración de la actividad antimicrobiana de la Microcina J25 por efecto de una modificación química alcalina. XXIII Congreso de la Sociedad

Española de Enfermedades Infecciosas y Microbiología Clínica.
23-25 May 2019. Madrid, Spain.

5. P. Betancourt, J. Sierra, O. Camps, **M. Jorba**, J. Arnabat, M. Viñas. Oral communication: Eficacia antimicrobiana de Irrigación activada por Láser Er,Cr:YSGG contra biofilm de *Enterococcus faecalis* en dientes extraídos. XXIII Congreso de la Sociedad Española de Enfermedades Infecciosas y Microbiología Clínica. 23-25 May 2019. Madrid, Spain.

ABSTRACT

Outer membrane: a key obstacle for new antimicrobial agents

Introduction: Antimicrobial resistance is one of the world's major challenges in both microbiology and public health since infections caused by multidrug-resistant bacteria are reaching alarming levels. The world is currently facing a global antibiotics crisis and some new strategies need to be explored to tackle these resistant infections.

The outer membrane is a differential structure of Gram-negative bacteria that works as a highly effective selective permeability barrier. Thus, the permeation through the Gram-negative cell envelope is a challenge for drug compounds to reach their targets.

One path to open new antimicrobial perspectives is the chemical modification of old antimicrobial compounds that may result in optimized drugs with improved antimicrobial properties. In this context, the activity exploration of the derivatives of Microcin J25 and Trimethoprim was carried out.

Hypothesis: The main hypotheses of this thesis are that chemical modifications of current antibiotics may significantly contribute to overcoming the problems arising from the increase and spread of antibiotic resistance in bacteria. Moreover, the combination of these modified compounds with old-rescued antibiotics may contribute to the solution bases of the problem caused by resistance.

Objectives: The main objective of this thesis is to determine the antimicrobial properties of chemically modified drug compounds. The secondary objectives of this thesis are divided in two parts:

Microcin J25: Study of the antimicrobial activity of the modified Microcin J25 as well as determination of its toxicity.

Trimethoprim: Study of the antimicrobial activity and cytotoxicity of the Trimethoprim derivatives, exploration of the effect of the new derivatives on the Dihydrofolate Reductase (DHFR) enzyme and start a computational approach to decipher the intimal mechanisms of action.

Methodology: The antimicrobial activity of the derived compounds was explored against planktonic bacteria (studying the Minimum Inhibitory Concentration and the FIC index) and against sessile bacteria (exploring the Minimum Biofilm Eradication Concentration and the Biofilm Prevention Concentration). The growth curves of several microorganisms in contact with these compounds and in combination with colistin were also studied. The cytotoxicity of all the compounds was tested. An enzymatic assay with *E. coli* DHFR as well as a docking modelling were carried out to investigate the mechanism of action of TMP derivatives.

Results: With respect to Microcin MccJ25, it has been detected that the chemical modification of the compound resulted in a new peptide without antimicrobial activity. It acted synergistically with sublethal concentrations of colistin.

When referring to Trimethoprim (TMP), some of the new derivatives showed antibacterial similar to that of TMP. Moreover, almost all the new TMP-like compounds acted synergistically with SMX. *P. aeruginosa* PAO1 was fully resistant to TMP and all its derivatives as well as to the combination of TMP-SMX. The combination of TMP, TMP-like molecules and SMX with colistin enhanced their antimicrobial efficacy against *E. coli*, *P. aeruginosa* and *S. marcescens*. Compounds 1a and 1b, like TMP, strongly inhibited the activity of the *E. coli* DHFR. Additionally, it was detected that the heterocyclic ring of the compound 1a fills the pocket occupied by the nicotinamide ring of NADPH.

Conclusions: The present PhD thesis has led to some relevant conclusions. With respect to Microcin MccJ25, the chemical modification of the compound avoided its detection by the membrane receptor FhuA. Moreover, it did not affect the interaction with the target and, as the polymyxin facilitated the microcin entrance across the membrane, once inside the cell, the new compound retained its ability to inhibit the growth of bacteria.

When referring to Trimethoprim (TMP), the derivatives showed interesting antimicrobial activities acting synergistically with SMX. The combination of TMP, TMP-like molecules and SMX with colistin enhances their antimicrobial efficacy by permeabilizing the cells. Compounds 1a and 1b, like TMP, strongly inhibited the activity of the *E. coli* DHFR and it was suggested that both molecules interact with the analogues during inhibition.

The search of new antimicrobial compounds is one of the main pathways to overtake bacterial resistance to antibiotics. All putative compounds should be tested in conditions in which outer membrane role as permeability barrier is inactivated. Their assay together with sublethal concentrations of colistin is proposed as one of the methods of election.

RESUMEN

Membrana externa: un obstáculo clave para los nuevos agentes antimicrobianos

Introducción: La resistencia a los antimicrobianos es uno de los principales desafíos del mundo tanto en microbiología como en salud pública, ya que las infecciones causadas por bacterias multirresistentes están alcanzando niveles alarmantes. Actualmente el mundo se enfrenta a una crisis de antibióticos y es necesario explorar nuevas estrategias para abordar estas infecciones resistentes.

La membrana externa es una estructura diferencial de bacterias Gramnegativas que funciona como una barrera de permeabilidad selectiva altamente efectiva. Por lo tanto, la permeación a través de la envoltura de células Gramnegativas es un desafío para que los compuestos farmacológicos alcancen sus dianas.

Una opción para abrir nuevas perspectivas antimicrobianas es la modificación química de compuestos antimicrobianos ya existentes que pueden resultar medicamentos optimizados con propiedades antimicrobianas mejoradas. En este contexto, en esta tesis se llevó a cabo la exploración de la actividad de los derivados de Microcina J25 y Trimethoprim.

Hipótesis: Las principales hipótesis de esta tesis son que las modificaciones químicas de los antibióticos actuales pueden contribuir significativamente a superar los problemas que surgen del aumento y la propagación de la resistencia a los antibióticos en las bacterias. Además, la combinación de estos compuestos modificados con antibióticos antiguos rescatados puede contribuir a resolver el problema causado por la resistencia.

Objetivos: El principal objetivo de esta tesis es determinar las propiedades antimicrobianas de compuestos químicamente modificados. Los objetivos secundarios de esta tesis se dividen en dos partes:

Microcina J25: Estudio de la actividad antimicrobiana de la Microcina J25 modificada, así como determinación de su citotoxicidad.

Trimethoprim: Estudio de la actividad antimicrobiana y citotoxicidad de los derivados de Trimethoprim, exploración del efecto de los nuevos derivados sobre la enzima Dihidrofolato Reductasa (DHFR) e inicio de una aproximación computacional para descifrar los mecanismos de acción de los derivados de TMP.

Metodología: Se exploró la actividad antimicrobiana de los compuestos derivados frente bacterias planctónicas (estudiando la Concentración Mínima Inhibidora y el índice FIC) y frente bacterias sésiles (explorando la Concentración Mínima de Erradicación de Biofilm y la Concentración de Prevención de Biofilm). También se estudiaron las curvas de crecimiento de varios microorganismos en contacto con estos compuestos y en combinación con colistina. Se ensayó la citotoxicidad de todos los compuestos. Se llevó a cabo un ensayo enzimático con *E. coli* DHFR así como un modelo de docking.

Resultados: Con respecto a la Microcina MccJ25, se detectó que la modificación química del compuesto dio como resultado un nuevo péptido sin actividad antimicrobiana. Esta actuó de forma sinérgica con concentraciones subletales de colistina.

En cuanto a Trimethoprim (TMP), algunos de los nuevos derivados mostraron un efecto antibacteriano similar al de TMP. Además, casi todos los nuevos compuestos actuaron sinérgicamente con SMX. *P.*

aeruginosa PAO1 fue totalmente resistente a TMP y todos sus derivados, así como a la combinación de TMP-SMX. La combinación de TMP, análogos de TMP y SMX con colistina mejoró su eficacia antimicrobiana contra *E. coli*, *P. aeruginosa* y *S. marcescens*. Los compuestos 1a y 1b, como TMP, inhibieron la actividad de la DHFR de *E. coli*. Además, se observó que el anillo heterocíclico del compuesto 1a llena el bolsillo ocupado por el anillo de nicotinamida de NADPH.

Conclusiones: La presente tesis doctoral ha identificado algunas conclusiones relevantes. Con respecto a la Microcina MccJ25, la modificación química del compuesto evitó su detección por el receptor de membrana FhuA. Además, no afectó la interacción con la diana celular debido a que la polimixina facilitó la entrada de la microcina a través de la membrana y, una vez dentro de la célula, el nuevo compuesto conservó su capacidad para inhibir el crecimiento de las bacterias.

En cuanto a Trimethoprim (TMP), los derivados mostraron actividades antimicrobianas interesantes actuando sinérgicamente con SMX. La combinación de TMP, derivados de TMP y SMX con colistina mejora su eficacia antimicrobiana al permeabilizar las células. Los compuestos 1a y 1b, como TMP, inhibieron fuertemente la actividad de la DHFR de *E. coli* y se sugirió que ambas moléculas interactúan con los análogos durante la inhibición.

La búsqueda de nuevos compuestos antimicrobianos es una de las principales vías para superar la resistencia bacteriana a los antibióticos. Todos los compuestos putativos deben ensayarse en condiciones en las que el papel de la membrana externa como barrera de permeabilidad esté inactivo. El ensayo de nuevos compuestos junto con concentraciones subletales de colistina se propone como uno de los métodos de elección.

1.INTRODUCTION

1. INTRODUCTION

Bacteria exist in varied sizes and shapes and it is crucial to understand their structure and the specialized functions of the different components that make them up to be able to identify potential antibiotic targets to treat infectious diseases.

1.1. Bacterial cell envelope structure: overview

The bacterial cell envelope is a complex and sophisticated structure, formed by multiple layers, that protect bacteria from their uncertain and frequently hostile environment. Bacterial cells must interact selectively with their environment since they need to acquire nutrients from the outside and eliminate waste from the inside¹. The different layers that form the cell envelopes are the cell membrane, the cell wall and periplasm; their structure and specialized functions are described below.

The cell or cytoplasmic membrane limits the cytoplasm and separates the inside of the cell from the extracellular space. It acts as a selectively permeable barrier, preventing or allowing the movement of some ions and molecules. Transport systems are used to help some compounds to cross the cell membrane².

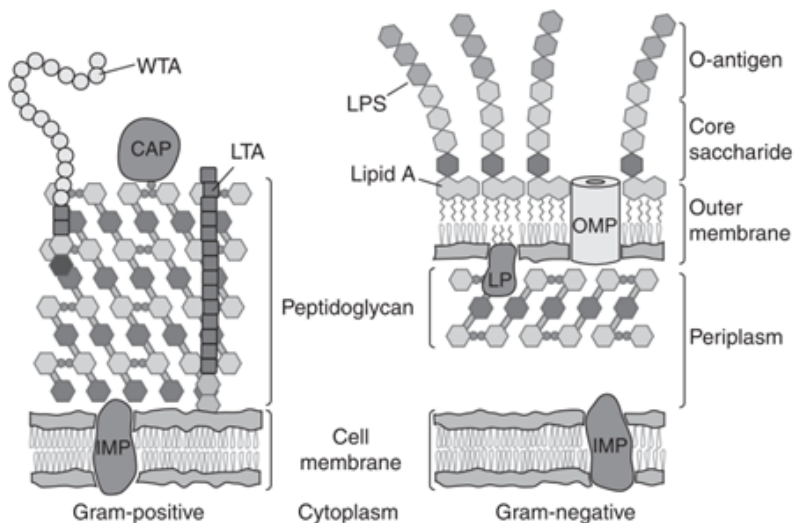
The cell wall is a relatively permeable layer found outside the cell membrane that gives structural strength and integrity to the cell since it

Outer membrane: a key obstacle for new antimicrobial agents

has a semi-rigid structure. The cell wall structure, chemical composition, and thickness are different in Gram-positive and Gram-negative bacteria (

Figure 1).

In 1884, the Danish bacteriologist Christian Gram developed a staining method to classify bacteria into two groups depending on the structural differences in their cell envelope. The first group (Gram-positive) stained purple whereas the second (Gram-negative) stained pink³.



Nowadays, it is a frequently used staining technique for the initial classification of unknown isolates of bacteria.

Figure 1. Gram-positive and Gram-negative cell envelopes. WTA: wall teichoic acid, CAP: covalently attached protein, LTA: Lipoteichoic acid, IMP: Integral membrane

protein, LPS: Lipopolysaccharide, OMP: Outer membrane protein and LP: lipoprotein.
Figure extracted from Silhavy *et al.*,2010⁴.

1.1.1. Gram-positive bacterial wall

The Gram-positive bacteria cell wall consists of a single mesh-like layer of peptidoglycan (PG) surrounding the cell membrane. Since Gram-positive bacteria lack an outer lipid membrane, the thickness constituting the cell wall is 30-100nm⁴.

Gram-positive bacteria usually contain teichoic acids attached to either the layers of peptidoglycan (WTA: wall teichoic acids) or the cell membrane lipids (LTA: Lipoteichoic acids). Both types are attractive targets for novel antimicrobial agents. These acids are negatively charged which gives Gram-positive bacteria their negative charge⁵. Moreover, some surface proteins used for the recognition of host components are attached to peptidoglycan or teichoic acids.

1.1.2. Gram-negative bacterial wall

In contrast, the Gram-negative cell wall is quite complex, and it varies in several ways from the Gram-positive envelopes. It has a thinner peptidoglycan layer surrounding the cell membrane or inner membrane (IM) which is covered by an outer membrane (OM). Between the IM and the OM, there is the periplasmic space filled with an aqueous substance, the periplasm, which contains proteins that participate in some relevant processes such as nutrient uptake or peptidoglycan synthesis².

Outer membrane: a key obstacle for new antimicrobial agents

The inner membrane is a 2 to 7 nm thick phospholipid bilayer and is where the proteins that are in charge of the energy production, lipid biosynthesis, protein secretion and transport, are located.

The outer membrane is a differential structure of Gram-negative bacteria that works as a highly effective selective permeability barrier that protects the cell from external toxics. Being the OM of *E. coli* the best studied, it is used as a model among the other species OMs. It is a lipid bilayer of 7 to 8 nm thick. The inner leaflet of the membrane is formed by phospholipids and the outer is composed of glycolipids, mainly lipopolysaccharides (LPS). LPSs are large and complex molecules composed of lipid and carbohydrate and formed by three differentiated parts: a) Lipid A, b) the core polysaccharide and c) the polysaccharide chain called the O-antigen. The chains of lipid A are embedded together within the membrane by van der Waal forces while divalent cations (Mg^{2+} and Ca^{2+}) are intercalated between LPS molecules which stabilize them⁶. LPS develop many significant functions such as stabilization of the OM structure, creation of a permeability barrier or the participation in the bacterial attachment to surfaces and biofilm formation.

The proteins attached to the OM can be divided into two main groups: lipoproteins and β -barrel proteins. The former are anchored in the inner leaflet of the membrane while the latter are transmembrane proteins and are named outer membrane proteins (OMPs). Despite being a permeability barrier, the OM allows the entrance of small molecules and nutrients through the narrow channels formed by a class of OMPs called

porins. Furthermore, some other minor proteins, synthesised mainly when required, exist. Some examples are TonB-dependent receptors (e.g. FhuA and FepA) or other porins (e.g. PhoE and LamB). *E. coli* produces three trimeric porins named OmpF, OmpC, and PhoE which are highly expressed. Nevertheless, there are some Gram-negative bacteria such as *P. aeruginosa* that lack these porins. They produce OprF, a non-specific porin that is a homolog of the *E. coli* OmpA and many specific porins⁷.

Larger molecules need to be transported across the OM by specific carriers. In addition, the OM works as an attachment surface of some organelles such as pili which are relevant in bacterial pathogenesis.

The cell envelope of Gram-negative bacteria harbours other essential structures such as multidrug efflux pumps. Efflux pumps are energy-dependent transporters capable to actively extrude a huge variety of toxic molecules such as antibiotics and non-antibiotic compounds like dyes, detergents, and heavy metals, among others⁸. Six families of bacterial drug efflux pumps have been identified. They are the ATP-binding cassette (ABC) family, the major facilitator superfamily (MFS), the multidrug and toxin extrusion (MATE) family, the small multidrug resistance (SMR) family, the resistance-nodulation-cell division (RND) superfamily and the proteobacterial antimicrobial compound efflux (PACE) family. The ABC family uses ATP as the energy source to drive transport while the other five families are powered by electrochemical energy obtained in transmembrane ion gradients^{9,10}. AcrAB-TolC is one

of the efflux pumps that are expressed in *E. coli*. It is formed by TolC, an outer membrane protein, AcrA, a periplasmic adaptor protein and AcrB, an inner membrane transporter from the RND superfamily^{11,12}.

These structures, coupled with porins, OMP and LPS, are crucial for the proper functioning of the cell and play a major role in antimicrobial resistance.

Drug permeation through Gram-negative cell envelope

The permeation through the Gram-negative cell envelope is a challenge for drug compounds to reach their targets¹³. In the outer membrane, the LPS layer is barely permeable for any compound and especially hydrophobic molecules. The existence of porins provides the only gates for antibiotics to cross the outer membrane. However, they have some limitations regarding the sort of chemical structures allowed to pass, usually small, hydrophilic and polar molecules. The inner membrane is permeable to small hydrophobic molecules and allows the limited diffusion of hydrophilic molecules. On top of that, once the drug compounds have been able to cross the outer membrane, the efflux pumps are likely to expel them from bacteria (Figure 2)¹⁴.

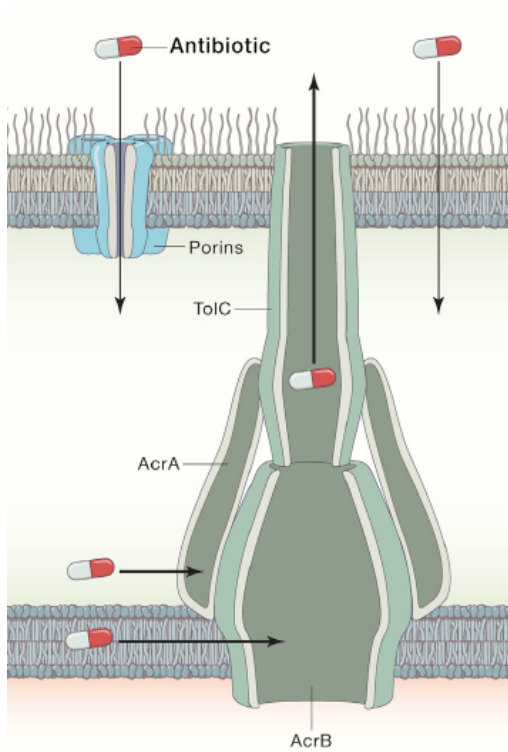


Figure 2. Drug permeation mechanisms through the Gram-negative cell envelope. Drugs pass through porins in the outer membrane or through the membrane itself. Once inside the cell they are extruded by efflux pumps such as AcrAB/TolC of *E. coli*. Figure extracted from Lewis, 2020¹².

Although academia and the pharmaceutical industry are making a great effort for the discovery of novel compounds, nowadays there are only a few drugs in development that are effective against Gram-negative bacteria.

1.2. Antimicrobials' overview

An antibiotic is a substance used to treat or prevent a microbial infection. It is a drug used to kill or control the growth of microorganisms in a host. Effective antimicrobial drugs display selective toxicity, at therapeutic concentrations killing or inhibiting pathogens without harming the host¹³.

The old concept of antibiosis was first used by Paul Vuillemin in 1889 who generated an antonym of symbiosis^{15,16}. The term was created to define the antagonistic action between different microorganisms such as bacteria, fungi and protozoan. The term was originally used to describe natural products, often secondary metabolites, produced by bacteria or fungi and able to inhibit the progression of other microbes. Later, it acquired a broader meaning and, nowadays, also includes molecules designed and totally or partially synthesized in chemistry laboratories. Nevertheless, the term antibiotic is being progressively displaced by the term antimicrobial or antimicrobial agent.

1.2.1. Antibiotics mechanisms of action

The mechanisms of action or modes of action of antibiotics are diverse. One possible classification is based on the cellular component or system they affect. They are mainly 5 antimicrobial targets(Figure 3)^{17,18}:

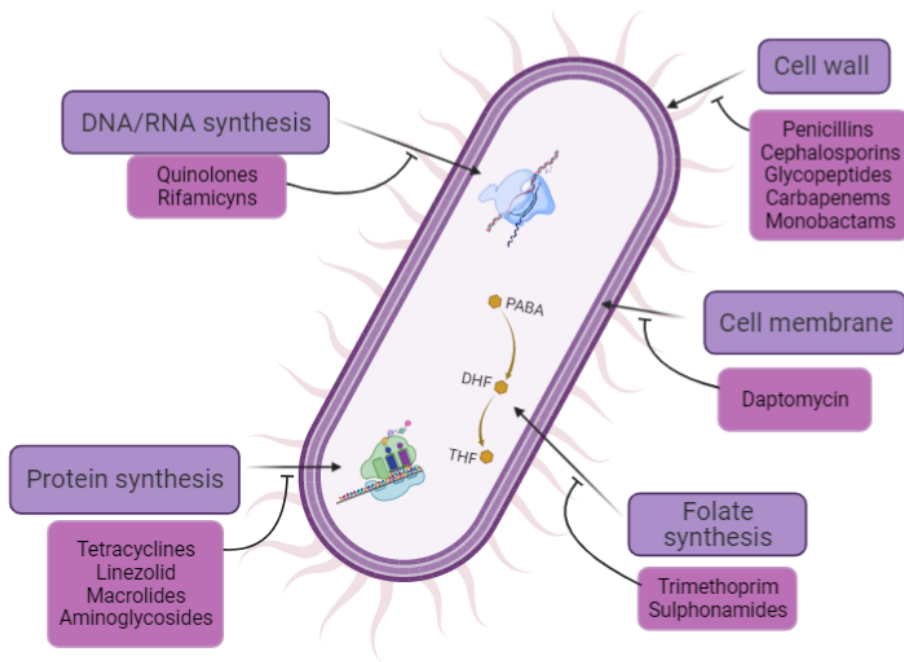


Figure 3. Antibiotic targets. Adapted from Lewis, 2013¹⁸ and Wright, 2010¹⁹ with BioRender.

- i. Cell wall synthesis inhibitors may cause modifications to cell shape and size, induction of cell stress responses and cell lysis (*e.g.*, β -lactams and glycopeptides).
- ii. Cell membrane synthesis disruptors produce changes in the permeability of the membrane (*e.g.* daptomycin).
- iii. Protein synthesis inhibitors are divided into the ones that affect subunit 50S (*e.g.* macrolides, amphenicols) and the ones that affect 30S (*e.g.* tetracyclines, aminoglycosides).
- iv. Nucleic acid synthesis inhibitors: This group includes inhibitors of DNA replication (DNA synthesis and DNA gyrase) and inhibitors of RNA synthesis (*e.g.* quinolones and rifampicin).

- v. Metabolism disruption such as inhibition of the folate synthesis pathway (*e.g.* Trimethoprim and Sulphonamides)

In addition, it is significant whether antimicrobial drugs are bactericidal and therefore induce cell death or bacteriostatic when they solely inhibit cell growth.

1.2.2. Antibiotics history

Infectious diseases have been a global challenge throughout time. Due to this fact, the introduction of antibiotics into clinical use was one of the greatest medical signs of progress of the XX century²⁰. In Figure 4, the timeline of the introduction of antibiotics to the clinic is shown.

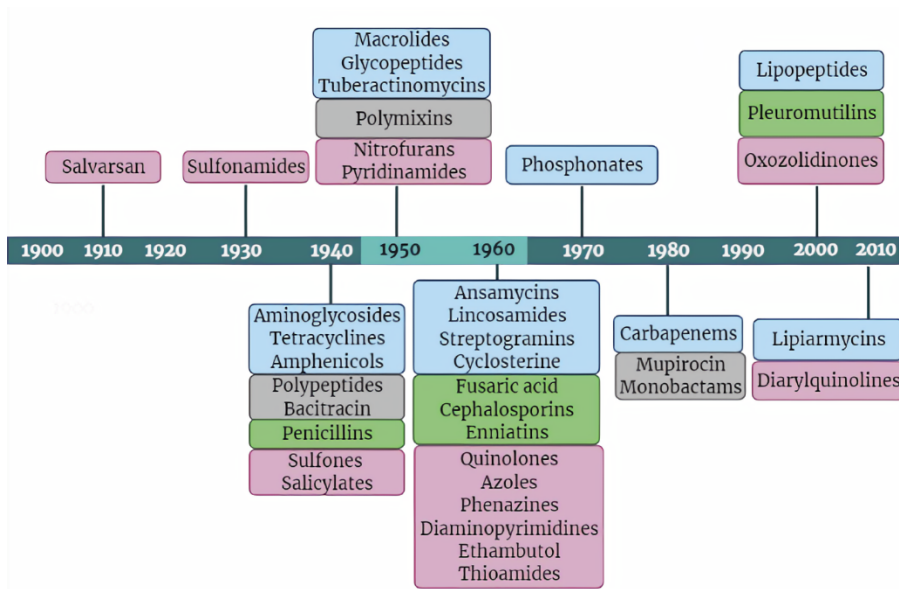


Figure 4. Antibiotics timeline. The compounds appear in the year of their introduction to the clinic. The colours of each antibiotic show their different sources: Pink globes represent synthetic antibiotics; blue globes represent Actinomycete natural products; grey globes represent natural products from other bacteria and green globes represent fungal natural products. The years in the clear zone show the Golden Era of antibiotic discovery. Adapted from Lewis, 2020¹² and Hutchings *et al.*, 2019²⁰.

Although the supply of the first antibiotics themselves began in the 1900s, there is evidence that they have been used for ages by ancient civilizations in Egypt, China, Serbia, Greece and Rome. There have been found many references to the benefits of the topical application of mouldy bread to treat open wounds among other naturally available treatments^{20,21}.

During the Middle Age, the $\mu\acute{\iota}\alpha\sigma\mu\alpha$ (miasma) theory was used to explain contagious diseases, its meaning was something like

contaminated air²². It was in 1546 when Fracastoro suggested that extremely small particles acting as seeds were the causative agents of such diseases²³, and more than three centuries later, the relationship between bacteria and disease was demonstrated. In a parallel history, the advance of knowledge allowed the start of the fight. On the one hand, the Hungarian physician Ignaz Semmelweis called attention to the convenience to apply hygiene measures in hospital, mainly stimulating the habit to wash hands and the use of chlorinated solutions when examining patients. His contribution led to such a spectacular reduction in puerperal infections that he was called 'saviour of mothers'. On the other hand, Joseph Lister, a surgeon of the Glasgow hospital started the treatment of surgical wounds with phenol reaching a drastic reduction of post-surgery infections²². The second half of the XIX century was the richest period in terms of research, mainly in France and Germany where the works of the schools of Louis Pasteur and Robert Koch did the decisive demonstration of the bacterial origin of infections as well as built the fundamentals of the modern microbiology²¹.

The first antibiotic was discovered in Italy in 1893 by Gosio¹⁵. It was a compound produced by *Penicillium brevicompactum* called mycophenolic acid. The molecule was active on *Bacillus anthracis* and it was the first antibiotic compound crystallized. This discovery was published in Italian and therefore it remained unnoticed until mycophenolic acid was rediscovered in 1913. It demonstrated a poorly selective spectrum having antibacterial, antiviral, antifungal, antitumor

and anti-psoriasis properties, in other words broadly toxic. In consequence, its clinical use was abandoned due to undesired adverse effects. Nevertheless, it is nowadays being used as an immunosuppressant to prevent transplant rejection²⁴.

It was not until Paul Ehrlich laboratories synthesized arsphenamine at the beginning of the XX century, that the synergism between microbiology and chemistry began and with it, the beginning of the modern chemotherapeutic era. It was an arsenic-based chemical active against *Treponema pallidum*, the causative agent of syphilis and it was approved as a drug under the name of Salvarsan in 1910^{21,25}. The finding was due to the fascination of Paul Ehrlich for the fact that biological structures could be stained differentially and that bacteria stain stronger than human tissues. This observation was the germ for the elaboration of the so-called *Zauberkegel* (magic bullet)²⁶. Microbiologists, cell biologists and chemists still work looking for magic bullets. For almost four decades Salvarsan and its improved forms (Neo-Salvarsan and Solu-Salvarsan) were the treatment of choice for syphilis and used in veterinarian medicine as well²⁷.

Several coincidences led to one of the major discoveries in microbiology ever. In 1928, when Alexander Fleming returned from his vacations, several plates of *Staphylococcus* were contaminated by a fungus. Despite discarding the plates, he did a careful examination and realized that the vicinity of the mould colonies was free of staphylococci²⁸. It was not until 1940 that Florey and Chain completed the purification of penicillin,

the substance responsible for the staphylococci inhibition^{26,27}. This event is regarded as the birth of the antibiotic era. At the beginning of the penicillin era, all products were natural and purified. However, attempts were immediately made to fully or partially synthesize molecules with similar characteristics. The first synthetic penicillin was produced in 1957 (Penicillin V)²⁷.

Similarly, sulphonamides have their own history. Discovered as antimicrobials by Domagk, emerged in the market in 1935²⁹. Throughout their history, sulphonamides have been used for many kinds of infection and later, almost always used associated with trimethoprim, a compound that inhibits the same metabolic pathway as sulphonamides (the folic acid synthesis) (see section 1.2.4.2).

The discovery of antimicrobial molecules produced by microorganisms led Selman Waksman to perform a systematic research of soil bacteria (largely actinomycetes) as producers of antimicrobials³⁰. This process is known as Waksman platform and is estimated that over 10,000 strains were examined^{20,27}. Subsequently, a worldwide search for antimicrobial compounds began and with it, the Golden Age of antibiotic discovery which lasted from 1940's to 1960's²⁰.

In 1945 Cephalosporins were discovered and, despite not being useful for clinical applications at the beginning, their mode of action, broad-spectrum and potency inspired many researchers who were involved in the synthesis of new antimicrobial molecules.

Unfortunately, after 50 years of drug discoveries, few new antimicrobial classes have been found. Some of them are nitrofurans (1953), quinolones (1960) and oxazolidinones (1987). In addition, some old antimicrobials such as linezolid (1955) and daptomycin (1986) have been modified and commercialized in recent years²⁵.

Currently, the number of antibiotics in the market comprises several molecules that act on different targets.

1.2.3. Bacteriocins

A particular kind of antimicrobials are bacteriocins. Bacteriocins are bioactive antimicrobial peptides (AMPs) produced by prokaryotes. They are amphipathic molecules with a positive net charge, synthesized in the ribosome and released extracellularly. Most of them interact with plasma membranes binding to the negatively charged phospholipids, forming pores that destroy the membrane potential which drives to cell death³¹.

In 1925, the Belgian microbiologist André Gratia succeeded in the detection of antagonisms between different Enterobacteriaceae strains³². Thereafter, it was in 1947 when Pierre Fredericq identified the first bacteriocins as toxic molecules for bacteria taxonomically and phylogenetically close to the producers³³.

Polymicrobial environments with scarce nutrients give rise to the production of peptides to eliminate other bacterial species which compete for space and resources. Normally, bacteriocins only affect bacteria closely related to the producer (narrow spectrum). Many of them, though, can be active against a wider range of bacteria (broad-spectrum)^{31,34}. Their mechanisms of action are diverse, from pore formation to enzyme inhibition.

Even though the broad majority of microcins are produced by Gram-Positive bacteria, especially by lactic acid bacteria, almost all bacteria can produce at least one bacteriocin. This large variety of antimicrobial molecules coupled with their specificity leads to their use in multiple applications such as pharmaceutical, industrial, or biotechnological^{34,35}. They are considered to play a key role in modulating the intestinal microbiota³⁶.

Bacteriocins are classified in an open-access database called DACTIBASE where they are characterized. Dactibase is available at: <http://bactibase.hammamilab.org/main.php>³⁷.

1.2.3.1. Microcins

Bacteriocins produced by Enterobacteria are called microcins. They are ribosomally synthesized molecules with low molecular weight (<10kDa)³⁶.

Microcins were originally studied in 1974 by a Spanish microbiology group whose leaders Fernando Baquero and Carlos Asensio gained a prominent position in the international scenario of microbiological research^{36,38}. It has been demonstrated that microcins play a crucial role in the output of the competition between the large amount and diversity of bacteria present in the human gut. The intestinal content is composed of a huge number of molecules. Some of them have a positive influence on bacteria while others exert a negative effect. The intestinal tract of mammals is complex and partially open, thus influenced by external microbiota. Because of that, it has been defined as “invironment,” a shared space where the interior and the exterior of the organism merge³⁹. The effect of chemical substances of bacterial origin on bacterial growth has led to consider the intestinal microbiota as a source of new antimicrobials. Thus, it makes microcins and other bacteriocins attractive to be investigated for the replacement of the obsolete conventional antibiotics.

In 1982 Aguilar *et al.*⁴⁰ reported the purification method and proposed a mechanism of action for a microcin so-called 15m, which was the origin of a long history of research dealing with microcins from *E. coli*. Microcin 15m inhibits RNA synthesis as a result of the methionine starvation caused by the antibiotic. Thus, a decrease in the RNA accumulation occurs, among other modifications.

Microcins are produced by multiple genera such as *Escherichia*, *Salmonella*, *Klebsiella*, *Shigella*, *Enterobacter* and *Citrobacter* and they are

important in the microbial competition^{36,41}. Most of them are plasmid-encoded although chromosome-encoded microcins have also been described. Their biosynthetic gene clusters present a partially conserved organization formed by a) a structural gene encoding the microcin precursor, b) a self-immunity gene that protects the microcin-producing strain against its toxic molecule, c) genes encoding the export system, and, frequently, d) several genes encoding auxiliary proteins or modification enzymes^{42,43}.

Microcins are active against enteropathogenic *E. coli*, *Salmonella*, *Klebsiella* and *Shigella*. Since they have a narrow spectrum of inhibition, their use may mean the preservation of the microbiota and have fewer side effects than current antibiotics. They normally hijack nutrient uptake pathways to penetrate their phylogenetically close bacterial targets. Their mechanisms of action are diverse, they act blocking vital functions on the target cell. Inside the bacteria, they perturb several and varied cellular targets such as transcription, translation, DNA structure, mannose transport, energy production or cell envelope function^{35,36,41}.

According to the classification proposed by Duquesne et al.⁴³, microcins are divided into two different groups:

- Class I formed by small molecules (<5 kDa) with posttranslational modifications of their peptide backbone (e.g., microcin B17, C7-C51, D93 and J25)

- Class II composed of higher molecular mass peptides (5-10 kDa) which may or may not undergo posttranslational modifications.

This group can be divided into two subclasses:

- o Class IIa: Microcins that require three different genes to synthesise and assemble functional peptides (e.g., microcin L, N, V)
- o Class IIb: Lineal peptides (e.g., microcin E492, M, H47)

Microcin J25

Microcin J25 (MccJ25) is the best studied microcin up to date. It was originally isolated in 1992 by Salomón and Farías from AY25, a faecal strain of *Escherichia coli*⁴⁴.

MccJ25 is produced by *E. coli* strains when cultures approach the stationary phase and its production is increased by iron limitations^{44,45}. For its production, a plasmid-borne mcjABCD biosynthetic gene cluster is required⁴⁶. The mcjA gene encodes a 58-residue precursor McjA, the mcjB and mcjC gene products catalyse the McjA maturation, and mcjD mediates the export of mature MccJ25 to the periplasm through the ABC transporter McjD and participates in the resistance to the microcin of the producing cells providing self-immunity^{42,46-49}.

MccJ25 is a plasmid-encoded and ribosomally synthesized peptide composed of 21 amino acids. It is a lasso peptide, and its peculiar structure consists of an 8-aminoacid ring and a 13 amino acid tail that loops through the ring. The ring is formed by a lactam bond between the α -amino group of Gly1 and the γ -carboxyl group of Glu8^{48,50,51} (Figure5). A β -hairpin structure is formed between the amino acids 10 and 16. This region is involved in the recognition of the molecule by the cell membrane proteins⁵¹. The unusual lasso topology of MccJ25 is responsible for the remarkably high stability of MccJ25. It makes the peptide resistant to denaturation by high temperatures and proteolysis^{52,53}.

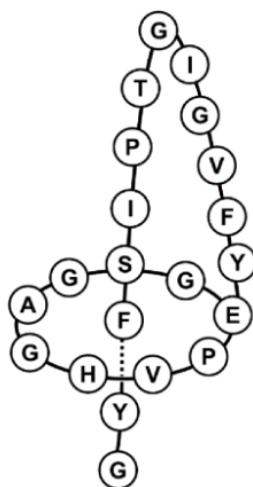


Figure 5. Schematic representation of Microcin J25. Adapted from Martín-Gómez *et al.*, 2019⁵⁴.

It shows bactericidal activity towards several Gram-negative pathogens related to the producer strain, including *E. coli*, *Salmonella* and *Shigella*

^{44,50}.

The microcin J25 uptake by target bacteria cells depends on the iron-siderophore receptor FhuA which is located on the outer membrane forming a closed channel^{45,55}. FhuA uses the electrochemical gradient of protons generated by the TonB-ExbB-ExbD inner-membrane complex to energize the transport of its substrates⁵⁶⁻⁵⁸. The inner membrane protein SbmA is responsible for transporting MccJ25 from the periplasm to the cytoplasmic space (Figure 6)⁵⁶.

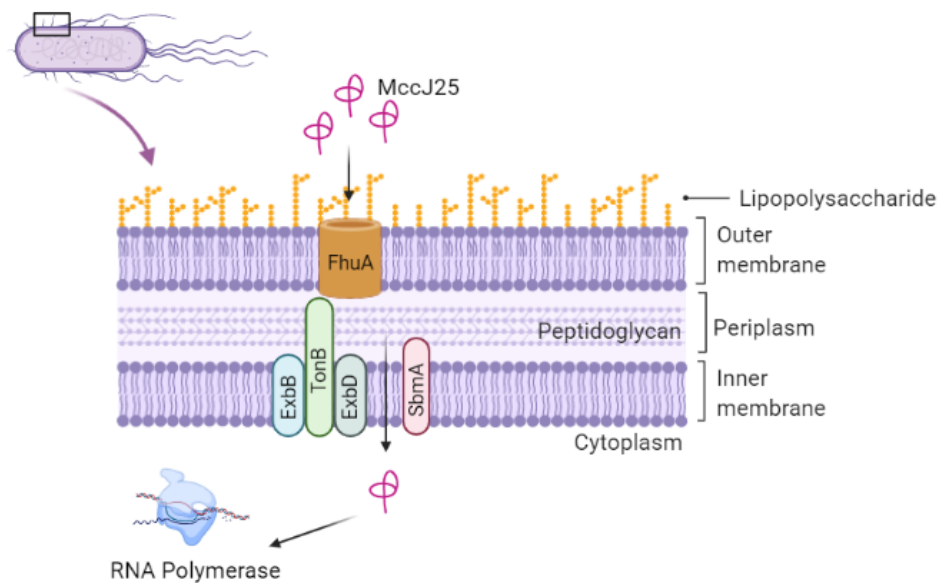


Figure 6. Microcin J25 uptake by target bacteria. Created with BioRender.

Once in the cytoplasm, the suggested mechanism of action of MccJ25 is the inhibition of the RNA polymerase (RNAP) of sensitive bacteria repressing the first two stages of transcription: abortive initiation and elongation^{31,48}.

The first step of gene expression is the transcription of DNA to RNA, carried out by RNA polymerase⁵⁹. The bacterial RNAP exists in two configurations: core and holoenzyme. The core enzyme consists of five subunits: α -dimer (α_2), β , β' , and ω . Although being catalytically active, the core enzyme needs to form a holoenzyme, binding an initiation factor, σ , to recognize the specific DNA sequences (promoters) and initiate the transcription^{60,61}. The RNAP molecule is formed by a "crab claw" structure, with an internal channel running along its full length, where the transcribed DNA binds. Apart from the main channel, RNAP has a secondary channel close to the catalytic centre through which the nucleoside triphosphates (NTPs) are supplied^{52,62}.

Microcin J25 first binds onto the secondary channel on the RNAP, and then blocks it interfering with the entry of NTPs to the RNAP active site⁶³. The MccJ25 β -hairpin loop structure appears to be necessary for the peptide uptake by the membrane protein FhuA but not for RNAP binding or respiration inhibition⁵⁰.

Being transcription essential for protein production, RNAP is seen as an interesting antibacterial target. One of the most studied bacterial RNAP inhibitors is rifampicin. This antibiotic acts binding to RNAP and blocking elongation of RNAs⁶⁴. It is nowadays one of the most powerful and broad-spectrum antibiotics against bacterial pathogens and is a key element of the therapy against mycobacterial infections⁵².

Moreover, it has been seen that MccJ25 has another independent mechanism of action in *E. coli*. It also acts at the level of the respiratory chain generating an increment in the production of reactive oxygen species (ROS)^{65,66}.

1.2.4. The antifolates

The antifolates are compounds that act blocking the folate biosynthesis. The folate biosynthetic pathway is an interesting key target for the development of new therapies against infectious diseases because it has an essential role in the synthesis of one-carbon (C1) donors in a variety of biosynthetic and degradative processes. It is crucial in the biosynthesis of purines, thymidylate, pantothenate, RNA and amino acids, such as methionine and glycine-to-serine conversion^{67,68}. In most microorganisms, dihydrofolate is synthesised *de novo* from early precursor molecules. Briefly, dihydropteroate synthetase (DHPS) is the enzyme that performs the condensation of 6-hydroxymethyl-7,8-dihydropterin pyrophosphate with *p*ABA yielding to the folate intermediate 7,8-dihydropteroate. DHPS is the target of sulfonamide drugs such as Sulfamethoxazole. Dihydrofolate synthetase (DHFS) catalyses the condensation of glutamate with 7,8-dihydropteroate to yield dihydrofolate. In the next step of the pathway, dihydrofolate reductase (DHFR) catalyses the reduction of dihydrofolate to tetrahydrofolate using nicotinamide adenine dinucleotide phosphate

(NADPH) as a cofactor^{69,70} (Figure 7). DHFR is the enzyme target of Trimethoprim.

The early steps of this pathway are selective for bacteria as higher eukaryote organisms obtain folic acid from diet, so they do not depend on its endogenous synthesis and generally lack DHPS. They do reduce folic acid to tetrahydrofolate using DHFR⁶⁷.

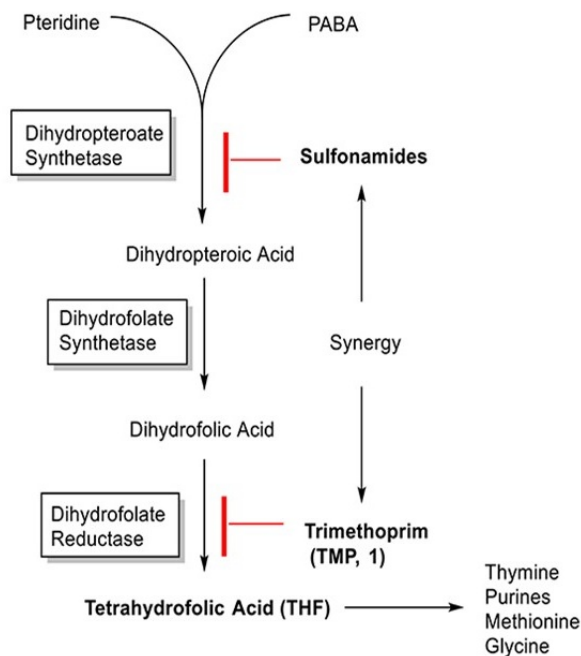


Figure 7. Folic acid biosynthetic route. Enzymes are shown inside a box and enzyme inhibitors marked in red. Figure extracted from Pedrola *et al.*, 2019⁷¹.

1.2.4.1. Trimethoprim

Trimethoprim (TMP, 5-[(3,4,5-trimethoxyphenyl) methyl] pyrimidine-2,4-diamine) is a well-known antimicrobial agent. It was discovered in 1956 by Gertrude Belle Elion and George Herbert Hitchings⁷².

It was first used for the treatment of infections in humans in 1962. It has been used clinically alone and in combination with sulphonamides since 1968, when it was registered⁷³.

Trimethoprim belongs to a group of antibacterial compounds called diaminopyrimidines (Figure 8).

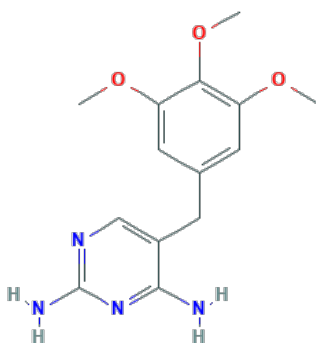


Figure 8. Trimethoprim chemical structure. Figure extracted from PubChem⁷⁴.

TMP is a synthetic, broad-spectrum antimicrobial agent that acts on a late step in the pathway of folate synthesis, inhibiting the dihydrofolate reductase of bacteria.

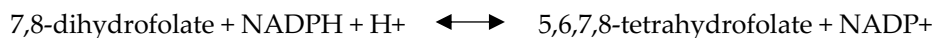
Since trimethoprim has excellent properties such as a wide antibacterial spectrum, low cytotoxicity and few side effects, it has been an extensively prescribed antimicrobial agent.

TMP is included in the Model List of Essential Medicines from the World Health Organization (WHO). In combination with sulfamethoxazole, it is recommended for the treatment of lower urinary tract infections (UTIs) as first choice and for the treatment of acute invasive diarrhoea and bacterial dysentery as second choice⁷⁵.

Dihydrofolate reductase

Dihydrofolate reductase (DHFR, EC 1.5.1.3) is an enzyme ubiquitously expressed in all kingdoms of life.

DHFR catalyses the reduction of 7,8-dihydrofolate (H₂F) to 5,6,7,8-tetrahydrofolate (H₄F) using NADPH as a cofactor (Equation 1)⁷⁶. This conversion is by hydride transfer from C4 of the NADPH cofactor to the C6 atom of the pterin ring of H₂F and an additional concomitant protonation of the dihydrofolate on N5⁷⁷.



Equation 1. Reduction of dihydrofolate to tetrahydrofolate. Reaction catalysed by dihydrofolate reductase (DHFR).

This reaction is essential in *the novo* pathway synthesis of purine, thymidine and certain amino acids⁷⁷.

Being the activity of DHFR fundamental, it is seen as an interesting therapeutic target to disrupt systems that require a fast DNA turnover. Therefore, it has been used as a drug target in the treatment of infectious diseases and the treatment of cancer⁷⁸. Trimethoprim and Methotrexate (MTX) are used as antibacterial and antitumor drugs respectively.

One of the key features concerning DHFR inhibitors is their species selectivity. The identification of small differences between the target enzyme and the host enzyme can lead to the development of successful treatments⁷⁶. Regarding *Escherichia coli* and human DHFR enzymes, they have less than 30% of sequence alignment^{77,79}. Despite this fact, both have a highly conserved structure.

DHFR is folded into an eight-stranded β -sheet which consists of seven parallel strands and an antiparallel one that leads to the carboxyl terminus. The β -strands are flanked by two α -helices on either side⁷⁶.

DHFR is composed of two subdomains, the adenosine-binding domain, which binds the adenosine portion of NADPH, and the loop domain, which is dominated by three loops. The Met20 loop, the β F- β G loop, and the β G- β H loop create the space where the active site is located. Regarding the reaction catalysed by *E. coli*, during the catalytic cycle, the DHFR Met20 loop (residues 9 to 24) adopts three conformations determined by crystallography, open, closed and occluded^{80,81}. The enzyme cycles through five complex intermediates (Figure 9 A).

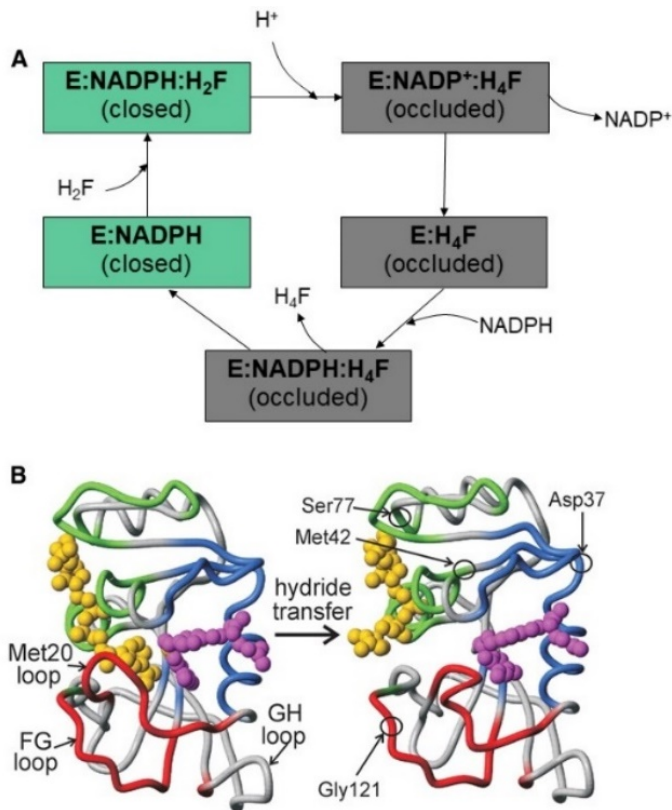


Figure 9. Conformational changes during the catalytic cycle of Dihydrofolate Reductase (DHFR). A) Met20 loop conformations for the five different complexes within the DHFR catalytic cycle. B) Representations of the structure of the ternary complexes of E:

NADPH: H₂F (left) and E: NADP⁺: H₄F (right) during the hydride transfer. Figure adapted from Boehr *et al.*, 2006⁸².

In the substrate complexes (the holoenzyme and Michaelis complex), the Met20 loop adopts the closed conformation. In the product complexes, the loop switches to the occluded conformation.

Fast hydride transfer from NADPH to H₂F occurs in the Michaelis complex (E: H₂F: NADPH) to yield the product complex (E: H₄F: NADP⁺) (Figure 9 B). The following liberation of the cofactor produces the binary complex E: H₄F and NADPH rebinds to assist the product release. Then, E: NADPH is formed again, and the cycle is completed^{80,82-84}.

In enzyme catalysis, protein catalysis plays a key role. Understanding the protein conformation movements may be relevant for the design of new DHFR inhibitors.

1.2.4.2. Sulphonamides: Sulfamethoxazole

Sulphonamides are structural analogues of pABA substrate. They inhibit competitively dihydropteroate synthase (DHPS).

The history of these compounds started in 1932 when Gerhard Domagk showed that the dye Prontosil rubrum prevented mice intraperitoneally

infected with *Streptococcus pyogenes* from contracting peritonitis²⁹. This compound had been synthesised in the laboratories of the Friedrich Bayer Company by Josef Klarer and Fritz Mietzsch. Afterwards, it was discovered that Prontosil hydrolysed *in vivo* to the active molecule sulphanilamide which was responsible for the antimicrobial activity of the dye. Prontosil started being commercially available in 1935^{26,27}.

Since then, a huge number of compounds derived from sulphanilamide, known as sulphonamides or sulpha drugs, have been synthesised. They were the first class of antimicrobials that went into large-scale production and, rapidly, became widely used in clinical settings. Because of the lack of regulation during that time, sulphonamides came to be victims of their own success. The resistance to these drugs became broadly disseminated.

Nowadays, the use of sulphonamides is quite limited. The reasons are the discovery of new and more effective antimicrobials, the sulphonamides widespread resistance and their hard and current side effects²⁹.

Sulfamethoxazole (SMX, 4-amino-N-(5-methyl-1,2-oxazol-3-yl) benzenesulphonamide) is an antibacterial sulfonamide (Figure 10). It is the most commonly used sulfonamide due to its combination with trimethoprim called cotrimoxazole. They act synergistically against a

wide range of bacteria because both drugs affect the same metabolic pathway.

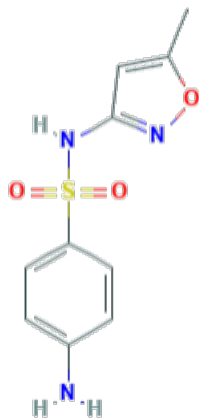


Figure 10. Sulfamethoxazole chemical structure. Figure extracted from PubChem⁸⁵.

1.2.5. Colistin

Polymyxins are a polypeptide antibiotic family and were first isolated in 1947 from the soil bacterium *Paenibacillus polymyxa*. They include five different compounds (A, B, C, D and E) and are characterized by its potent and specific activity against Gram-negative bacteria⁸⁶. Polymyxins were used clinically until they reported severe nephrotoxicity and neurotoxicity in many patients and new drugs were available and, consequently, their use was abandoned.

The emergence of multidrug-resistant bacteria and the need for new effective antibiotics brought back colistin (also known as Polymyxin E). It is nowadays seen as a last-resort antibiotic to treat Gram-negative MDR infections and, therefore, it is on the WHO model list of essential medicines⁷⁵. Unfortunately, with the revived interest for colistin as a

last-line treatment against MDR infections and its overuse in veterinary medicine, colistin resistance in clinical pathogens is on a global rise^{87,88}. Despite this fact, colistin is often the last feasible option for treating infections caused by MDR Gram-negative bacteria.

Polymyxins are cationic polypeptides that consist of a cyclic heptapeptide with a tripeptide side chain acylated at the N terminus by a fatty acid tail^{89,90} (Figure 11).

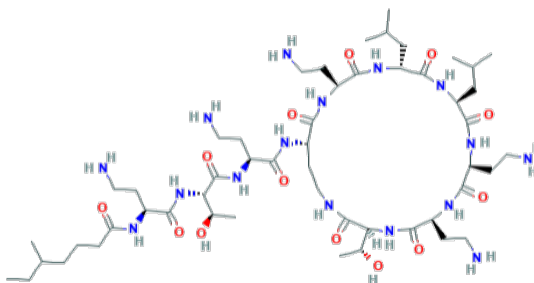


Figure 11. Colistin chemical structure. Figure extracted from PubChem⁹¹.

The specific mode of action of colistin is still not well understood and various mechanisms are stated. Principally, it acts on the LPS of the bacterial outer membrane interacting with its lipid A component⁸⁶. Because of an electrostatic interaction between the diaminobutyric acid (Dab) residue of colistin on the one side and the anionic phosphate groups of the lipid A on the other side, Mg^{2+} and Ca^{2+} are competitively displaced. LPS is therefore destabilized leading to permeability changes in the cell envelope, leakage of the cytoplasmatic content, and consequently, cell death^{86,92}.

1.3. Antimicrobial resistance

Infectious diseases have been a threat throughout the years. The introduction of antimicrobial compounds to treat infections transformed modern medicine and remodelled the therapeutic paradigm⁹³. Unfortunately, antimicrobial resistance appeared almost at the same time as antimicrobial drugs⁹⁴(Table 1).

Table 1. Microorganisms showing antibiotic resistance over time. The year the antibiotics where released is shown as well as the first resistant microorganism and the year it was first identified. Adapted from CDC ⁹⁴.

| Antibiotic Approved or Released | Year Released | Resistant Microorganism Identified | Year Identification |
|----------------------------------|--------------------|--|---------------------|
| Penicillin | 1941 | Penicillin-resistant <i>Staphylococcus aureus</i> | 1942 |
| | | Penicillin-resistant <i>Streptococcus pneumoniae</i> | 1967 |
| | | Penicillinase-producing <i>Neisseria gonorrhoeae</i> | 1976 |
| Vancomycin | 1958 | Plasmid-mediated vancomycin-resistant <i>Enterococcus faecium</i> | 1988 |
| | | Vancomycin-resistant <i>Staphylococcus aureus</i> | 2002 |
| AmphotericinB | 1959 | Amphotericin B-resistant <i>Candida auris</i> | 2016 |
| Methicillin | 1960 | Methicillin-resistant <i>Staphylococcus aureus</i> | 1960 |
| Extended spectrum cephalosporins | 1980 Cefotaxime | Extended-spectrum beta-lactamase-producing <i>Escherichia coli</i> | 1983 |

Outer membrane: a key obstacle for new antimicrobial agents

| | | | |
|-----------------------|------|---|------|
| Azithromycin | 1980 | Azithromycin-resistant <i>Neisseria gonorrhoeae</i> | 2011 |
| Imipenem | 1985 | <i>Klebsiella pneumoniae</i> carbapenemase (KPC)-producing <i>Klebsiella pneumoniae</i> | 1996 |
| Ciprofloxacin | 1987 | Ciprofloxacin-resistant <i>Neisseria gonorrhoeae</i> | 2007 |
| Fluconazole | 1990 | Fluconazole-resistant <i>Candida</i> | 1988 |
| Caspofungin | 2001 | Caspofungin-resistant <i>Candida</i> | 2004 |
| Daptomycin | 2003 | Daptomycin-resistant methicillin-resistant <i>Staphylococcus aureus</i> | 2004 |
| Ceftazidime-avibactam | 2015 | Ceftazidime-avibactam-resistant KPC-producing <i>Klebsiella pneumoniae</i> | 2015 |

It is important to notice that antimicrobial resistance (AMR) is a natural phenomenon. Thus, during the years of evolution of the microbial world, as a result of their interaction with the environment, microorganisms have acquired a huge variety of metabolic and protective mechanisms used in response to big selective pressure such as the one exerted by antimicrobials^{26,95}. Despite this, the main focus of the AMR crisis is not the intrinsic resistance of some bacteria to some antibiotics but the acquired resistance due to the extreme overuse of these drugs during the last decades and the increasing rate at which the resistances are emerging and spreading. The widespread and persistent use of antibiotics, the exposure to nosocomial pathogens and bad practices as self-medication and over medication of humans and

animals, has led to the emergence of multidrug-resistant bacteria (MDR)⁹⁶. This, coupled with the lack of new effective antimicrobials, represents one of the major public-health issues worldwide for the coming decades⁹⁷⁻⁹⁹. Nowadays, approximately 700,000 deaths per year are attributed to antimicrobial resistance and it is estimated that it will get worse, up to 10 million people by the year 2050⁹⁹.

Antimicrobial resistance occurs when microorganisms are capable to survive to a concentration of drug that would otherwise kill them or inhibit their growth. Since they lack competition, the survivor strains can grow and spread. Infectious diseases caused by resistant microorganisms are complex and, in some cases, impossible to treat. They represent substantial costs to the healthcare systems⁹⁴. Superbugs can be classified as either multi-drug resistant (MDR) when resistant to at least one agent in three or more antimicrobial categories, extensively drug resistant (XDR) when resistant to at least one agent in all but two or fewer antimicrobial categories or pan-drug resistant (PDR) displaying resistance to all antibiotic classes¹⁰⁰.

In recent years, the WHO has emphasized the need for investment and research of new drugs against antibiotic-resistant bacteria highlighting the urgency to find anti-tuberculosis medicines. In 2016, they created for the first time a priority list of antibiotic-resistant bacteria against which new antibiotics are critically needed^{97,101}. The prioritization was based on the levels of drug resistance, the number of deaths they cause, the frequency with which they infect people and the burden they create in

health care systems. The first target pathogen of the rank was *Mycobacterium tuberculosis* since it is considered as the top infectious disease killer from a single infectious pathogen. Aside from *M. tuberculosis*, other twelve pathogenic bacteria were enumerated and grouped in three categories^{101,102}:

Priority 1: Critical

- *Acinetobacter baumannii*, carbapenem-resistant
- *Pseudomonas aeruginosa*, carbapenem-resistant
- Enterobacteriaceae, carbapenem-resistant, third generation cephalosporin-resistant

Priority 2: High

- *Enterococcus faecium*, vancomycin-resistant
- *Staphylococcus aureus*, methicillin-resistant, vancomycin-resistant
- *Helicobacter pylori*, clarithromycin-resistant
- *Campylobacter* spp., fluoroquinolone-resistant
- *Salmonella* spp., fluoroquinolone-resistant
- *Neisseria gonorrhoeae*, third-generation cephalosporin-resistant, fluoroquinolone-resistant

Priority 3: Medium

- *Streptococcus pneumoniae*, penicillin non-susceptible
- *Haemophilus influenzae*, ampicillin-resistant
- *Shigella* spp., fluoroquinolone-resistant

It should be noted that 9 of them are Gram-negative bacteria. Moreover, six pathogens from the WHO list have also been grouped using the term “ESKAPE” which stands for *Enterococcus faecium*, *Staphylococcus aureus*, *Klebsiella pneumoniae*, *Acinetobacter baumannii*, *Pseudomonas aeruginosa* and *Enterobacter* spp.^{93,103}. They currently cause most of the nosocomial infections in the US and other parts of the world and can “escape” the effect of antimicrobial compounds.

1.3.1. Mechanisms of antimicrobial resistance

The mechanisms of antimicrobial resistance can be classified according to the metabolic route involved in such resistance (Figure 12)^{95,104}:

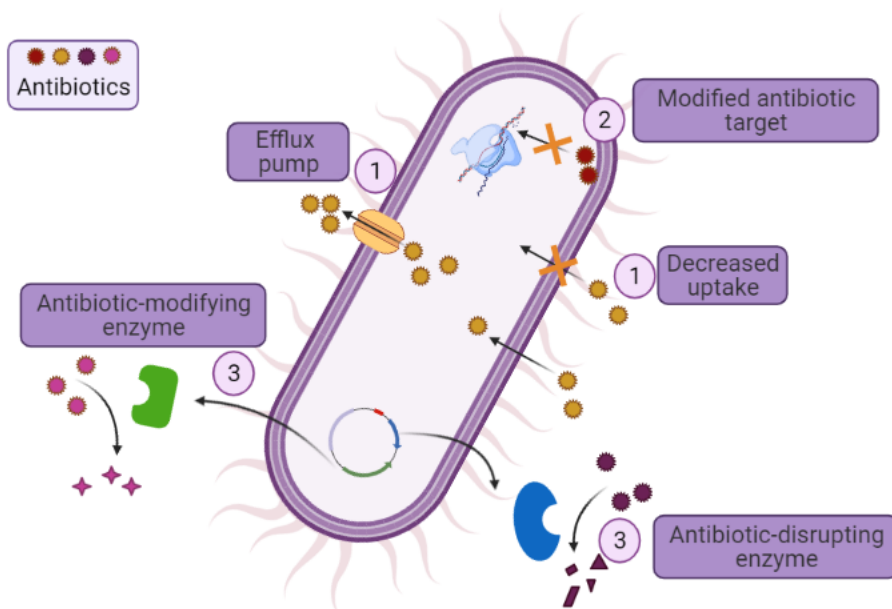


Figure 12. Schematic representation of the antibiotic resistance mechanisms in bacteria. 1) Exclusion of the antimicrobial agent by changes in permeability or efflux pumps 2) Alteration of the antimicrobial target and 3) Modifications of the antimicrobial agent. Adapted from Ryan and Ray, 2003¹⁰⁴ and Allan *et al.*, 2010¹⁰⁵ with BioRender.

1. Exclusion of the antimicrobial agent

To exert their antimicrobial effect, antibiotics must penetrate bacterial cells and reach a sufficient concentration in their target site. Therefore, the molecule must penetrate the bacterial cell wall, being the outer membrane (in Gram-negative bacteria) and/or the cytoplasmic membrane a challenging barrier to enter the cell. Bacteria can prevent the antibiotic molecules to reach their target by two different mechanisms:

- Reducing permeability by decreasing the antimicrobial uptake. Porins are used by antimicrobial compounds as protein channels to cross the outer membrane depending on their physical characteristics. Some of the best-characterized porins are OmpF, OmpC and PhoE produced by *E. coli* and OprD by *P. aeruginosa*. Mutations in the protein porins may produce changes in permeability.
- Actively extruding the molecule using efflux pumps⁹. They are complex bacterial pieces of machinery able to force a toxic compound out of the cell. They are energy-dependent bacterial mechanisms able to force toxic compounds, which have penetrated the cell, back out.

2. Alterations of the target

Once antibiotics have penetrated the cell, they act by binding to the target site and inactivating it. A typical strategy of antimicrobial resistance is interference with the target site. Protection or modification of the target structure may result in a decrease in the antimicrobial-target affinity and effect.

3. Modifications of the antimicrobial agent

One of the most powerful bacterial tactics of antimicrobial resistance is the enzymatic inactivation of the compound. Bacterial enzymes may disrupt or chemically modify antimicrobial compounds making them incapable to interact with the target site. One of the best examples of such disruption is β -lactam resistance. The enzyme β -lactamase breaks open the β -lactam ring of the β -lactamic group. An example of the chemical modification of the compounds is the presence of aminoglycoside modifying enzymes that modify the hydroxyl or amino groups of aminoglycoside molecules.

1.4. Present and future perspectives of antibiotics

As mentioned before, because of the alarming increase of Antimicrobial Resistance, the world is currently facing a global antibiotics crisis. It is relevant to notice that since the golden age of antibiotics, when all the major classes were discovered, there has been a huge development gap and the number of newly available molecules has been critically scarce,

being Daptomycin the last new discovered class of antibiotic in 1986²⁵. From 2011 to 2014 the Food and Drug Administration (FDA) only approved eight new antibiotics or combinational therapies. According to the Pew Charitable Trusts¹⁰⁶ and the WHO⁹⁸ reviews, nowadays there are 43 new antibiotics in clinical development and none of them addresses the problem of resistance in the most dangerous bacteria of the WHO list or ESKAPE pathogens. Thus, because of all the challenges they may face during the process, it is clear that the number of candidates is alarmingly low.

The development of new drugs requires a vast investment of time, research effort from the scientific community and huge expenses. To notably complicate the matters, antibiotics are seen as an unattractive business by the pharmaceutical industry. On the one hand, a huge amount of money is required for the process of discovery of a new drug, from the initial research to final commercialization. On the other hand, once the new compound reaches clinical application, the risk may exist in two different scenarios: the rapid antimicrobial resistance spread and the use of the new drug only as a last resort therapeutic. In both cases, the company's investment may not be worthy^{12,27}.

Immediate actions need to be taken to avoid the critical dangers of a post-antibiotic era in which many common infections would no longer have a cure.

The antibiotics found in the market in the last years are variations or combinations of existing drugs. New and effective antibacterial drugs need to be discovered and developed and innovative and alternative therapies must be explored to fill the pipeline. In order to overcome existent resistant mechanisms, novel compounds acting by unexplored mechanisms, or a new chemical class of antimicrobials are needed although being a major issue.

1.4.1. Strategies to fight MDR bacteria

a) Natural products antibiotic discovery

From the Waksman platform until today, numerous natural products produced by bacteria as secondary metabolites, have been investigated as antimicrobials. Several compounds principally produced by *Actinomycetes* and specifically, *Streptomyces*, have been identified²⁰. Microorganisms produce these natural products to kill competitors, as signalling molecules or to mediate interactions with eukaryotic organisms.

The exploitation of these natural products sources, coupled with new powerful tools and techniques such as whole genome sequencing (WGS) and CRISPR/cas9 may make it easier to explore microorganisms that had not been screened yet as difficult to cultivate bacteria^{12,107}. Nowadays, with these advanced methods, many shortcomings of the natural products drug discovery can be quickly and efficiently solved. Some studies have demonstrated that many bacteria and fungi possess

biosynthetic gene clusters (BGCs) that are not expressed *in vitro* and when activated or expressed in heterologous cells, they encode pathways to produce functional natural products^{12,20}.

Despite this, the options of success in the finding of new classes of antibiotics are conditioned by the ability to find promising types of producers.

b) Synthesis of new molecules

New classes of antibiotics may arise from fully synthetic approaches to drug discovery which may result in novel scaffolds²⁷. There are many relevant examples of fully synthetic current antibacterials such as chloramphenicol, metronidazole, trimethoprim, and fosfomycin. Although the most widely appreciated ones may be quinolones, carbapenems, and oxazolidinones¹⁰⁸.

Despite this, now there is a low rate of discovery of new fully synthetic antimicrobials. The cause is unclear because of the progress in chemistry such as the raise of compound libraries¹².

c) Combination of already known compounds

The interaction between new molecules and conventional antimicrobials should be examined with the aim to find possible synergistic activities^{109,110}. The combination of synergistic drugs for infectious diseases treatment has several advantages. Firstly, it increases

the spectrum of coverage and the antibacterial effect and, secondly, the possibility to develop resistance decreases⁹⁷. An example is the use of colistin in combination with other antibiotics to facilitate the entry and enhance the effect of other antimicrobials against some intrinsically resistant species¹¹¹.

d) Alternative therapies

The use of antibiotics in combination with adjuvants such as permeabilizers, lactamase inhibitors, efflux pumps inhibitors, etc. is seen as a feasible option to reduce resistant rates⁹⁷. Moreover, there has recently been a notable rise in the interest of the scientific community for emergent therapeutic agents and technologies such as phage therapy¹¹², antimicrobial peptides¹¹³, metal nanoparticles, vaccines, antibodies, quorum sensing inhibitors, drug nanoencapsulates¹¹⁴ and photodynamic light, although they have some limitations^{20,115-117}.

e) Improvement of already known compounds

Another approach to open new antimicrobial perspectives is the examination of new synthetic compounds mimicking the structure and mechanisms of action of old antimicrobial compounds^{108,118}. Therefore, chemically modifying old backbones should result in optimized drugs which can be promising antimicrobial compounds. What is sought in the new compounds is to enhance antimicrobial properties either by broadening their mode of action, by reducing their cytotoxicity or by

Outer membrane: a key obstacle for new antimicrobial agents

tackling resistance issues as well as improving their pharmacokinetic and pharmacodynamic characteristics ¹¹⁹.

During the development of this thesis, we have focused on the exploration of the antimicrobial activity of chemical modifications of Microcin J25 and the first-line antibiotic Trimethoprim.

2.HYPOTHESIS AND OBJECTIVES

2.1. Hypothesis

Two partial hypotheses are presented:

- Chemical modifications of current antibiotics may significantly contribute to overcoming the problems arising from the increase and spread of antibiotic resistance in bacteria.
- The combination of these modified compounds with old-rescued antibiotics (door-opener peptides) may contribute to the solution bases of the problem caused by resistance, as it may enhance the bacterial permeability

2.2. Justification of the study and objectives

Antimicrobial resistance is one of the world's major challenges in both microbiology and public health since infections caused by multidrug-resistant bacteria have reached alarming levels. One approach to open new antimicrobial perspectives is the chemical modification of old antimicrobial compounds that may result in optimized drugs with promising antimicrobial properties.

The main purpose of our studies was the activity exploration of the derivatives of two drugs. On the one hand, Microcin J25, which is a potent antimicrobial lasso peptide. On the other hand, Trimethoprim, which is a first line antimicrobial agent present in the WHO model list and used normally in combination with Sulfamethoxazole.

Main objective:

Determine the antimicrobial properties of chemically modified drug compounds.

The secondary objectives of this thesis are divided in two parts:

1. Microcin J25

1.1. Study of the antimicrobial activity of the modified Microcin J25

1.1.1. Determination of their antimicrobial effect on planktonic bacteria

1.1.2. Determination of their antimicrobial effect on biofilm

1.1.3. Exploration of the antimicrobial synergistic effect of the new compound with colistin

1.2. Determination of the toxicity of the modified MccJ25

2. Trimethoprim

2.1. Study of the antimicrobial activity of the Trimethoprim derivatives

2.1.1. Determination of their antimicrobial effect on planktonic bacteria

2.1.2. Determination of their antimicrobial effect on biofilm

2.1.3. Exploration of their antimicrobial synergistic effect in combination with Sulfamethoxazole

2.1.4. Exploration of their antimicrobial synergistic effect with colistin

2.2. Determination of the cytotoxicity of the new derivatives

2.3. Exploration of the effect of the new derivatives on the Dihydrofolate Reductase (DHFR) enzyme

2.4. Start a computational approach to decipher the intimal mechanisms of action.

3. RESULTS

3.1. ARTICLE 1

ARTICLE 1: Chemical Modification of Microcin J25 Reveals New Insights on the Stereospecific Requirements for Antimicrobial Activity.

Martin-Gómez H, **Jorba M**, Albericio F, Viñas M, Tulla-Puche J.

International Journal of Molecular Sciences 2019

Addressed objectives in this article:

1. Microcin J25

1.1. Study of the antimicrobial activity of the modified Microcin J25

1.1.1. Determination of their antimicrobial effect on planktonic bacteria

1.1.2. Determination of their antimicrobial effect on biofilm

1.1.3. Exploration of the antimicrobial synergistic effect of the new compound with colistin

1.2. Determination of the toxicity of the modified MccJ25



Article

Chemical Modification of Microcin J25 Reveals New Insights on the Stereospecific Requirements for Antimicrobial Activity

Helena Martín-Gómez ¹, Marta Jorba ², Fernando Albericio ^{3,4,5}, Miguel Viñas ^{2,*} and Judit Tulla-Puche ^{3,4,6,*}

¹ Institute for Research in Biomedicine, Baldiri Reixac 10, 08028 Barcelona, Spain; marting.helena@gmail.com

² Department of Pathology & Experimental Therapeutics, Medical School & IDIBELL Bellvitge, University of Barcelona, Campus Bellvitge, 08907 Hospitalet de Llobregat, Spain; m.jorba.pedrosa@gmail.com

³ Department of Inorganic and Organic Chemistry–Organic Chemistry Section, University of Barcelona Martí i Franquès 1-11, 08028 Barcelona, Spain; albericio@ub.edu

⁴ CIBER-BBN, Networking Centre on Bioengineering, Biomaterials and Nanomedicine, Baldiri Reixac 10, 08028 Barcelona, Spain

⁵ School of Chemistry and Physics. University of KwaZulu-Natal, Durban 4001, South Africa

⁶ Institut de Biomedicina de la Universitat de Barcelona (IBUB), 08028 Barcelona, Spain

* Correspondence: mvinyas@ub.edu (M.V.); judit.tulla@ub.edu (J.T.P.)

Received: 13 September 2019; Accepted: 13 October 2019; Published: 17 October 2019



Abstract: In this study, microcin J25, a potent antimicrobial lasso peptide that acts on Gram-negative bacteria, was subjected to a harsh treatment with a base in order to interrogate its stability and mechanism of action and explore its structure-activity relationship. Despite the high stability reported for this lasso peptide, the chemical treatment led to the detection of a new product. Structural studies revealed that this product retained the lasso topology, but showed no antimicrobial activity due to the epimerization of a key residue for the activity. Further microbiological assays also demonstrated that it showed a high synergistic effect with colistin.

Keywords: antimicrobial peptide; microcin J25; epimerization; lasso peptide; mechanism of action

1. Introduction

Microcin J25 (MccJ25) is a 21-residue lasso peptide with an 8-residue macrolactam ring, formed between the *N*-terminal Gly1 and the Glu8 side-chain, and a 13-residue *C*-terminal tail, which is threaded through the ring (Figure 1). It is a class II lasso peptide in which the residues Phe19 and Tyr20 are the steric locks. The threaded lasso structure is stabilized by two short double-stranded antiparallel β -sheets. The first comprises residues 6–7 and 19–20, and it is formed between part of the ring and the threaded *C*-terminal tail. The second sheet, which involves residues 10–11 and 15–16, is associated with a β -turn involving residues 11–14, and it forms a hairpin-like structure [1–3]. MccJ25 shows antimicrobial activity against a relatively wide range of Gram-negative bacteria. In particular, it exhibits remarkable antibiotic activity towards *Salmonella newport* and several strains of *E. coli*, with minimum inhibitory concentrations typically in the submicromolar range [4].

MccJ25 shows high thermal and proteolytic stability against several proteases, including chymotrypsin, trypsin and pepsin [5]. Moreover, it is stable to highly denaturing conditions, such as 8 M urea and temperatures above 100 °C [6].

Most antimicrobial peptides (AMPs) are characterized by a large number of hydrophobic positive charges and are generally considered to interact with bacterial membrane structures, like indolicidin [7] or LL-37, the active form of human cathelicidin [8]. Once they have crossed the bacterial membrane,

they can interfere with internal targets, such as DNA [9,10]. However, MccJ25 has only one positive charge and it inhibits bacterial transcription by interacting with the β' subunit of the *E. coli* RNA polymerase (RNAP), which is the target of its antibiotic action [6]. MccJ25 also disrupts the inner membrane of *S. Newport* by inhibiting several essential processes for cell viability, such as oxygen consumption [11]. In contrast, the peptide inhibits the RNA transcription in many *E. coli* strains [6], without affecting oxygen consumption [12,13]. This peptide has also been reported to exhibit a second mode of action. In this regard, MccJ25 interacts with the membrane, thus depolarizing it and decreasing oxygen consumption. However, the underlying mechanism behind these effects is not yet understood [14]. The uptake of MccJ25 by *E. coli* is dependent on the outer membrane receptor FhuA [15–17]. For example, treatment of MccJ25 with thermolysin abolishes its binding to FhuA and results in the suppression of its antibacterial activity, although it is still able to inhibit *E. coli* RNAP activity and *S. Newport* respiration *in vitro* [18]. Additional supporting evidence that the Val11 to Pro16 residues are relevant for MccJ25 uptake emerged from an extensive mutational scanning analysis [19].

To gain further insight into the stability and mode of action of the lasso peptide MccJ25, we performed a chemical modification by treatment with basic conditions (0.5 M NaOH), which produced an alteration in the topology of the peptide and the consequent modification of biological activity. We examined how the alteration in the structure affected the mechanism of action through its comparison with the natural lasso peptide.

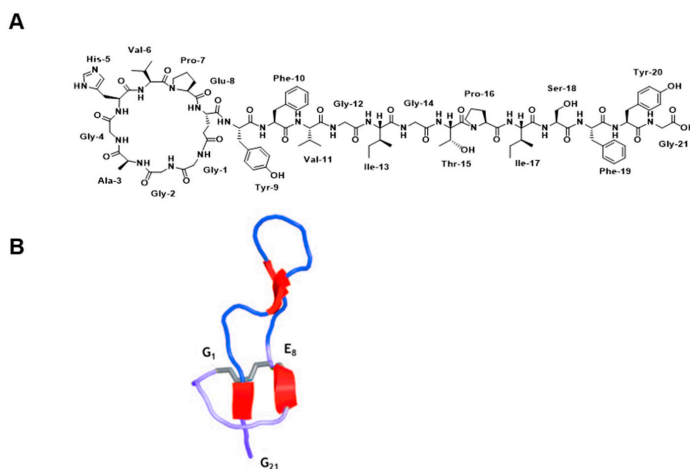


Figure 1. (A) Chemical structural and (B) ribbon representation of the 3D structure of MccJ25 (Protein Data Bank (PDB) code: 1Q71). The four fragments of antiparallel β -sheets are shown in red. Reprinted (adapted) with permission from Knappe, T.A.; Linne, U.; Zirah, S.; Rebuffat, S.; Xie, X.; Marahiel, M.A. Isolation and structural characterization of capistrucin, a lasso peptide predicted from the genome sequence of *Burkholderia thailandensis* E264. *J. Am. Chem. Soc.* 2008, 130, 11446–11454. Copyright 2019 American Chemical Society [20].

2. Results

2.1. Chemical Treatment

The RP-HPLC analysis denotes that the structure of the native lasso peptide was affected by the harsh extended treatment with a base (Figure S1). In this way, a new peak was detected (Figure S2A,B). After being left overnight, the ratio between the starting material and the new product was 1:1 and even with the addition of more NaOH or an increase in reaction time, no reaction progress was observed. The new product, which is shown in Figure S2A, was purified and isolated. RP-HPLC revealed that

the new compound and the native peptide did not co-elute, and distinct chemical equivalence was confirmed by different retention times (t_R), even though these two compounds had the same molecular mass (2107.8 Da) (Figure S2C). Furthermore, the new compound was subjected to the same treatment with basic conditions, and no differences were observed after overnight. This result suggested that the modification was not reversible.

2.2. Minimum Inhibitory Concentration (MIC)

The antimicrobial activity was then evaluated against eight Gram-negative strains, among them four were Multidrug-Resistant bacteria (MDR). As expected, the native MccJ25 displayed activity against four of them: two *E. coli* and two *S. enterica* strains (Table 1). On the contrary, the new compound showed the lowest activity against the eight strains tested. Its MIC values were in all cases higher than 128 $\mu\text{g/mL}$. Thus, we addressed whether the loss of activity was due to the inability of the new compound to penetrate the target bacteria, whether it was caused by changes in its antibacterial properties exerted inside the bacterial cell, or if it was a combination of both factors.

Table 1. Minimum inhibitory concentration (MIC) in $\mu\text{g/mL}$ of the native MccJ25 and the new compound against eight Gram-negative strains [a]. The sensitive strains to the native MccJ25 are highlighted in bold.

| Strains[a] | Native MccJ25 | New Compound |
|--|---------------|--------------|
| <i>Escherichia coli</i> MDR 39255 | 0.5 | >256 |
| <i>Escherichia coli</i> MDR 208691 | >128 | >128 |
| <i>Escherichia coli</i> MDR 246415 | 0.0625 | >128 |
| <i>Escherichia coli</i> MDR 239910 | >128 | >128 |
| <i>Salmonella enterica</i> ATCC 14028 | >128 | >128 |
| <i>Salmonella enterica</i> ATCC 13076 | <0.0625 | >128 |
| <i>Salmonella enterica</i> ATCC 49214 | 0.8 | >128 |
| <i>Salmonella typhimurium</i> SY5015 | >128 | >128 |

2.3. Synergy Study

Colistin, a cationic antimicrobial peptide, even at low concentrations severely disrupts the outer membrane, allowing chemicals to penetrate Gram-negative bacteria. The inability to penetrate bacteria is a major cause of resistance. Although the medical use of colistin was abandoned 30 years ago as a result of its very high toxicity, it was rescued when superbugs (extreme pan-resistant strains) emerged. The recovery of colistin has spurred research into various strategies that allow the preservation of its antimicrobial action and a reduction of its negative side effects. One such strategy involves its combination with drugs with low toxicity to achieve synergistic activity. Colistin may serve as a “door opener” even at concentrations at which the negative side effects are negligible. A checkerboard assay using a combination of the new compound and colistin was performed against the *E. coli* MDR 39255 strain and the *S. enterica* ATCC 13076 (American Type Culture Collection) strain, which are susceptible to native MccJ25 but not to the new compound, as shown in the MIC assay (Table 1). Moreover, two strains resistant to native MccJ25 (*E. coli* MDR 208691 and 239910) were also tested in order to compare results in both types of bacteria.

The fractional inhibitory concentration (FIC_i) values for the bacterial strains tested with combinations of the new compound and colistin are shown in Table S1. According to the international standard, FIC_i values below 0.5 should be interpreted as synergistic (see “Methods” section for more details) [21]. Thus, these experiments indicated a synergistic effect between colistin and the new compound.

These results show that the new compound retained the ability to inhibit the growth of these two strains (*E. coli* MDR 39255 and *S. enterica* ATCC 13076), although it was unlikely to have the capacity to enter the bacteria through the outer membrane, the reasons for that have to be investigated and

may probably involve its ability to bind the receptor FhuA. In contrast, when the new compound was combined with colistin, it penetrated the outer membrane, thereby demonstrating that the antibacterial mechanisms of action were conserved after the chemical treatment. On the other hand, when the combination of colistin and the new compound was tested in bacteria resistant to native Mcc25, namely *E. coli* MDR 208691 and *E. coli* MDR 239910, a weak synergistic effect was observed. These results could be explained by the change in the peptide topology observed by RP-HPLC.

2.4. Minimal Biofilm Eradication Concentration (MBEC)

The MBEC values were, in all cases, greater than 128 $\mu\text{g/mL}$. Such value is thousands of times greater than the inhibitory values against planktonic bacteria. Therefore, it should be assumed that neither MccJ25 nor the new compound can be considered antibiofilm agents.

2.5. Stability Assays

In order to understand the loss in biological activity of the new compound, the stability and structure of the peptide was analyzed. Initially, the chemical treatment was believed to have converted the lasso peptide into a branched cyclic peptide. However, the carboxypeptidase assay rendered the same cleavage pattern for the native peptide and the new product, corresponding to the loss of 81 Da (Figure S3). This loss was attributed to the double cleavage in the loop between the amide bond of Phe10-Val11 and Val11-Gly12, resulting in the loss of Val11 and maintenance of the threaded structure. We obtained a total conversion carboxypeptidase Y treatment, in contrast to previous studies in which only minor traces of the (MccJ25–18) Da were detected [22]. Although the two peptides showed the same cleavage pattern, their t_R differed, as shown in the co-injection in Figure S3C. Both peptides were also thermally stable for 4 h at 95 °C (Figure S4). Carboxypeptidase Y treatment was also performed on the resulting peptides after heating for 4 h at 95 °C. In this regard, the same cleavage pattern as in Figure S3 was observed.

To further characterize the new compound, both this peptide and the native MccJ25 were subjected to proteolytic hydrolysis with stronger proteases, such as pepsin and thermolysin. As expected from the pepsin treatment, no hydrolysis was observed, even after several hours at pH 2 at 37 °C [5]. Given this result, the temperature was increased to 50 °C, as pepsin is stable at this temperature. However, no cleavage was detected after 19 h, thereby indicating that both the native peptide and new compound were stable (Figure S5). These results ruled out the formation of the unthreaded structure. On the other hand, thermolysin treatment produced the same cleavage pattern for the two peptides, corresponding to the loss of 137 Da (m/z 1969.9) (Figure S6A,B) [23–25]. This loss could be attributed to the double cleavage between Phe10-Val11 and Gly12-Ile13, with the loss of Val11-Gly12 and the subsequent gain of 18 Da. This cleavage led to a structure with two fragments stabilized by the steric hindrance of Phe19 and Tyr20 and the presence of non-covalent interactions (Figure 2) [24]. Of note, after the treatment with thermolysin, the two peptides showed the same t_R value (Figure S6C). This result indicated that the cleavage led to the same structure, thereby suggesting that the variable part of the compound was removed during hydrolysis (Val11-Gly12). In this regard, this result can be explained only by the inversion of the chiral center of Val11. This question will be addressed in future structural studies.

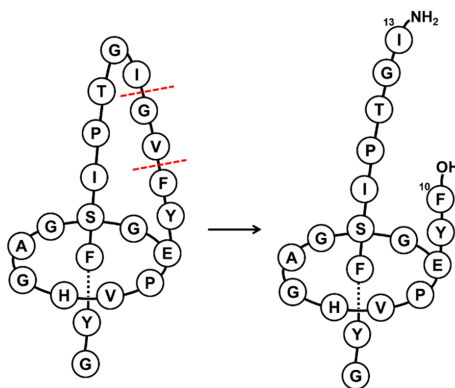


Figure 2. Schematic representation of thermolysin cleavage in the native MccJ25 and in the new compound. Dashed red lines indicate the cleavage sites.

2.6. MS/MS Analysis

The tandem mass spectrometry (MS^2) fragmentation spectra revealed that the main fragmentations took place around Pro16 (Figure S7). The same fragmentations were obtained for the two peptides, but with different intensities (Table S2). These fragmentations were characteristic of a lasso structure, since they contained both the *N*-terminal and *C*-terminal parts of the molecule. The steric hindrance between the ring and the bulky side chains of a putatively threaded *C*-terminal part of the peptide would explain this remarkable fragmentation pattern. Regarding the native MccJ25, the fragmentations obtained were in agreement with those already described in the literature [1,24].

The MS^3 spectra of the main fragmentations showed the same pattern for the native MccJ25 and the new product, the only difference being that the MS^3 fragmentations of $b_{13} + y_6$ were more intense for the former (Figure S8). On the basis of these results, we confirmed that the new compound showed the lasso topology and that, with the exception of its t_R , its structure was very similar or even the same as that of the native MccJ25.

2.7. Ion-Mobility Mass Spectrometry (IM-MS) Analysis

Small changes in collision cross section (CCS) values were observed upon increasing the charge state of both the native MccJ25 and the new peptide (Table S3). This feature was demonstrated by the low range of CCS values ($\Delta\Omega$) and the concomitant low $\Delta\Omega/\Omega$ value (Table S4). Small changes in CCS values are characteristic of lasso peptides, as an increase in charge state brings about more unfolding and, consequently, lower drift times (t_d). However, due to the organized and constrained structure of lasso peptides, the increase in the CCS was very low compared to branched cyclic or lineal peptides. The $\Delta\Omega/\Omega$ value of the new compound was within the accepted range for lasso peptides (0 to 10.9%) [26]. It was therefore deduced that this peptide had a lasso structure.

The number of multiple conformations was higher for lower charge states, as expected due to the larger number of available protonation sites and the coexistence of several protomers [27]. However, when the charge state increases, narrow ion mobility peaks, associated with the existence of few conformations, are expected (Figure 3).

IM-MS revealed that the new compound showed the same features as those of native MccJ25, thus allowing us to confirm once again the lasso structure of the former.

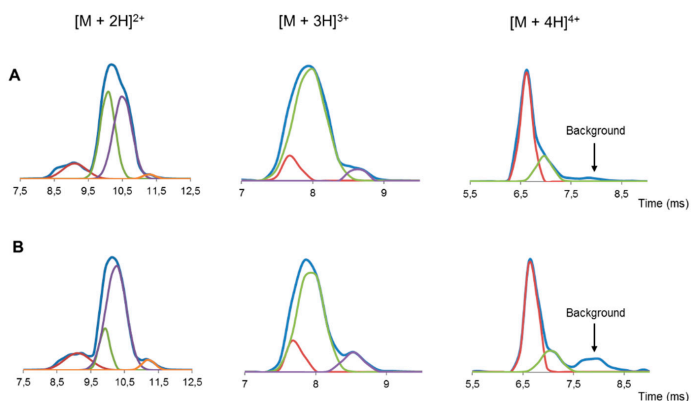


Figure 3. Drift times profiles (blue trace) and fitted peaks (red, green, purple and orange trace) of double, triple and quadruple protonated ion of (A) the new compound obtained after treatment with a base and (B) native MccJ25. Background is the residual drift time profile, in which no more peaks could be fitted.

2.8. Circular Dichroism (CD) Spectroscopy

The CD spectra of the two peptides were recorded in methanol [28,29]. They displayed a clear minimum at 200 nm, which is characteristic of unstructured peptides, indicating a predominant random coil state (Figure 4). The native MccJ25 in methanol showed a maximum at 220 nm and a smooth positive shoulder at 210 nm. These bands have been previously attributed to the Phe L_{α} and Tyr L_{α} transitions [30]. However, for the native MccJ25 in H_2O with 5% of 2,2,2-trifluoroethanol (TFE), the maximum was located at 222 nm and was more intense than in methanol. In addition, the shoulder at 210 nm was not marked. On the contrary, the positive band at 220 nm for the new compound was displaced to 225 nm and the one at 210 nm was more defined and clearer than for the native peptide. This behavior suggested that the L_{α} transition of these residues had greater relevance for the new compound than for the native MccJ25.

In conclusion, the CD spectra revealed some differences in the positive bands of the two peptides, but the clear minimum at 200 nm indicated a random coil structure for both. The changes in the positive bands may indicate distinct topologies.

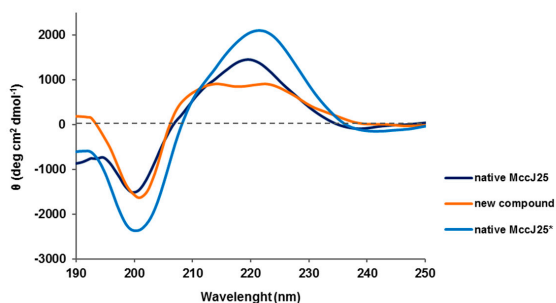


Figure 4. CD spectra of new compound after treatment with a base and native MccJ25 in methanol. * in H_2O with 5% TFE.

2.9. Nuclear Magnetic Resonance (NMR) Spectroscopy

The NMR data for the structural characterization of the new compound were recorded in methanol- d_3 and compared with those of the native MccJ25 (Tables S5–S8 and Figures S9–S14) [1,24,25,28,31]. The resonance assignments of the native MccJ25 were identical to those of the structure already published (PDB code 1PP5) [31]. Given our previous results from the thermolysin assay, we hypothesized that the difference between the two peptides may reside in the peptide loop, between residues 10–12 in particular, which are involved in the β -hairpin, and that after thermolysin treatment the cleaved product showed the same t_R .

Regarding 1H assignment, the chemical shift deviation values of αH of the loop residues in the new compound differed to those of the native structure (Figure 5). The most remarkable residue was Val11, indicating that the β -hairpin had been lost, as demonstrated by the negative value [18]. On the other hand, the structure of the ring and the tail had been conserved, including the β -hairpin between residues 6–7 and 19–20, as shown by the high positive values in Figure 5. In addition, the overlapping of several peaks was observed for the new compound in the amide proton region around 7.80, 7.90 and 8.40 ppm (Table 2).

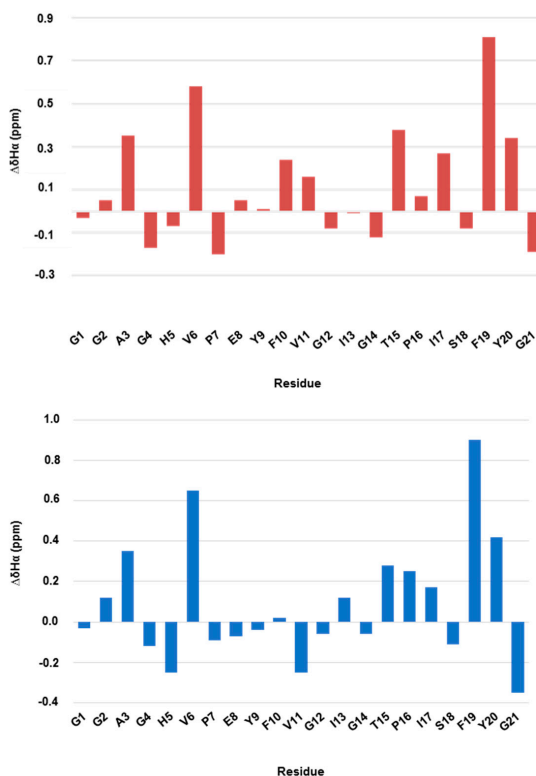


Figure 5. Histograms of chemical shift deviations from random coil for $\Delta H\alpha$ in the native MccJ25 (red) and new compound (blue) in methanol. Random coil values were obtained from Wishart et al. [32].

Table 2. ¹H chemical shift of the amide protons of the new compound that underwent peak overlapping [a]. From the total correlated spectroscopy (TOCSY) spectrum in methanol-d₃ at 298 K.

| Residue | δ (ppm)[a] | Residue | δ (ppm)[a] |
|---------|------------|---------|------------|
| Ser18 | 7.80 | Glu8 | 7.90 |
| Gly4 | 7.80 | Ile13 | 7.89 |
| Tyr9 | 7.84 | Ala3 | 8.44 |
| His5 | 7.79 | Val11 | 8.42 |
| | | Gly12 | 8.39 |

Evidence that the tail was threaded through the ring in the new compound was provided by the presence of the characteristic Nuclear Overhauser Effect (NOE) cross-peaks between residues 1–8 and residues 19–21 (Figures S15–S17A) [24]. For example, the NOEs between NH Tyr20 and αH Gly2 and δH Phe19 and βH Ser18 were also more intense than for the native MccJ25. Moreover, some NOEs, such as βH Phe19–NH Glu8 and δH Tyr9–αH Gly14, were detected only in the new compound (Figure S17B). Analysis of the two β-hairpins in the native MccJ25 structure reveals clear differences (Table S9). The disappearance of the β-sheet in the loop can also be detected by the lack of NOEs between αH Val11 and δH Pro16 (Figure S17C). The two Pro (7 and 16) in both structures adopted a trans conformations, as shown by the presence of the NOE between the δH Pro(i) and the αH residue(i-1).

With respect to Val11, various NOE cross-peaks were observed, thereby revealing a distinct topology for the new compound (Table S10). In general, the intensities of the NOEs for the new compound were lower than those of the native one. However, the new compound showed a stronger connectivity with Phe10 and Thr15 (Table S11). The ring protons of Phe10 adopted a different conformation. In the new compound, this residue interacted with δH Pro16, βH Ile17, NH Val11 and αH Ala3, while in the native peptide it interacted with αH, γH Pro16, βH, γH Glu8, βH Phe19 and NH Thr15 (Figure S17D).

All the results pointed to the epimerization of Val11 during the treatment with a base, a process that yielded a new peptide topology. This epimerization explains the loss of the β-sheet in the loop region, producing a lack of organization and consequently a high signal overlap.

2.10. Structure Calculation

The structure of the new compound was determined using a macrocyclic conformational sampling tool [33], and the constraints are described in Table S12. The lowest-energy structure was compared with the native MccJ25. The lasso structure was maintained and the modification was mainly in the loop region (Figure 6). The interaction between the side-chains of Val11 and Pro16, characteristic of a β-sheet, was not present. The αC of Val11 underwent racemization and the side-chain of Val11 adopted a new orientation. Furthermore, the high root-mean-square deviation value (RMSD = 8.5 Å) exhibited that the structures of the native peptide and new product differed.

The Ramachandran plots for the two peptides differed (Figure S17). The native MccJ25 showed a well-defined and compact structure, with the individual backbone conformations of all residues located mainly in highly favored regions. On the contrary, the new compound showed more dispersion. The β-sheet in the loop was absent, and Pro16 was observed to be involved in a right-handed α-helix and Val11 in a left-handed one (Figure S18). Gly12 and Ile17 also adopted a left-handed α-helix conformation. On the other hand, the ring residues 5–8 of the new compound remained in the same conformation as that of the native structure.

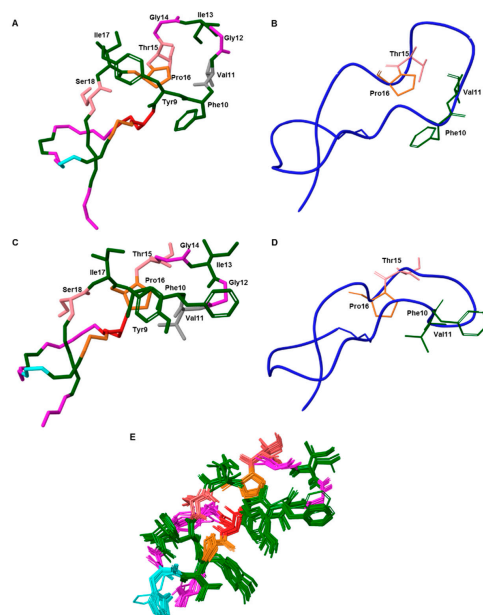


Figure 6. (A) and (C) 3D structure of the native MccJ25 (PDB code 1PP5) and NMR-derived lowest-energy structure of the new compound, respectively. Only the side chains of the loop are shown. (B) and (D) Ribbon representation of the native peptide and new compound, respectively. The four residues involved in the β -sheet located in the loop are shown. (E) Ensemble of the 20-lowest energy structures derived from the NMR restraints of the new compound. The maximum RMSD value between structures 1–20 is 0.6 Å. Aromatic and hydrophobic residues are shown in green, negatively charged residue (Glu8) in red, positively charged residues (His5) in blue, polar residues in light pink and non-polar residues in pink (Gly) and (Pro). In (A) and (C) Val11 residue is shown in grey.

3. Discussion

We have demonstrated that basic chemical treatment of MccJ25 produced a new compound that maintained the threaded lasso structure but lost its antimicrobial activity. Three independent properties corroborated the presence of the lasso topology: high proteolytic stability; identical MS² fragmentation pattern; and ion-mobility spectra as the native MccJ25. Circular dichroism revealed slight differences in the positive bands between the two peptides, thereby pointing to distinct topologies.

The microbiological results showed that the new compound did not exert antimicrobial activity, as shown by its incapacity to penetrate the outer bacterial membrane. However, when used in combination with colistin, the new compound did show antimicrobial activity. These findings were consistent with the NMR results, in which a change in the loop topology, caused by epimerization at the Val11 residue, was detected. This observation suggests that Val11 is highly base-sensitive and is essential for conferring antimicrobial activity, because it governs binding to the FhuA receptor [34]. This epimerization produced a conformational change on the loop between Val11 and Pro16, which is in agreement with previous evidence that this section is relevant for the antimicrobial activity of MccJ25 [19]. Ile13 is also an essential residue for the uptake of MccJ25 into cells [35]. The new compound showed an alteration in the orientation of the Ile13 side chain, which led to the suppression of biological activity.

The weak synergistic effect observed when the new compound was used in combination with colistin and assayed on resistant bacteria (*E. coli* MDR 208691 and *E. coli* MDR 239910), is consistent

with the hypothesis that penetration is the main handicap for antimicrobial activity. In the case of such resistant strains the entry is not the reason for resistance. Although the microbiological results are preliminary, we propose that the combination of bacteriocins with “door openers”, such as colistin, may provide a promising strategy to fight multidrug-resistant infections. In this regard, the treatment of such infections is becoming increasingly unsuccessful and has thus emerged as a key challenge in current microbiological research [36].

4. Materials and Methods

4.1. Heterologous Expression of MccJ25

Overnight cultures were prepared in Luria broth (LB) medium containing 17 µg/mL of Chloramphenicol at 37 °C through inoculation with *E. coli* BL21 cells carrying the MccJ25 plasmid (pTUC202). Subsequently, 500 mL of M9 minimal medium ((17.1 g/L Na₂HPO₄ × 12 H₂O, 3 g/L KH₂PO₄, 0.5 g/L NaCl, 1.0 g/L NH₄Cl, 1.0 mL/L MgSO₄ 2 M, 0.2 mL/L CaCl₂ 0.5 M at pH 7.0), after autoclaving 10 mL/L glucose solution (40% *w/v*), 0.2 mL/L vitamin mix (Table S13), and 17 µg/mL amphenicol) were inoculated with 5 mL of culture and incubated for 3 days at 37 °C. Once the OD₆₀₀ reached ~1.5, cells were harvested by centrifugation (2 × 20 min at 7000 rpm), and the supernatant was treated with 10 mL of XAD-16. After 1 h of shaking at 100 rpm, the supernatant was removed by filtration, and the resin was washed with water and extracted with 50 mL of MeOH. Solvent was removed under vacuo. Dried extract was resuspended in a total of 1 mL of MeOH-H₂O (1:1, *v/v*), cleared by centrifugation, and analyzed by RP-HPLC. For the isolation and purification of MccJ25, the expression was carried out with 6 L of M9 minimal medium. In this case, the procedure was the same, and the dried extract was resuspended in 6 mL of MeOH-H₂O (1:1, *v/v*), cleared by centrifugation and filtration, and then subjected to preparative HPLC.

4.2. Minimum Inhibitory Concentration (MIC)

MIC values were determined by the broth microdilution method and interpreted following the guidelines of the Clinical & Laboratory Standards Institute (CLSI) and European Committee on Antimicrobial Susceptibility Testing (EUCAST) [37]. The different strains were grown in Mueller-Hinton broth (MHB) overnight at 37 °C with shaking at 200 rpm. The bacterial cultures were then adjusted to OD_{625nm} of 0.08–0.1 and diluted 1:100 in fresh MHB medium. Next, 5 µL of each diluted suspension was added to 96-well plates previously filled with MHB and serially diluted peptides. The plates were incubated at 37 °C for 24 h, after which the MIC was determined macroscopically, based on the visually turbidity of the wells. All experiments were performed in triplicate.

4.3. Synergy Study

A checkerboard test was used to determine the fractional inhibitory concentrations (FICs) of colistin in combination with the new compound. Each well in a 96-well plate was inoculated with 100 µL of a bacterial inoculum of 1 × 10⁵ CFU/mL, and the plates were incubated at 37 °C for 24 h. The FIC was calculated after identifying the first well in each row without growth (MIC), following Equations (1) and (2).

$$FIC_A = \frac{MIC \text{ drug A in combination}}{MIC \text{ drug A}} \quad (1)$$

$$FIC_B = \frac{MIC \text{ drug B in combination}}{MIC \text{ drug B}} \quad (2)$$

The FIC index (FIC_i) values were calculated by adding the FIC A (colistin) to the FIC B (peptide). FIC_i values were interpreted as follows: FIC_i < 0.5, synergistic; FIC_i ≥ 0.5 and < 4, no interaction; FIC_i > 4, antagonistic [38]. This assay was performed in triplicate.

4.4. Minimal Biofilm Eradication Concentration (MBEC)

MBEC was determined as described by Moskowitz et al. [39]. Bacterial biofilms were formed by immersing the pegs of a modified polystyrene microtiter lid into 96-well microtiter plates, each containing 200 μ L of Muller-Hinton broth cation adjusted (MHBCA), followed by incubation at 37 °C for 24 h. Pegs were then gently rinsed in a 0.9% *w/v* NaCl solution and biofilms were exposed to a range of concentrations of antimicrobials for 24 h at 37 °C. Pegs were again rinsed with a 0.9% *w/v* NaCl solution and biofilms were removed by 10 min sonication. Recovered bacteria were incubated for 24 h at 37 °C. Optical densities at 620 nm were measured in order to determine MBEC values, defined as the lowest concentration of antimicrobial that prevented bacterial regrowth from the treated biofilm. All experiments were performed in triplicate.

4.5. NMR Spectroscopy

1D and 2D NMR spectra were acquired on a Bruker 600 Avance II Ultrashield, equipped with a cryoprobe. Chemical shifts (δ) are shown in parts per million (ppm) using tetramethylsilane (TMS) as internal standard.

1.5 mg and 1.0 mg of the native MccJ25 and the new compound, respectively, were dissolved in 600 μ L of methanol- d_3 to a final concentration of 1.2 mM and 0.86 mM, respectively. The spectrum was recorded at 25 °C and the residue assignments were obtained from 2D total correlated spectroscopy (TOCSY), while 2D nuclear Overhauser effect spectroscopy (NOESY) permitted sequence-specific assignments. ^{13}C resonances were assigned from 2D ^{13}C - ^1H HSQC spectra. The TOCSY and NOESY mixing times were 70 and 250 ms, respectively.

4.6. Ion-Mobility Mass Spectrometry (IM-MS)

IM-MS experiments were recorded on a Synapt G1-HDMS mass spectrometer (Waters). 0.1 mg of peptide was dissolved in 500 μ L of water at 100 μ M. Samples were then diluted 1/10 in water-acetonitrile (H_2O -ACN) (1:1) with 4% of formic acid and adding 200 mM and 400 mM sulfolane up to 10 μ M. Samples were directly injected into the instrument using a Triversa Nanomate system (AdvionBioSciences, Ithaca, NY, USA) as the interface. Ionization was recorded in positive mode using a gas pressure and spray voltage of 0.5 psi and 1.75 kV, respectively. Source temperature, extraction cone and cone voltage were set to 20 °C, 3 V and 40 V, respectively. Transfer and trap collision energies were set to 4 V and 6 V, respectively. Ion-mobility spectrometry (IMS) and trap gas flows were 25 and 8 mL/sec, respectively. The pressure in the Trap and Transfer T-Wave regions were 5.97×10^{-2} mbar of argon and the pressure in the IMS T-Wave was 0.478 mbar of N_2 . The wave amplitude was a linear ramp from 1.0 to 28.0 V. The traveling wave operated at a velocity of 250 m/sec. The bias voltage for getting in the T-wave cell was 15 V. Cesium iodide was used to calibrate the instrument over the m/z range of 200–3000 Da. MassLynx 4.1 SCN 704 (Waters, Spain) and Drift scope version 2.4 software were used for data processing.

4.7. MS/MS Analysis

MS^2 and MS^3 analyses were carried out on a linear trap quadrupole fourier transform (LTQ-FT) Ultra mass spectrometer (Thermo Scientific). 0.1 mg of peptide was dissolved in 500 μ L of water at 100 μ M. Then, 10 μ L was diluted 1/1 with ACN (1% formic acid) to obtain a concentration of 50 μ M (20 μ L). Solutions were directly injected into the instrument using a Nanomate system (AdvionBioSciences, Ithaca, NY, USA) as the interface. Ionization was recorded in positive mode using a gas pressure and spray voltage of 0.5 psi and 1.75 kV, respectively. Voltage and capillary temperature were set to 44 V and 200 °C, respectively. Collision-induced dissociation (CID) was used as a fragmentation technique. Data were recorded using Xcalibur software vs.2.0SR2 (ThermoScientific).

4.8. Structure Calculation

The structure was calculated with the Schrödinger Suite Macrocylic Conformational Sampling tool [33]. The coordinates were extracted from the native MccJ25 solution NMR structure (PDB ID: 1PP5). The stereochemistry of Val11 was manually mutated to R. The resulting structure was used as input for structural modeling. NOEs were classified as strong, medium and weak (upper limits for structure calculation were set as 2.2 Å, 3.0 Å and 4.0 Å, respectively), and were then applied to the structure (Table S12). Optimized potentials for liquid simulations (OPLS) 2005 force field and Generalized Born surface area (GBSA) for electrostatic treatment were used to generate a total of 56 conformations. They were kept when energies were below 10 kcal/mol, and superfluous conformations (RMSD > 0.75 Å) were removed. 5000 simulation cycles were applied with 5000 Large-scale Low Mode (LLMOD) search steps.

4.9. Circular Dichroism (CD)

CD spectra were recorded using a Jasco 810 UV-Vis spectropolarimeter, equipped with a CD/Fluorescence 426S/426L Peltier temperature controller. Peptide samples were dissolved in MeOH, and spectra were recorded at 200 µM. One sample was dissolved in H₂O with 5% TFE. The following parameters were used: sensitivity (standard, 100 mdeg); start (260 nm); end (190 nm); data pitch (0.5 nm); scanning mode (continuous); scanning speed (200 nm/min); response (1 s); band width (1.0 nm); and accumulation (3). A blank spectrum of the buffer was subtracted from all recordings, and molar ellipticity values were calculated from experimental ellipticity using the Equation (3):

$$\theta = \frac{\theta_{\text{exp}} \cdot 10^6}{b \times C \times n} \quad (3)$$

where θ is the molar ellipticity in deg·cm²·dmol⁻¹, θ_{exp} is the measured ellipticity in mdeg, b is the optical path length in mm, C is the peptide concentration in µM and n is the number of residues in the peptide. After unit conversion, the spectrum was smoothed using the Savitzky-Golay method (convolution width = 21) and taken to zero at the far-UV region ($\lambda = 260$ nm).

Supplementary Materials: Supplementary Materials can be found at <http://www.mdpi.com/1422-0067/20/20/5152/s1>.

Author Contributions: Conceptualization, H.M.-G., F.A., and J.T.-P.; investigation, H.M.-G., and M.J.; writing—original draft preparation, H.M.-G., M.J., and M.V.; writing—review and editing, H.M.-G., M.J., F.A., M.V., and J.T.-P.; supervision, F.A., M.V., and J.T.-P.

Acknowledgments: This study was partially financed by MINECO (CTQ2015-67870-P to F.A., and CTQ2015-68677-R and EUIN2017-88320 to J.T.-P), and the Institute for Research in Biomedicine Barcelona (IRB Barcelona). Helena Martín-Gomez and Judit Tulla-Puche thank MINECO for a Severo Ochoa Predoctoral fellowship and a Ramon y Cajal contract, respectively. Miquel Viñas is a member of the ENABLE consortium. The research of this group has been awarded by the Marató TV3 foundation 2018.

Conflicts of Interest: The authors declare no conflict of interest.

References

1. Rosengren, K.J.; Clark, R.J.; Daly, N.L.; Göransson, U.; Jones, A.; Craik, D.J. Microcin J25 has a threaded sidechain-to-backbone ring structure and not a head-to-tail cyclized backbone. *J. Am. Chem. Soc.* **2003**, *125*, 12464–12474. [CrossRef]
2. Knappe, T.A.; Manzenrieder, F.; Mas-Moruno, C.; Linne, U.; Sasse, F.; Kessler, H.; Xie, X.; Marahiel, M.A. Introducing Lasso Peptides as Molecular Scaffolds for Drug Design: Engineering of an Integrin Antagonist. *Angew. Chem. Int. Ed.* **2011**, *50*, 8714–8717. [CrossRef]
3. Hegemann, J.D.; De Simone, M.; Zimmermann, M.; Knappe, T.A.; Xie, X.; Di Leva, F.S.; Marinelli, L.; Novellino, E.; Zahler, S.; Kessler, H.; et al. Rational improvement of the affinity and selectivity of integrin binding of grafted lasso peptides. *J. Med. Chem.* **2014**, *57*, 5829–5834. [CrossRef]

4. Salomón, R.A.; Fariás, R.N. Microcin 25, a novel antimicrobial peptide produced by *Escherichia coli*. *J. Bacteriol.* **1992**, *174*, 7428–7435. [[CrossRef](#)]
5. Blond, A.; Péduzzi, J.; Goulard, C.; Chiuchiolo, M.J.; Barthélémy, M.; Prigent, Y.; Salomón, R.A.; Fariás, R.N.; Moreno, F.; Rebuffat, S. The cyclic structure of microcin J25, a 21-residue peptide antibiotic from *Escherichia coli*. *Eur. J. Biochem.* **1999**, *259*, 747–755. [[CrossRef](#)]
6. Delgado, M.A.; Rintoul, M.R.; Fariás, R.N.; Salomon, R.A. *Escherichia coli* RNA Polymerase Is the Target of the Cyclopeptide Antibiotic Microcin J25. *J. Bacteriol.* **2001**, *183*, 4543–4550. [[CrossRef](#)]
7. Selsted, M.E.; Novotny, M.J.; Morris, W.L.; Tang, Y.Q.; Smith, W.; Cullor, J.S. Indolicidin, a novel bactericidal tridecapeptide amide from neutrophils. *J. Biol. Chem.* **1992**, *267*, 4292–4295. [[PubMed](#)]
8. Turner, J.; Cho, Y.; Dinh, N.-N.; Waring, A.J.; Lehrer, R.I. Activities of LL-37, a Cathelin-Associated Antimicrobial Peptide of Human Neutrophils. *Antimicrob. Agents Chemother.* **1998**, *42*, 2206–2214. [[CrossRef](#)] [[PubMed](#)]
9. Xhindoli, D.; Pacor, S.; Benincasa, M.; Scocchi, M.; Gennaro, R.; Tossi, A. The human cathelicidin LL-37—A pore-forming antibacterial peptide and host-cell modulator. *Biochim. Biophys. Acta—Biomembr.* **2016**, *1858*, 546–566. [[CrossRef](#)] [[PubMed](#)]
10. Falla, T.J.; Karunaratne, D.N.; Hancock, R.E.W. Mode of Action of the Antimicrobial Peptide Indolicidin. *J. Biol. Chem.* **1996**, *271*, 19298–19303. [[CrossRef](#)] [[PubMed](#)]
11. Rintoul, M.R.; De Arcuri, B.F.; Salomón, R.A.; Fariás, R.N.; Morero, R.D. The antibacterial action of microcin J25: Evidence for disruption of cytoplasmic membrane energization in *Salmonella* Newport. *FEMS Microbiol. Lett.* **2001**, *204*, 265–270. [[CrossRef](#)] [[PubMed](#)]
12. Vincent, P.A.; Bellomio, A.; De Arcuri, B.F.; Fariás, R.N.; Morero, R.D. MccJ25 C-terminal is involved in RNA-polymerase inhibition but not in respiration inhibition. *Biochem. Biophys. Res. Commun.* **2005**, *331*, 549–551. [[CrossRef](#)] [[PubMed](#)]
13. Mukhopadhyay, J.; Sineva, E.; Knight, J.; Levy, R.M.; Ebright, R.H. Antibacterial peptide Microcin J25 inhibits transcription by binding within and obstructing the RNA polymerase secondary channel. *Mol. Cell* **2004**, *14*, 739–751. [[CrossRef](#)] [[PubMed](#)]
14. Bellomio, A.; Vincent, P.A.; De Arcuri, B.F.; Fariás, R.N.; Morero, R.D. Microcin J25 has dual and independent mechanisms of action in *Escherichia coli*: RNA polymerase inhibition and increased superoxide production. *J. Bacteriol.* **2007**, *189*, 4180–4186. [[CrossRef](#)]
15. Bonhivers, M.; Plançon, L.; Ghazi, A.; Boulanger, P.; Le Maire, M.; Lambert, O.; Rigaud, J.L.; Letellier, L. FhuA, an *Escherichia coli* outer membrane protein with a dual function of transporter and channel which mediates the transport of phage DNA. *Biochimie* **1998**, *80*, 363–369. [[CrossRef](#)]
16. Destoumieux-Garzón, D.; Duquesne, S.; Peduzzi, J.; Goulard, C.; Desmadril, M.; Letellier, L.; Rebuffat, S.; Boulanger, P. The iron-siderophore transporter FhuA is the receptor for the antimicrobial peptide microcin J25: Role of the microcin Val11–Pro16 β -hairpin region in the recognition mechanism. *Biochem. J.* **2005**, *389*, 869–876. [[CrossRef](#)]
17. Salomon, R.A.; Fariás, R.N. The fhuA protein is involved in microcin 25 uptake. *J. Bacteriol.* **1993**, *175*, 7741–7742. [[CrossRef](#)]
18. Bellomio, A.; Vincent, P.A.; de Arcuri, B.F.; Salomón, R.A.; Morero, R.D.; Fariás, R.N. The microcin J25 β -hairpin region is important for antibiotic uptake but not for RNA polymerase and respiration inhibition. *Biochem. Biophys. Res. Commun.* **2004**, *325*, 1454–1458. [[CrossRef](#)]
19. Pavlova, O.; Mukhopadhyay, J.; Sineva, E.; Ebright, R.H.; Severinov, K. Systematic structure-activity analysis of microcin J25. *J. Biol. Chem.* **2008**, *283*, 25589–25595. [[CrossRef](#)]
20. Knappe, T.A.; Linne, U.; Zirah, S.; Rebuffat, S.; Xie, X.; Marahiel, M.A. Isolation and structural characterization of capistruin, a lasso peptide predicted from the genome sequence of *Burkholderia thailandensis* E264. *J. Am. Chem. Soc.* **2008**, *130*, 11446–11454. [[CrossRef](#)]
21. Rudilla, H.; Fusté, E.; Cajal, Y.; Rabanal, F.; Vinuesa, T.; Viñas, M. Synergistic antipseudomonal effects of synthetic peptide AMP38 and carbapenems. *Molecules* **2016**, *21*, 1223. [[CrossRef](#)] [[PubMed](#)]
22. Ducasse, R.; Yan, K.P.; Goulard, C.; Blond, A.; Li, Y.; Lescop, E.; Guittet, E.; Rebuffat, S.; Zirah, S. Sequence determinants governing the topology and biological activity of a lasso peptide, microcin J25. *ChemBioChem* **2012**, *13*, 371–380. [[CrossRef](#)] [[PubMed](#)]

23. Rosengren, K.J.; Blond, A.; Afonso, C.; Tabet, J.C.; Rebuffat, S.; Craik, D.J. Structure of Thermolysin Cleaved Microcin J25: Extreme Stability of a Two-Chain Antimicrobial Peptide Devoid of Covalent Links. *Biochemistry* **2004**, *43*, 4696–4702. [CrossRef] [PubMed]
24. Wilson, K.-A.A.; Kalkum, M.; Ottesen, J.; Yuzenkova, J.; Chait, B.T.; Landick, R.; Muir, T.; Severinov, K.; Darst, S.A. Structure of microcin J25, a peptide inhibitor of bacterial RNA polymerase, is a lassoed tail. *J. Am. Chem. Soc.* **2003**, *125*, 12475–12483. [CrossRef]
25. Blond, A.; Cheminant, M.; Destoumieux-Garzón, D.; Ségalas-Milazzo, I.; Peduzzi, J.; Goulard, C.; Rebuffat, S. Thermolysin-linearized microcin J25 retains the structured core of the native macrocyclic peptide and displays antimicrobial activity. *Eur. J. Biochem.* **2002**, *269*, 6212–6222. [CrossRef]
26. Fouque, K.J.D.; Lavanant, H.; Zirah, S.; Hegemann, J.D.; Zimmermann, M.; Marahiel, M.A.; Rebuffat, S.; Afonso, C. Signatures of Mechanically Interlocked Topology of Lasso Peptides by Ion Mobility–Mass Spectrometry: Lessons from a Collection of Representatives. *J. Am. Soc. Mass Spectrom.* **2017**, *28*, 315–322. [CrossRef]
27. Jeanne Dit Fouque, K.; Afonso, C.; Zirah, S.; Hegemann, J.D.; Zimmermann, M.; Marahiel, M.A.; Rebuffat, S.; Lavanant, H. Ion mobility-mass spectrometry of lasso peptides: Signature of a rotaxane topology. *Anal. Chem.* **2015**, *87*, 1166–1172. [CrossRef]
28. Blond, A.; Cheminant, M.; Ségalas-Milazzo, I.; Péduzzi, J.; Barthélémy, M.; Goulard, C.; Salomón, R.; Moreno, F.; Farías, R.; Rebuffat, S. Solution structure of microcin J25, the single macrocyclic antimicrobial peptide from *Escherichia coli*. *Eur. J. Biochem.* **2001**, *268*, 2124–2133. [CrossRef]
29. Soudy, R.; Wang, L.; Kaur, K. Synthetic peptides derived from the sequence of a lasso peptide microcin J25 show antibacterial activity. *Bioorganic Med. Chem.* **2012**, *20*, 1794–1800. [CrossRef]
30. Woody, R.W. Aromatic side-chain contributions to the far ultraviolet circular dichroism of peptides and proteins. *Biopolymers* **1978**, *17*, 1451–1467. [CrossRef]
31. Bayro, M.J.; Mukhopadhyay, J.; Swapna, G.V.T.; Huang, J.Y.; Ma, L.C.; Sineva, E.; Dawson, P.E.; Montelione, G.T.; Ebricht, R.H. Structure of antibacterial peptide microcin J25: A 21-residue lariat protoknot. *J. Am. Chem. Soc.* **2003**, *125*, 12382–12383. [CrossRef] [PubMed]
32. Wishart, D.S.; Bigam, C.G.; Holm, A.; Hodges, R.S.; Sykes, B.D. ^1H , ^{13}C and ^{15}N random coil NMR chemical shifts of the common amino acids. I. Investigations of nearest-neighbor effects. *J. Biomol. NMR* **1995**, *5*, 67–81. [CrossRef] [PubMed]
33. Watts, K.S.; Dalal, P.; Tebben, A.J.; Cheney, D.L.; Shelley, J.C. Macrocycle Conformational Sampling with MacroModel. *J. Chem. Inf. Model.* **2014**, *54*, 2680–2696. [CrossRef]
34. Semenova, E.; Yuzenkova, Y.; Peduzzi, J.; Rebuffat, S.; Severinov, K. Structure-activity analysis of microcin J25: Distinct parts of the threaded lasso molecule are responsible for interaction with bacterial RNA polymerase. *J. Bacteriol.* **2005**, *187*, 3859–3863. [CrossRef] [PubMed]
35. Socias, S.B.; Severinov, K.; Salomon, R.A. The Ile13 residue of microcin J25 is essential for recognition by the receptor FhuA, but not by the inner membrane transporter SbmA. *FEMS Microbiol. Lett.* **2009**, *301*, 124–129. [CrossRef] [PubMed]
36. Sierra, J.M.; Fusté, E.; Rabanal, F.; Vinuesa, T.; Viñas, M. An overview of antimicrobial peptides and the latest advances in their development. *Expert Opin. Biol. Ther.* **2017**, *17*, 663–676. [CrossRef]
37. Committee, T.E.; Testing, A.S.; Changes, N.; Pseudomonas, E. European Committee on Antimicrobial Susceptibility Testing Breakpoint Tables for Interpretation of MICs and Zone Diameters European Committee on Antimicrobial Susceptibility Testing Breakpoint Tables for Interpretation of MICs and Zone Diameters 0–77. Available online: http://www.eucast.org/fileadmin/src/media/PDFs/EUCAST_files/Breakpoint_tables/v_6.0_Breakpoint_table.pdf (accessed on 12 January 2018).
38. Odds, F.C. Synergy, antagonism, and what the checkerboard puts between them. *J. Antimicrob. Chemother.* **2003**, *52*, 1. [CrossRef]
39. Moskowitz, S.M.; Foster, J.M.; Emerson, J.; Burns, J.L. Clinically feasible biofilm susceptibility assay for isolates of *Pseudomonas aeruginosa* from patients with cystic fibrosis. *J. Clin. Microbiol.* **2004**, *42*, 1915–1922. [CrossRef]



3.2. ARTICLE 2

ARTICLE 2: Multicomponent Reactions Upon the Known Drug Trimethoprim as a Source of Novel Antimicrobial Agents.

Pedrola M*, **Jorba M***, Jardas E, Jordi F, Ghashghaei O, Viñas M, Lavilla R.

Frontiers in Chemistry 2019

Addressed objectives in this article:

2. Trimethoprim

2.1. Study of the antimicrobial activity of the Trimethoprim derivatives

- 2.1.1. Determination of their antimicrobial effect on planktonic bacteria
- 2.1.2. Exploration of their antimicrobial synergistic effect in combination with Sulfamethoxazole

The microbiological part of the supplementary material of this article is also included.



Multicomponent Reactions Upon the Known Drug Trimethoprim as a Source of Novel Antimicrobial Agents

Marina Pedrola^{1†}, Marta Jorba^{2,3†}, Eda Jardas¹, Ferran Jordi¹, Ouldouz Ghashghaei¹, Miguel Viñas^{2,3*} and Rodolfo Lavilla^{1*}

¹ Laboratory of Medicinal Chemistry, Faculty of Pharmacy and Food Sciences and Institute of Biomedicine (IBUB), University of Barcelona, Barcelona, Spain, ² Laboratory of Molecular Microbiology & Antimicrobials, Department of Pathology & Experimental Therapeutics, Medical School, Hospitalet de Llobregat, University of Barcelona, Barcelona, Spain, ³ Bellvitge Institute for Biomedical Research (IDIBELL), Barcelona, Spain

OPEN ACCESS

Edited by:

Jonathan G. Rudick,
Stony Brook University, United States

Reviewed by:

Jean-François Brière,
UMR6014 Chimie Organique,
Bioorganique Réactivité et Analyse
(COBRA), France

Andrea Trabocchi,
University of Florence, Italy

Fabio De Moliner,
University of Edinburgh,
United Kingdom

*Correspondence:

Miguel Viñas
mvinyas@ub.edu
Rodolfo Lavilla
rlavilla@ub.edu

[†] These authors have contributed
equally to this work

Specialty section:

This article was submitted to
Organic Chemistry,
a section of the journal
Frontiers in Chemistry

Received: 04 April 2019

Accepted: 20 June 2019

Published: 04 July 2019

Citation:

Pedrola M, Jorba M, Jardas E, Jordi F,
Ghashghaei O, Viñas M and Lavilla R
(2019) Multicomponent Reactions
Upon the Known Drug Trimethoprim
as a Source of Novel Antimicrobial
Agents. *Front. Chem.* 7:475.
doi: 10.3389/fchem.2019.00475

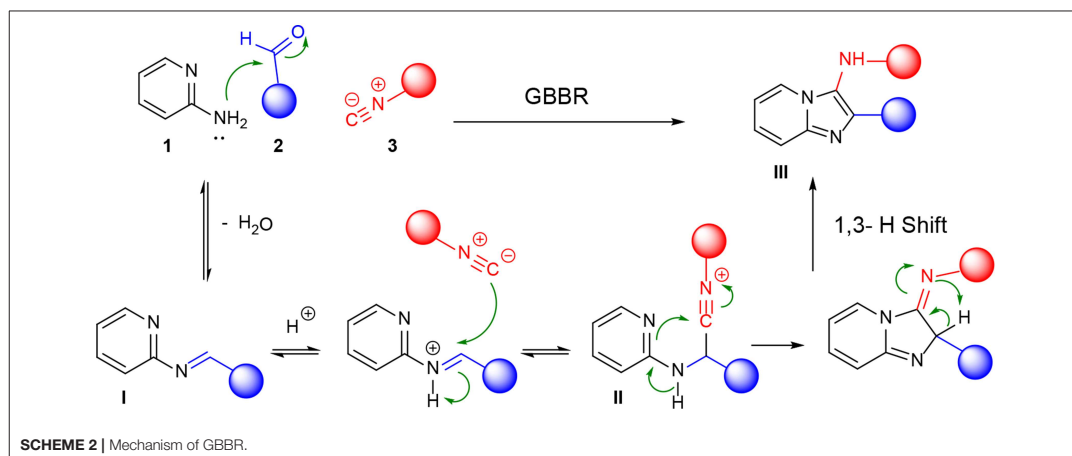
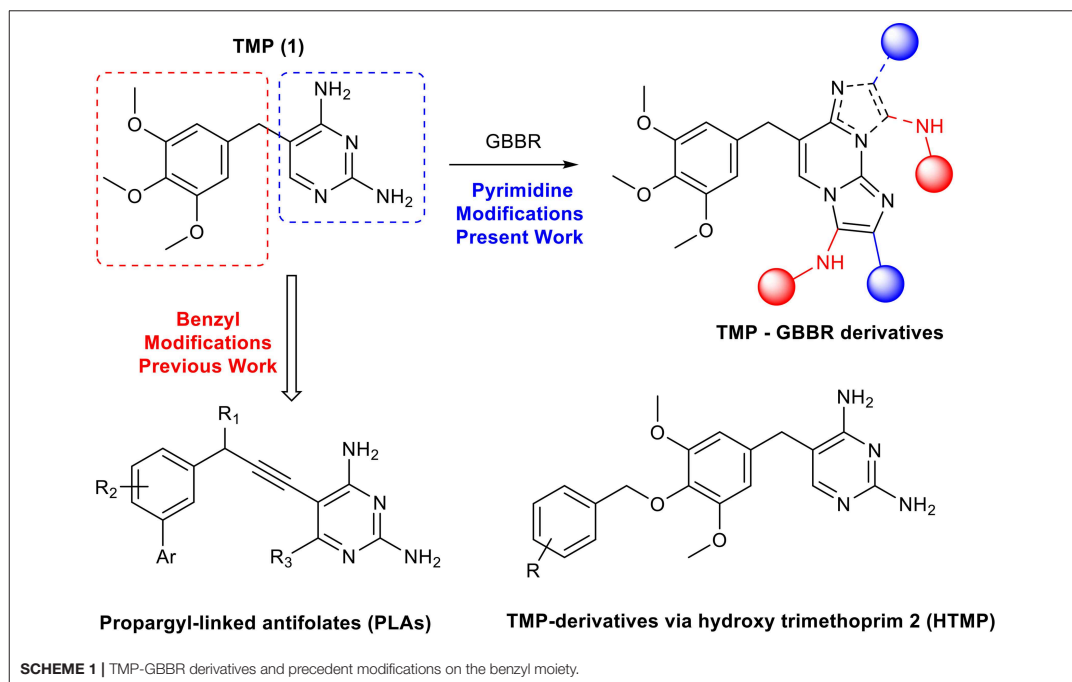
Novel antibiotic compounds have been prepared through a selective multicomponent reaction upon the known drug Trimethoprim. The Groebke-Blackburn-Bienaymé reaction involving this α -aminoazine, with a range of aldehydes and isocyanides afforded the desired adducts in one-step. The analogs display meaningful structural features of the initial drug together with relevant modifications at several points, keeping antibiotic potency and showing satisfactory antimicrobial profile (good activity levels and reduced growth rates), especially against methicillin-resistant *Staphylococcus aureus*. The new products may open new possibilities to fight bacterial infections.

Keywords: antibiotics, drugs, isocyanides, multicomponent reactions, resistant bacteria

INTRODUCTION

Trimethoprim (TMP, **1**, **Figure 1A**) is a well-known antibiotic, present in the *Model List of Essential Medicines* from the World Health Organization. TMP is usually used in combination with Sulfamethoxazole (SMX) to treat lower urinary tract infections and acute invasive diarrhea/bacterial dysentery as first and second choice, respectively (WHO, 2017), respiratory infections in cystic fibrosis patients caused by *Staphylococcus aureus*, among other many infections. Lately, it has also been used for preventing infections from the opportunistic pathogen *Pneumocystis carinii* (Urbancic et al., 2018), which normally causes pneumonia in patients with AIDS. Both drugs act on the folic acid biosynthetic route by inhibiting two enzymes: dihydrofolate reductase (DHFR) and dihydropteroate synthetase, respectively. Folate needs to be synthesized by bacteria and it is crucial in the biosynthetic pathway of thymidine, essential in DNA synthesis. Hence, when used in combination, these antibiotics display a synergistic effect in inhibiting bacterial growth and leading to eventual cell death (**Figure 1B**) (Torok et al., 2009; Katzung et al., 2012).

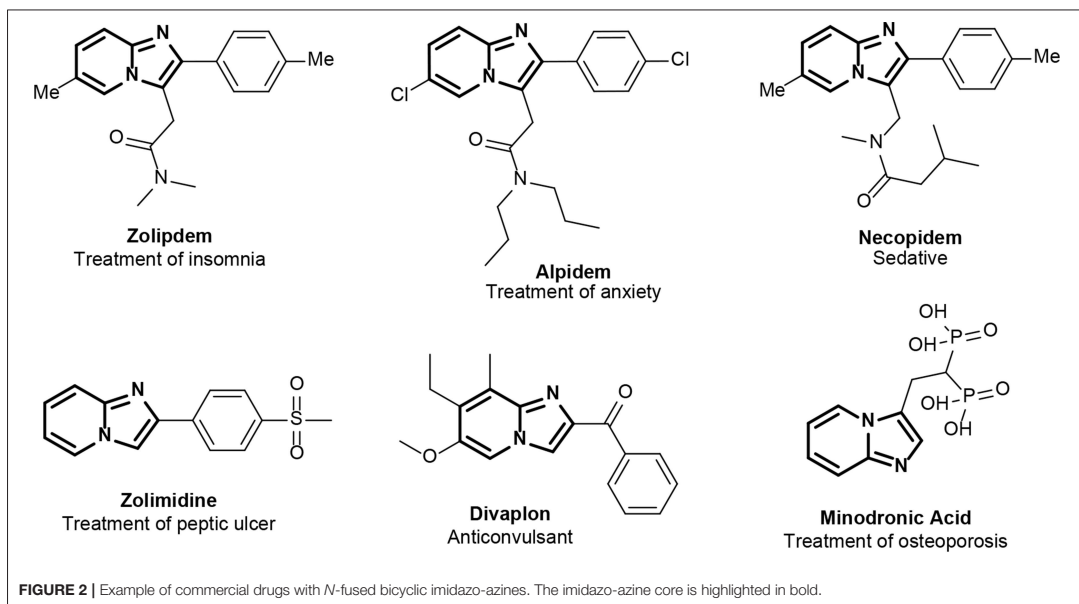
The combination of sulfonamides and DHFR inhibitors has been clinically used since 1968 when it was first approved in the UK (Cody et al., 2008; Torok et al., 2009). Unfortunately, resistance emerged soon and has become widespread (Huovinen et al., 1995; Ventola, 2015). Nowadays, antibiotic resistance is one of the world's most pressing public health problems with high morbidity and mortality rates (Centers for Disease Control and Prevention, 2017). Furthermore, finding active drugs to fight both multidrug resistant infections and organisms is becoming extremely challenging, as is often the case of methicillin-resistant *Staphylococcus aureus* (MRSA) and multidrug resistant *Pseudomonas aeruginosa*. In this context, the co-therapy with TMP and SMX turns out to be



Minodronic acid (approved for treatments of insomnia, anxiety, peptic ulcers, epilepsy, osteoporosis, etc.) (Figure 2). It is also well-known that α -polyamino-polyazines are important aromatic polyheterocycles present in a wide variety of clinical drugs, such as the antibacterial drug Trimethoprim, the anticonvulsant drug Lamotrigine and the anticancer drug Methotrexate. Furthermore, specific GBBR adducts have been identified as

active antibiotics through phenotypic analyses, addressing a variety of targets (Al-Tel and Al-Qawasmeh, 2010; Shukla et al., 2012; Semreen et al., 2013; Kumar et al., 2014). These facts back our project to modify TMP via GBBR processes to deliver potentially useful novel antibiotics, either improving the activity of the original drug upon DHFR or acting through independent mechanisms.

Outer membrane: a key obstacle for new antimicrobial agents



RESULTS AND DISCUSSION

Chemical Synthesis

In this context, we planned to develop a series of TMP derivatives through the GBBR by interaction of the original drug (TMP, **1**) with a range of aldehydes (**2**) and isocyanides (**3**), and analyse the resulting MCR adducts as novel antibiotics, determining their potency, and efficiency, also considering their potential impact on resistant bacteria (**Scheme 3**).

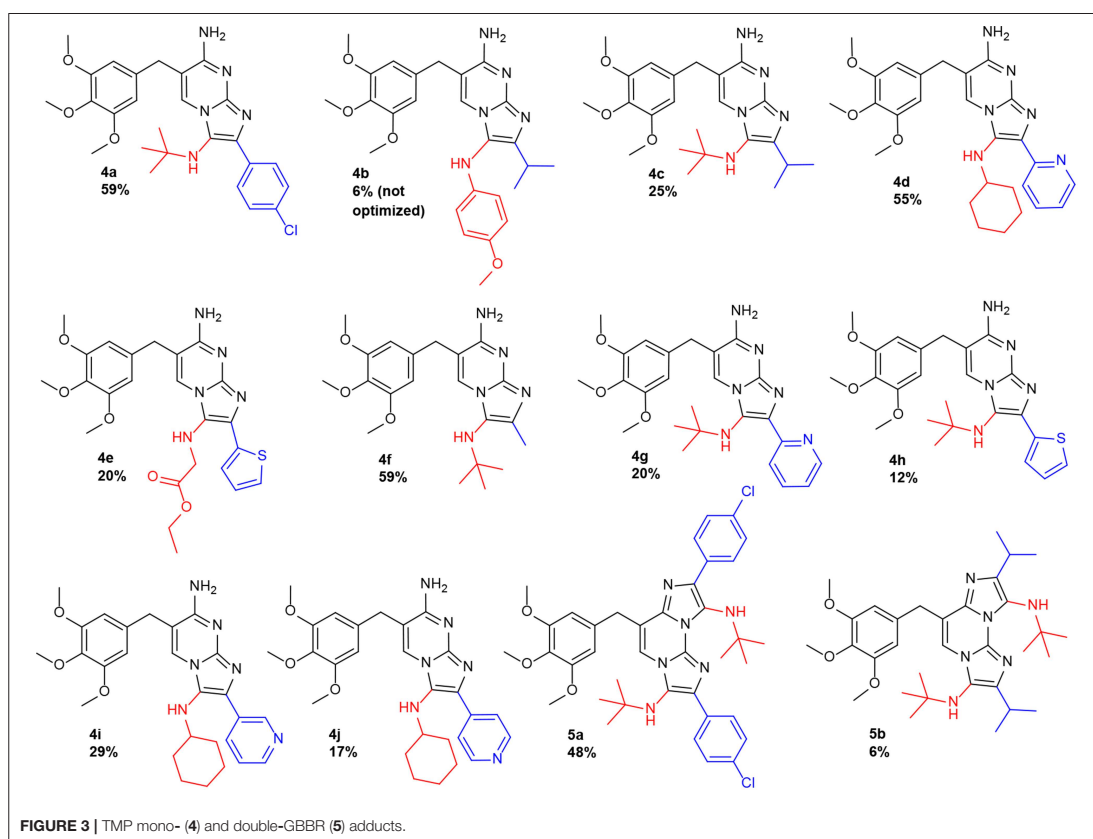
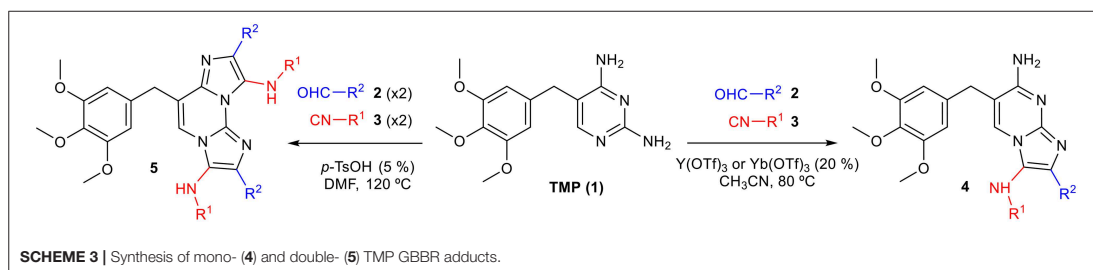
The chemical modifications on TMP are based in our recent discoveries on GBBRs upon diaminopyrimidines, involving selective and multiple MCRs (Ghashghaei et al., 2018). In this way, the preparation of TMP analogs consisted in a regioselective mono-GBBR with an aldehyde/isocyanide pair, to yield derivatives **4**; it is worth mentioning that a kinetic control justifies the preferential formation of the observed isomer. Furthermore, double GBBR processes upon TMP yield doubly substituted derivatives **5**, with two equivalents of each reactant class (**Scheme 3**). The participation of a variety of Lewis acids catalyst is required to suitably generate and activate the imine intermediate and to achieve a moderate yield. In addition, standard flash chromatography purification was normally needed to afford the pure product. The designed analogs featured the *N*-fused bicyclic imidazo-azine scaffolds from the TMP reactant and displayed the variability points at substituents R^1 , derived from the isocyanide input (**3**) and R^2 arising from the aldehyde reactant (**2**).

The processes worked in our TMP system as expected, yielding the corresponding products, showing the same reactivity and selectivity trends that were described in the unsubstituted

diaminopyrimidine studies (Ghashghaei et al., 2018). For the initial screening, we prepared a series of TMP analogs featuring a variety of substituents on the imidazole amino group (R^1 , being *tert*-butyl, 4-methoxyphenyl, cyclohexyl, and ethoxycarbonylmethyl) whereas at its carbon position a range of aromatic or alkyl substituents were introduced (R^2 being 4-chlorophenyl, α -, β -, or γ -pyridinyl, α -thienyl, methyl, and isopropyl). All the reactions were successful, yielding the mono-GBBR derivatives **4** and the doubly substituted-GBBR adducts **5** in acceptable yields (unoptimized). In this way, 12 new products (**4a-4j** and **5a-b**) arising from the corresponding aldehyde/isocyanide combinations were suitably prepared as pure materials (**Figure 3**).

The connectivity of the first analog synthesized (**4a**) was assigned through two-dimensional NMR experiments: HSQC, HMBC and NOESY spectra (see **Supplementary Material**) and matched with the expected structure, displaying the regioselectivity previously described (Ghashghaei et al., 2018). The rest of derivatives showed the same spectroscopical trends and their structures were assigned by analogy. Furthermore, the doubly substituted GBBR adducts **5** synthetically derived from the corresponding precursors **4**, then securing their identity.

We planned to incorporate an unsubstituted amino group in the imidazole ring of the novel derivatives **4** and **5** in order to favor their recognition by the DHFR active site, in line with the natural substrate. Then, we tackled the preparation of such compounds through the acidic removal of a *tert*-butyl group from a suitable precursor adduct coming from MCRs involving *tert*-butyl isocyanide. Precedent work by Krasavin et al. (2008) demonstrated that this transformation is feasible in GBBR



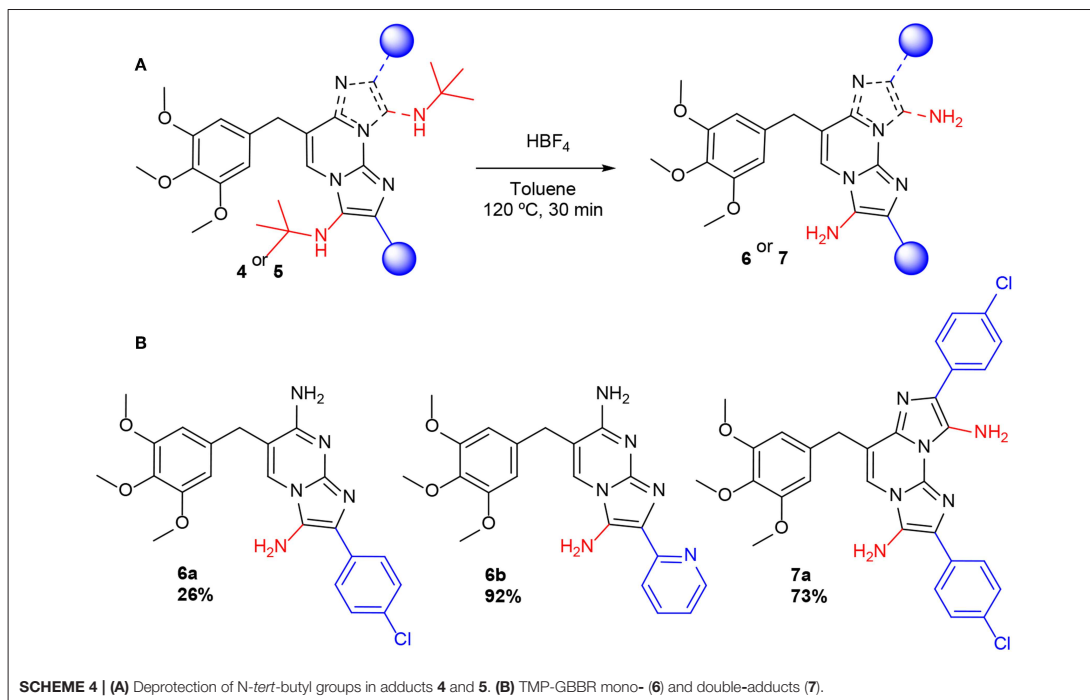
adducts. In this way, compounds **6a-6b** and **7a** were obtained as pure unsubstituted amino derivatives from *tert*-butyl precursors **4** and **5**, after HBF₄ treatment (Scheme 4). All the synthesized compounds were suitably obtained in pure form, characterized and forwarded to microbiological analyses.

Biological Analyses

The Minimum Inhibitory Concentration (MIC) values of the 15 TMP analogs against control strains are shown in Table 1

(for details, see the **Supplementary Material**). Although all the compounds showed MIC values against *E. coli* ATCC 25922 and *S. aureus* ATCC 29213 higher than TMP, some of them were almost as potent as TMP (**4c**, **4f**, **4h**, **4i**, **4j** and **6a**). *P. aeruginosa* PAO1 was found to be fully resistant to TMP, as well as to all new compounds. A preliminary inspection of the results showed that double GBBR adducts **5** lacked activity, probably meaning that they were unsuitable for binding to the target sites. Whereas for derivatives **4** some combinations were unproductive

Outer membrane: a key obstacle for new antimicrobial agents



(especially the ones with aromatic and acetate R¹ substituents and *p*-chlorophenyl group at R² position), those featuring *tert*-butyl groups at R¹ and isopropyl, methyl, β-, γ- (but not α-) pyridyl, and α-thienyl groups at R² were particularly favored. Moreover, comparing compounds 4d, 4g and 6b, we are able to confirm that the reduction of R¹ substituents size allowed to decrease the MIC. It is also worthy to emphasize that all compounds resulted to be more active on *E. coli* than on *S. aureus*; 4i, 4c, and 4f being the most potent ones. Thus, chemical modifications do not seem to limit the ability of the different new compounds to penetrate the outer membrane in Gram negative bacteria.

Almost all the new compounds acted synergistically with SMX as the control drug TMP did, against *E. coli* ATCC 25922 and *S. aureus* ATCC 29213 (Table 2); the latter species being much more sensitive to the SMX combination than to the treatment with the TMP-GBBR analogs alone. It also becomes apparent that nearly all the new compounds presented high activity against a set of clinical isolates of MRSA isolated from hospitalized or Cystic fibrosis (CF) patients. In CF patients, *Staphylococcus aureus* (and particularly MRSA) infection is the main challenge of antibiotic therapy, since the persistent infection caused by this bacterium is strongly associated with increased rates of decline in respiratory function and high mortality (Dolce et al., 2019). Thus, new approaches to fight this kind of bacterium are mandatory and should be based on new antimicrobials, most

probably combined with conventional ones (Lo et al., 2018; Xhemali et al., 2019).

Again, derivatives 4c, 4f, 4h, 4i, 4j, and 6b were the most potent, but interestingly, some adducts which were not meaningful acting alone (Table 1), on SMX combination displayed a relevant potency (4a, 4d, 4e, 4g, and 6a). Disappointingly, no effect either of adducts alone or in combination with SMX was observed on *Pseudomonas aeruginosa* in any case, in line with the detected TMP activity. Particularly interesting are the activities against MRSA isolates as can be seen in Table 2, with many derivatives being as active as the TMP reference.

A relevant feature in the use of an antibiotic is its kinetic profile. Specifically, a fast reduction of the growth rates of the infective microorganism is of capital interest in therapeutics, arguably as important or more than the effective dose. Thus, the effect of TMP analogs in combination with SMX on the growth curves of *E. coli* ATCC 25922 and *S. aureus* ATCC 29213 was studied for the most interesting compounds (Figure 4 and Supplementary Material). Some differences were observed at subinhibitory concentrations of the antimicrobials (1/2 MIC and 1/4 MIC). In both tested bacteria, full inhibition occurred for derivatives 4g and 4i with SMX (1:20) at 1/2 the MIC value (Figures 4A,C,D). On the other hand, compounds 4g and 4f, at a concentration of 1/4 MIC, gave similar results than

TMP at 1/2 MIC against *E. coli* ATCC 25922 (Figures 4A,B). In all the cases, significant reductions in the growth rates were observed when compared with the antimicrobial-free control, being comparatively better for some conditions than

the TMP reference, especially compound **4i** for long culture times (Figure 4D).

CONCLUSION

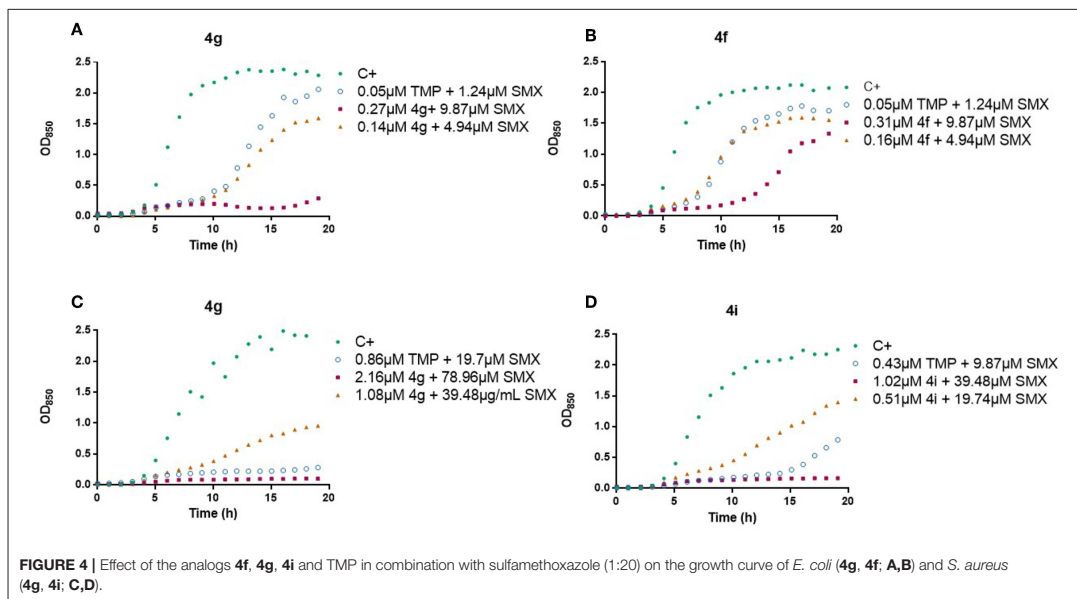
The marketed antibiotic TMP (**1**) has been successfully modified by a GBB MCR with a range of commercially available aldehydes and isocyanides in selective processes yielding mono- or double- imidazo-azine adducts **4** and **5**. A short synthetic (one or two steps) protocol allowed access to a focused library of 15 TMP analogs featuring a novel heterocyclic scaffold with a relevant degree of chemical diversity at selected positions, including hydrogen atoms, small alkyl groups, aromatic and heteroaromatic rings. Incidentally, this work shows the possibility of using known drugs as substrates for MCRs and, in this manner, opens new ways to develop novel chemical entities of biological interest from this unusual origin. Antimicrobial activity of the novel analogs has been assayed in Grampositive (*S. aureus*) and Gramnegative (*E. coli*) microorganisms as well as on a bacterium considered the paradigm of resistance (*P. aeruginosa*). Despite the latter was resistant to all the new compounds, several mono-adducts **4** displayed MICs in the micromolar range against *E. coli* and *S. aureus*, what make us think that the TMP-derivatives bind to DHFR as well. The observed impact on growth kinetics allows us to conclude that the association of these new products with SMX exert a very similar effect than TMP itself. It is worthy to emphasize the excellent activities detected against MRSA strains. Given the reduced size of the focused chemset analyzed, and the relevant results found, we can conclude that the novel scaffold synthesized has potential to become a source for novel antibiotics. Further on going studies along these

TABLE 1 | Minimum Inhibitory Concentration (MIC, μM) of TMP and the new GBBR analogs against *E. coli* ATCC 25922, *S. aureus* ATCC 29213, and *P. aeruginosa* PAO1.

| | MIC (μM) | | |
|--------------|------------------------------|-----------------------------|---------------------------|
| | <i>E. coli</i> ATCC 25922 | <i>S. aureus</i> ATCC 29213 | <i>P. aeruginosa</i> PAO1 |
| TMP 1 | 0.43 | 13.78 | > 110.22 |
| 4a | 16.13 | > 64.52 | > 64.52 |
| 4b | > 67.01 | > 67.01 | > 67.01 |
| 4c | 1.17 | 18.71 | > 74.85 |
| 4d | 8.19 | > 65.50 | > 65.50 |
| 4e | 5.19 | > 83.07 | > 83.07 |
| 4f | 1.25 | 80.10 | > 80.10 |
| 4g | 17.30 | > 69.18 | > 69.18 |
| 4h | 2.14 | > 68.44 | > 68.44 |
| 4i | 1.02 | 65.50 | > 65.50 |
| 4j | 2.05 | 65.50 | > 65.50 |
| 5a | > 45.60 | > 45.60 | > 45.60 |
| 5b | > 56.66 | > 56.66 | > 56.66 |
| 6a | 4.55 | > 72.75 | > 72.75 |
| 6b | 2.46 | 78.73 | > 78.73 |
| 7a | > 54.29 | > 54.29 | > 54.29 |

TABLE 2 | Minimum Inhibitory Concentration (MIC, μM) of TMP and the new GBBR analogs in combination with Sulfamethoxazole (1:20) against *E. coli* ATCC 25922, *S. aureus* ATCC 29213, *P. aeruginosa* PAO1, *S. aureus* 8125304770, *S. aureus* 8139265926, *S. aureus* 8125255044, and *S. aureus* 8124825998.

| | MIC (μM) | | | | | | |
|--------------|------------------------------|--------------------------------|------------------------------|--------------------------------|--------------------------------|--------------------------------|--------------------------------|
| | <i>E. coli</i> ATCC 25922 | <i>S. aureus</i> ATCC 29213 | <i>P. aeruginosa</i> PAO1 | <i>S. aureus</i> 8125304770 | <i>S. aureus</i> 8139265926 | <i>S. aureus</i> 8125255044 | <i>S. aureus</i> 8124825998 |
| TMP 1 | 0.11 | 0.43 | 13.78 | 0.431 | 0.86 | 0.22 | 0.43 |
| 4a | 2.02 | 8.06 | > 64.52 | 4.03 | 8.06 | 1.01 | 4.03 |
| 4b | 67.01 | > 67.01 | > 67.01 | 67.01 | > 67.01 | 67.01 | > 67.00 |
| 4c | 1.17 | 4.88 | 37.42 | 4.68 | 9.36 | 0.292 | 1.17 |
| 4d | 2.05 | 4.09 | > 65.50 | 4.09 | 4.093 | 1.02 | 4.09 |
| 4e | 1.30 | 5.19 | > 83.07 | 1.298 | 2.60 | 0.65 | 1.30 |
| 4f | 0.63 | 5.01 | 40.05 | 0.63 | 2.50 | 0.63 | 1.25 |
| 4g | 0.54 | 4.32 | > 69.18 | 2.16 | 8.65 | 1.08 | 4.32 |
| 4h | 0.27 | 2.14 | 34.22 | 1.07 | 1.07 | 0.27 | 1.07 |
| 4i | 0.13 | 2.05 | 32.75 | 0.51 | 1.02 | 0.51 | 1.02 |
| 4j | 0.26 | 2.05 | 32.75 | 1.02 | 2.05 | 0.51 | 1.02 |
| 5a | > 45.60 | > 45.60 | > 45.60 | > 45.60 | > 45.60 | > 45.60 | > 45.60 |
| 5b | 28.33 | > 56.66 | > 56.66 | 28.331 | > 56.66 | 14.17 | 56.66 |
| 6a | 2.27 | 9.09 | > 72.75 | 2.27 | 4.55 | 1.14 | 4.55 |
| 6b | 0.31 | 2.46 | 78.73 | 1.23 | 2.46 | 0.62 | 2.46 |
| 7a | > 54.29 | > 54.29 | > 54.29 | > 54.9 | > 54.29 | > 54.29 | > 54.29 |



lines tackle toxicity, the mechanism of action and bacterial resistance issues.

DATA AVAILABILITY

All datasets generated for this study are included in the manuscript and/or the **Supplementary Files**.

AUTHOR CONTRIBUTIONS

MP was responsible for designing and performing the initial experiments. EJ, FJ, OG, and RL performed the rest of the experimentation of the chemical section and analyzed the results. MJ designed and performed the microbiological experiments. MJ and MV analyzed the results of this section. All authors discussed the whole project and wrote the publication.

FUNDING

Financial support from the Ministerio de Economía y Competitividad-Spain (MINECO, CTQ2015-67870-P) and

REFERENCES

- Akritisoulou-Zanze, I., and Djuric, S. W. (2010). "Applications of MCR-derived heterocycles in drug discovery," in *Topics in Heterocyclic Chemistry*, eds. B. U. W. Maes, R. V. A. Orru, and E. Ruijter (Berlin: Springer), 231–287. doi: 10.1007/7081_2010_46
- Al-Tel, T. H., and Al-Qawasmeh, R. A. (2010). Post Groebke-Blackburn multicomponent protocol: synthesis of new polyfunctional imidazo[1,2-a]pyridine and imidazo[1,2-a]pyrimidine derivatives as potential antimicrobial agents. *Eur. J. Med. Chem.* 45, 5848–5855. doi: 10.1016/j.ejmech.2010.09.049
- Bienaymé, H., and Bouzid, K. (1998). A new heterocyclic multicomponent reaction for the combinatorial synthesis of fused 3-aminoimidazoles. *Angew. Chemie Int. Ed.* 37, 2234–2237. doi: 10.1002/(SICI)1521-3773(19980904)37:16<2234::AID-ANIE2234>3.0.CO;2-R
- Blackburn, C., Guan, B., Fleming, P., Shiosaki, K., and Tsai, S. (1998). Parallel synthesis of 3-aminoimidazo[1,2-a]pyridines

Generalitat de Catalunya (2017 SGR 1439) is gratefully acknowledged. The Microbiology group was financed by the Generalitat de Catalunya (GGC2017A-SGR-1488) and Marató TV3 (201C/2018) and its own funding.

ACKNOWLEDGMENTS

We thank Dr. Josep M. Sierra (U. Barcelona, IDIBELL) for useful suggestions and discussions. MV is a member of JIPAMR (Joint Programming Initiative on Antimicrobial Resistance) translocation-transfer and of ENABLE consortia. Clinical strains were kindly supplied by Servei de Microbiologia Hospital Vall d'Hebron (Barcelona).

SUPPLEMENTARY MATERIAL

The Supplementary Material for this article can be found online at: <https://www.frontiersin.org/articles/10.3389/fchem.2019.00475/full#supplementary-material>

- and pyrazines by a new three-component condensation. *Tetrahedron Lett.* 39, 3635–3638. doi: 10.1016/S0040-4039(98)00653-4
- Centers for Disease Control and Prevention (2017). *Facts about Antibiotic Resistance and Antibiotic Prescribing: Attitudes, Behaviors, Trends and Cost*. Available at: <http://www.cdc.gov/getsmart/community/about/fast-facts.html> (accessed March 10, 2019).
- Cernak, T., Dykstra, K. D., Tyagarajan, S., Krskab, P. V., and Shane, W. (2016). The medicinal chemist's toolbox for late stage functionalization of drug-like molecules. *Chem. Soc. Rev.* 45, 456–576. doi: 10.1039/C5CS00628G
- Cody, V., Pace, J., Chisum, K., and Rosowsk, A. (2008). New insights into DHFR interactions: analysis of *Pneumocystis carinii* and mouse DHFR complexes with NADPH and two highly potent 5-x-carboxy(alkoxy) trimethoprim derivatives reveals conformational correlations with activity and novel parallel ring stack. *Proteins* 70, 311–319. doi: 10.1002/prot.21131
- Devi, N., Rawal, R. K., and Singh, V. (2015). Diversity-oriented synthesis of fused-imidazole derivatives via Groebke-Blackburn-Bienaymé reaction: a review. *Tetrahedron* 71, 183–232. doi: 10.1016/j.tet.2014.10.032
- Dolce, D., Neri, S., Grisotto, L., Campana, S., Ravenni, N., Miselli, F., et al. (2019). Methicillin-resistant *Staphylococcus aureus* eradication in cystic fibrosis patients: a randomized multicenter study. *PLoS ONE* 14, 1–15. doi: 10.1371/journal.pone.0213497
- Domling, A., Wang, W., and Wang, K. (2012). Chemistry and biology of multicomponent reactions. *Chem. Rev.* 112, 3083–3135. doi: 10.1021/cr100233r
- Ghashghaei, O., Caputo, S., Sintes, M., Reves, M., Kielland, N., Estarellas, C., et al. (2018). Multiple multicomponent reactions: unexplored substrates, selective processes, and versatile chemotypes in biomedicine. *Chem. Eur. J.* 24, 14513–14521. doi: 10.1002/chem.201802877
- Groebke, K., Weber, L., and Mehlin, F. (1998). Synthesis of imidazo[1,2-a]annulated pyridines, pyrazines and pyrimidines by a novel three-component condensation. *Synlett* 1998, 661–663. doi: 10.1055/s-1998-1721
- Heaslet, H., Harris, M., Fahnoe, K., Sarver, R., Putz, H., Chang, J., et al. (2009). Structural comparison of chromosomal and exogenous dihydrofolate reductase from *Staphylococcus aureus* in complex with the potent inhibitor trimethoprim. *Proteins* 76, 706–717. doi: 10.1002/prot.22383
- Hulme, C. (2005). “Applications of multicomponent reactions in drug discovery—lead generation to process development,” in *Multicomponent Reactions*, eds. J. Zhu and H. Bienaymé (Weinheim: Wiley-VCH), 311–341. doi: 10.1002/3527605118.ch11
- Huovinen, P., Sundstrom, L., Swedberg, G., and Skold, O. (1995). Trimethoprim and sulfonamide resistance. *Antimicrob. Agents Chemother.* 39, 279–289. doi: 10.1128/AAC.39.2.279
- Katzung, B. G., Masters, S. B., and Trevor, A. J. (2012). *Basic and Clinical Pharmacology*. 12th Edn. Oxford; San Francisco, CA: McGraw-Hill.
- Krasavin, M., Tsurulnikov, S., Nikulnikov, M., Sandulenko, Y., and Bukhryakov, K. (2008). Tert-Butyl isocyanide revisited as a convertible reagent in the Groebke-Blackburn reaction. *Tetrahedron Lett.* 49, 7318–7321. doi: 10.1016/j.tetlet.2008.10.046
- Kumar, M., Makhal, B., Gupta, V. K., and Sharma, A. (2014). *In silico* investigation of medicinal spectrum of imidazo-azines from the perspective of multitarget screening against malaria, tuberculosis and chagas disease. *J. Mol. Graph. Model.* 50, 1–9. doi: 10.1016/j.jmgm.2014.02.006
- Lo, D., Muhlebach, M., and Smyth, A. (2018). Interventions for the eradication of methicillin-resistant *Staphylococcus aureus* (MRSA) in people with cystic fibrosis. *Cochrane Database Syst. Rev.* 21, 1–58. doi: 10.1002/14651858.CD009650.pub4
- Lombardo, M. N., G-dayanandan, N., Wright, D. L., and Anderson, A. C. (2016). Crystal structures of trimethoprim-resistant DfrA1 rationalized potent inhibition by Propargyl-linked antifolates. *Infect. Dis.* 2, 149–156. doi: 10.1021/acinfeddis.5b00129
- Pericherla, K., Kaswan, P., Pandey, K., and Kumar, A. (2015). Recent developments in the synthesis of imidazo[1,2-a]pyridines. *Synthesis* 47, 887–912. doi: 10.1055/s-0034-1380182
- Rashid, U., Ahmad, W., Hassan, S. F., Qureshi, N. A., Niaz, B., Muhammad, B., et al. (2016). Design, synthesis, antibacterial activity and docking study of some new trimethoprim derivatives. *Bioorganic Med. Chem. Lett.* 26, 5749–5753. doi: 10.1016/j.bmcl.2016.10.051
- Semreen, M. H., El-Awady, R., Abu-Odeh, R., Saber-Ayad, M., Al-Qawasmeh, R. A., Chouaib, S., et al. (2013). Tandem multicomponent reactions toward the design and synthesis of novel antibacterial and cytotoxic motifs. *Curr. Med. Chem.* 20, 1445–1459. doi: 10.2174/0929867311320110007
- Shaban, S., and Abdel-Wahab, B. F. (2016). Groebke-Blackburn-Bienaymé multicomponent reaction: emerging chemistry for drug discovery. *Mol. Divers.* 20, 233–254. doi: 10.1007/s11030-015-9602-6
- Shukla, N. M., Salunke, D. B., Yoo, E., Mutz, C. A., Balakrishna, R., and David, S. A. (2012). Antibacterial activities of Groebke-Blackburn-Bienaymé-derived imidazo[1,2-a]pyridin-3-amines. *Bioorg. Med. Chem.* 20, 5850–5863. doi: 10.1016/j.bmc.2012.07.052
- Slobbe, P., Ruijter, E., and Orru, R. V. A. (2012). Recent applications of multicomponent reactions in medicinal chemistry. *Med. Chem. Commun.* 3, 1189–1218. doi: 10.1039/c2md20089a
- Torok, E., Moran, E., and Cooke, F. (2009). *Oxford Handbook of Infectious Diseases and Microbiology*. Oxford: Oxford University.
- Urbancic, K. F., Ierino, F., Phillips, E., Mount, P., Mahony, A., and Trubiano, J. (2018). Taking the challenge: a protocolized approach to optimize *Pneumocystis pneumonia* prophylaxis in renal transplant recipients. *Am. J. Transpl.* 18, 462–466. doi: 10.1111/ajt.14498
- Ventola, C. L. (2015). The antibiotic resistance crisis: causes and threats. *Pharm. Ther.* 40, 277–283.
- WHO (2017). *20th WHO Model List of Essential Medicines*. Essential Medicines and Health Products. Available online at: https://www.who.int/medicines/publications/essentialmedicines/20th_EML2017.pdf?ua=1 (accessed March 10, 2019).
- Xhemali, X., Smith, J., Kebraie, R., Rice, S., Stamper, K., Compton, M., et al. (2019). Evaluation of dalbavancin alone and in combination with β -lactam antibiotics against resistant phenotypes of *Staphylococcus aureus*. *J. Antimicrob. Chemother.* 74, 82–86. doi: 10.1093/jac/dky376
- Zarganes-Tzitzikas, T., and Doemling, A. (2014). Modern multicomponent reactions for better drug synthesis. *Org. Chem. Front.* 1, 834–837. doi: 10.1039/C4QO00088A
- Zhou, W., Scocchera, E. W., Wright, D. L., and Anderson, A. C. (2013). Antifolates as effective antimicrobial agents: new generations of trimethoprim analogs. *Med. Chem. Commun.* 4, 908–915. doi: 10.1039/c3md00104k
- Zhu, J., Wang, Q., and Wang, M. (2014). *Multicomponent Reactions in Organic Synthesis*. 1st Edn. Weinheim: Wiley-VCH.

Conflict of Interest Statement: The authors declare that the research was conducted in the absence of any commercial or financial relationships that could be construed as a potential conflict of interest.

The reviewer FD declared a past co-authorship with one with the authors OG, RL to the handling editor.

Copyright © 2019 Pedrola, Jorba, Jardas, Jardi, Ghashghaei, Viñas and Lavilla. This is an open-access article distributed under the terms of the Creative Commons Attribution License (CC BY). The use, distribution or reproduction in other forums is permitted, provided the original author(s) and the copyright owner(s) are credited and that the original publication in this journal is cited, in accordance with accepted academic practice. No use, distribution or reproduction is permitted which does not comply with these terms.



Supplementary Material

Multicomponent Reactions upon the Known Drug Trimethoprim as a Source of Novel Antimicrobial Agents

Marina Pedrola¹, Marta Jorba², Eda Jardas¹, Ferran Jordi¹, Ouldouz Ghashghaei¹, Miguel Viñas² and Rodolfo Lavilla¹

¹Laboratory of Medicinal Chemistry, Faculty of Pharmacy and Food Sciences and Institute of Biomedicine (IBUB), University of Barcelona, Av. de Joan XXIII, 27-31, 08028 Barcelona, Spain

²Laboratory of Molecular Microbiology & Antimicrobials, Dept. Pathology & Experimental Therapeutics. Medical School. University of Barcelona and IDIBELL, Feixa Llarga, s/n. 08907 Hospitalet de Llobregat, Barcelona, Spain

Contents

| | |
|--|----|
| Chemistry | 3 |
| General Information..... | 3 |
| Experimental Procedures for the Synthesis of Trimethoprim GBB Adducts and Related Compounds | 4 |
| Synthesis of Trimethoprim Mono GBBR Adducts | 4 |
| Synthesis of Trimethoprim Double GBBR Adducts..... | 4 |
| The tert-Butyl Removal from Trimethoprim GBBR Adducts | 5 |
| Characterization Data for the Isolated Compounds | 6 |
| Copies of the NMR Spectra | 11 |
| Microbiology | 28 |
| Material and Methods | 28 |
| Bacterial strains, bacteriological media and antimicrobials..... | 28 |
| Susceptibility testing..... | 28 |
| Determination of the Minimum Inhibitory Concentrations (MIC) | 28 |
| Effect of TMP-SMX and the GBBR analogues on bacterial growth curves | 29 |
| Growth Curves | 29 |

Microbiology

Material and Methods

Bacterial strains, bacteriological media and antimicrobials

Three different control strains were selected; *Escherichia coli* ATCC 25922, *Staphylococcus aureus* ATCC 29213 and *Pseudomonas aeruginosa* PAO1. Four clinical isolates of methicillin-resistant *S. aureus* from nasal and wound smear were used (*S. aureus* 8125304770, *S. aureus* 8139265926, *S. aureus* 8125255044, *S. aureus* 8124825998).

Tryptic soy broth (TSB, Scharlau Microbiology, Sentmenat, Spain) was used to determine the minimum inhibitory concentrations (MICs) and in the growth curves. Sulfamethoxazole and Trimethoprim were purchased from Sigma-Aldrich (St. Louis, USA).

Susceptibility testing

Determination of the Minimum Inhibitory Concentrations (MIC)

MIC values were determined by the broth microdilution method and interpreted according to the European Committee on Antimicrobial Susceptibility Testing (EUCAST) guidelines.¹ Briefly, the strains were grown overnight at 37 °C with orbital shaking at 200 rpm in Tryptone Soy Broth (TSB). After doing a refresh of 2 h in the same conditions, the bacterial cultures were adjusted to OD_{625nm} of 0.08–0.1 (10⁸ CFUs/mL) in fresh TSB medium. 5 µL of each suspension was added to 96-well plates previously filled with TSB and serially diluted TMP analogues. Concentrations assayed were 32, 16, 8, 4, 2, 1, 0.5, 0.25, 0.125 and 0.062 µg/ml. The plates were incubated at 37 °C for 24 h, after which the MIC was determined macroscopically, based on the visually turbidity of the wells by placing the plates on top of a viewing device in form of a stand with an enlarging mirror.

The antimicrobial activity of these 15 new Trimethoprim (TMP) analogues was evaluated against *Escherichia coli* ATCC 25922, *Staphylococcus aureus* ATCC 29213, *Pseudomonas aeruginosa* 01. Moreover, susceptibility was examined using the new compounds alone and in combination with Sulfamethoxazole in a 1:20 ratio in the three previous strains and also in *S. aureus* 8125304770, *S. aureus* 8139265926, *S. aureus* 8125255044 and *S. aureus* 8124825998. Serial dilutions of the antimicrobials starting from 32 µg/mL were tested.

Minimal inhibitory concentrations were determined in triplicate in at least three different experiments. Values resulted to be repetitive with undetectable differences by this method.

¹ EUCAST. European Committee on Antimicrobial Susceptibility Testing Breakpoint Tables for Interpretation of MICs and Zone Diameters European Committee on Antimicrobial Susceptibility Testing Breakpoint tables for Interpretation of MICs and Zone Diameters 0–99. Available online: http://www.eucast.org/fileadmin/src/media/PDFs/EUCAST_files/Breakpoint_tables/v_9.0_Breakpoint_Tables.pdf (accessed on 10 March 2019).

Effect of TMP-SMX and the GBBR analogues on bacterial growth curves

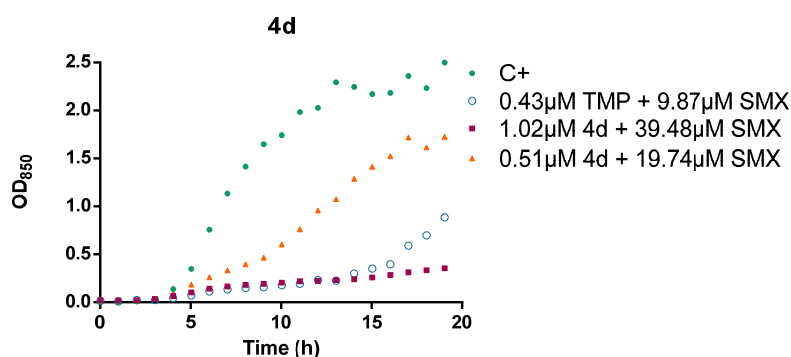
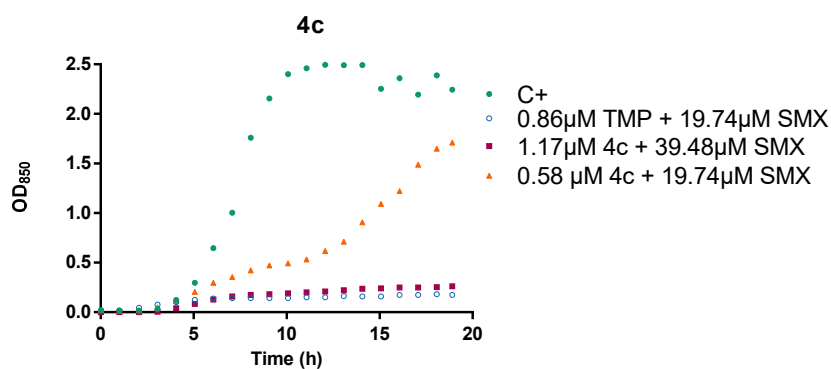
The combination of some of the most active analogues and Sulfamethoxazole (1:20) was assayed for their effect on the growth curve. A Gram-negative (*E. coli* ATCC 25922) and a Gram-positive (*S. aureus* ATCC 29213) were used to examine the effect of these new compounds in real time.

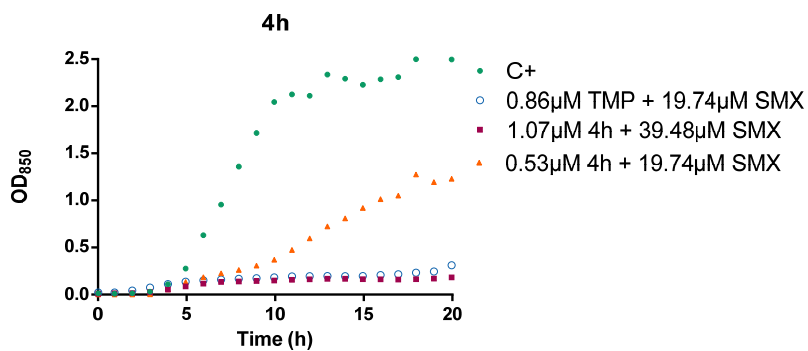
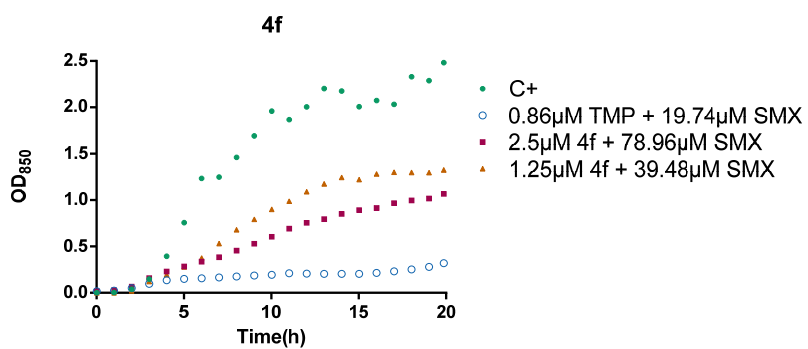
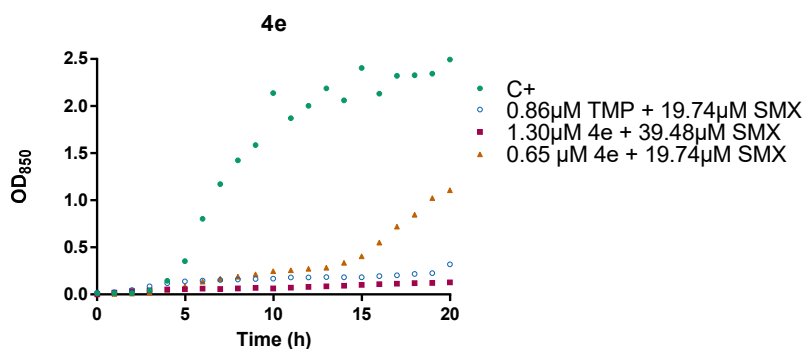
Volumes of 10 mL TSB liquid cultures with $1-5 \times 10^8$ CFU/mL in logarithmic-phase were adjusted. Antimicrobials were then added at sublethal concentrations ($\frac{1}{2}$ MIC and $\frac{1}{4}$ MIC). Trimethoprim was also evaluated as a control.

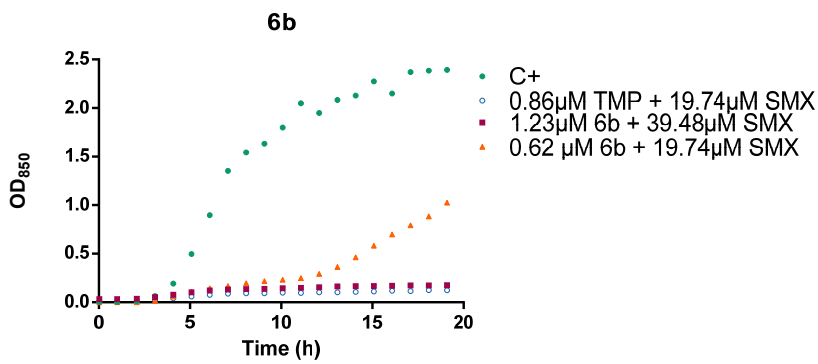
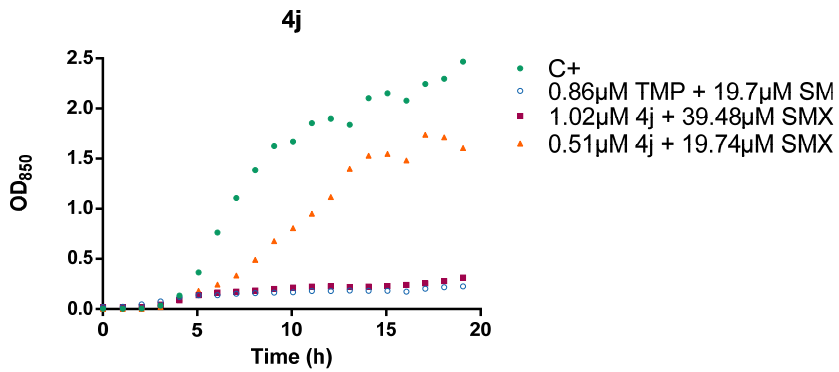
The incubation was performed in RTS-1C real-time cell growth loggers (Biosan) for 20h at 37 °C and 2000 rpm. Growth was measured as optical density (OD 850 nm) every 10 minutes.

Growth Curves

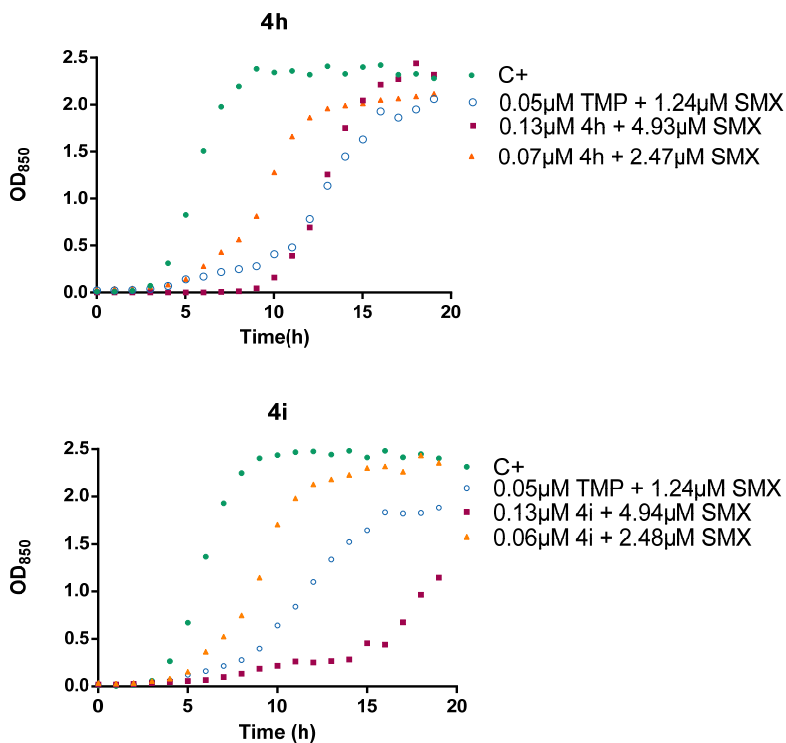
Effect of the analogues **4c**, **4d**, **4e**, **4f**, **4h**, **4j**, **6b** and **TMP** in combination with sulfamethoxazole (1:20) on the growth curve of *S. aureus*.







Effect of the analogues **4h** and **4i** and TMP in combination with sulfamethoxazole (1:20) on the growth curve of *E. coli*.



3.3. ARTICLE 3

ARTICLE 3: New trimethoprim-like molecules: bacteriological evaluation and insights into their action.

Jorba M, Pedrola M, Ghashghaei O, Herráez R, Campos-Vicens L, Luque FJ, Lavilla R, Viñas M.

Antibiotics. 2021..

Addressed objectives in this article:

2. Trimethoprim

2.1. Study of the antimicrobial activity of the Trimethoprim derivatives

- 2.1.1. Determination of their antimicrobial effect on planktonic bacteria
- 2.1.2. Determination of their antimicrobial effect on biofilm
- 2.1.3. Exploration of their antimicrobial synergistic effect in combination with Sulfamethoxazole
- 2.1.4. Exploration of their antimicrobial synergistic effect with colistin

2.2. Determination of the cytotoxicity of the new derivatives

2.3. Exploration of the effect of the new derivatives on the Dihydrofolate Reductase (DHFR) enzyme

2.4. Start a computational approach to decipher the intimal mechanisms of action



Article

New Trimethoprim-Like Molecules: Bacteriological Evaluation and Insights into Their Action

Marta Jorba ¹, Marina Pedrola ², Ouldouz Ghashghaei ², Rocío Herráez ¹, Lluís Campos-Vicens ^{3,4}, Francisco Javier Luque ³, Rodolfo Lavilla ² and Miguel Viñas ^{1,*}

- ¹ Laboratory of Molecular Microbiology & Antimicrobials, Department of Pathology & Experimental Therapeutics, Medical School, University of Barcelona, Bellvitge Institute for Biomedical Research (IDIBELL), Hospitalet de Llobregat, 08907 Barcelona, Spain; mjorba@ub.edu (M.J.); rherraez@ub.edu (R.H.)
 - ² Laboratory of Medicinal Chemistry, Faculty of Pharmacy and Food Sciences and Institute of Biomedicine (IBUB), University of Barcelona, 08028 Barcelona, Spain; mpedrola@ub.edu (M.P.); ghashghaei@ub.edu (O.G.); rlavilla@ub.edu (R.L.)
 - ³ Department of Nutrition, Food Science and Gastronomy, Faculty of Pharmacy and Food Sciences, Institute of Biomedicine (IBUB), Institute of Theoretical and Computational Chemistry (IQTC-UB), University of Barcelona, Av. Prat de la Riba 171, 08921 Santa Coloma de Gramenet, Spain; lluis.campos@pharmacelera.com (L.C.-V.); flluque@ub.edu (F.J.L.)
 - ⁴ Pharmacelera, Torre R, 4a planta, Despatx A05, Parc Científic de Barcelona, Baldiri Reixac 8, 08028 Barcelona, Spain
- * Correspondence: mvinyas@ub.edu



Citation: Jorba, M.; Pedrola, M.; Ghashghaei, O.; Herráez, R.; Campos-Vicens, L.; Luque, F.J.; Lavilla, R.; Viñas, M. New Trimethoprim-Like Molecules: Bacteriological Evaluation and Insights into Their Action. *Antibiotics* **2021**, *10*, 709. <https://doi.org/10.3390/antibiotics10060709>

Academic Editor: Carlos M. Franco

Received: 18 May 2021

Accepted: 10 June 2021

Published: 12 June 2021

Publisher's Note: MDPI stays neutral with regard to jurisdictional claims in published maps and institutional affiliations.



Copyright: © 2021 by the authors. Licensee MDPI, Basel, Switzerland. This article is an open access article distributed under the terms and conditions of the Creative Commons Attribution (CC BY) license (<https://creativecommons.org/licenses/by/4.0/>).

Abstract: This work reports a detailed characterization of the antimicrobial profile of two trimethoprim-like molecules (compounds **1a** and **1b**) identified in previous studies. Both molecules displayed remarkable antimicrobial activity, particularly when combined with sulfamethoxazole. In disk diffusion assays on Petri dishes, compounds **1a** and **1b** showed synergistic effects with colistin. Specifically, in combinations with low concentrations of colistin, very large increases in the activities of compounds **1a** and **1b** were determined, as demonstrated by alterations in the kinetics of bacterial growth despite only slight changes in the fractional inhibitory concentration index. The effect of colistin may be to increase the rate of antibiotic entry while reducing efflux pump activity. Compounds **1a** and **1b** were susceptible to extrusion by efflux pumps, whereas the inhibitor phenylalanine arginyl β -naphthylamide (PA β N) exerted effects similar to those of colistin. The interactions between the target enzyme (dihydrofolate reductase), the coenzyme nicotinamide adenine dinucleotide phosphate (NADPH), and the studied molecules were explored using enzymology tools and computational chemistry. A model based on docking results is reported.

Keywords: trimethoprim; multidrug-resistant (MDR) bacteria; mechanisms of action; dihydrofolate reductase

1. Introduction

Unlike eukaryotes, prokaryotes must produce their own nucleotides. In bacteria, a prerequisite for the biosynthesis of thymidine is the production of folate. Trimethoprim (TMP), included in the World Health Organization's Model List of Essential Medicines, was first used in 1962 and remains a first-line antibiotic in many countries, usually in combination with sulfamethoxazole (SMX), with which it acts synergistically. TMP and SMX target two key enzymes of the folate pathway, acting as inhibitors of dihydrofolate reductase (DHFR) and dihydropteroate synthetase (DHPS), respectively (Figure 1).

Antimicrobial resistance remains a major challenge for microbiologists and public health officials, as infections by multidrug-resistant bacteria have reached worrisome levels. Resistant bacteria include: (i) multi-resistant strains, which are resistant to antimicrobials from at least three different families, (ii) extremely resistant strains, which are resistant

to all antimicrobials except colistin, and (iii) pan-drug-resistant strains, resistant to all available antimicrobials [1].

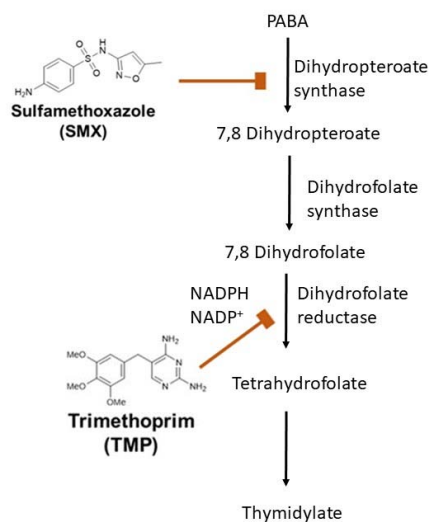
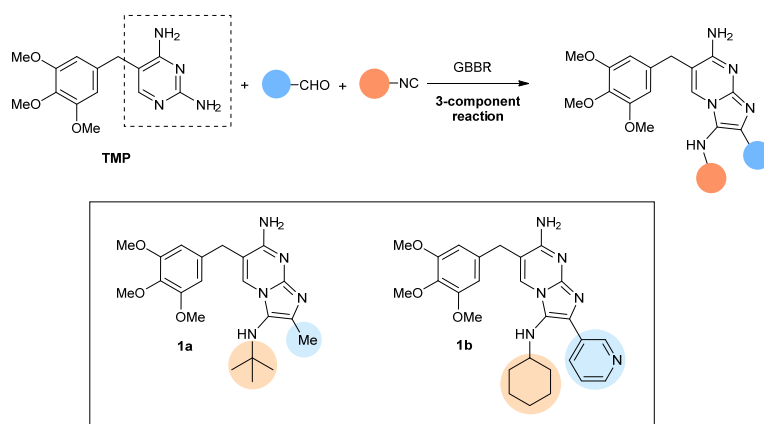


Figure 1. Folic acid biosynthesis pathway.

Among the lines of research aimed at overcoming antimicrobial resistance are: (i) the “green” approach, based on innovative eco-friendly antimicrobials [2], and (ii) the chemical approach, based on the synthesis of new molecules with antimicrobial action, including: (a) inhibitors of the resistance mechanisms to potentiate already existing antimicrobials [3]; (b) bioactive peptides [4], (c) the conjugation of different molecules to generate new ones with improved properties [5], and (d) a combination of two or more of these strategies. The interests of our laboratories include the synthesis of molecules whose active sites resemble those of already known antibiotics [6], the improvement of molecular delivery, such as the use of nanoparticles as antibiotics carriers in nano-medical devices [7], and the modification of natural molecules such that they acquire antimicrobial properties [8].

In this article we examine two TMP-like molecules that have been recently reported [6], focusing on their antibacterial effects and their mechanisms of action. TMP acts directly on dihydrofolate reductase (DHFR, EC 1.5.1.3), which catalyzes the reduction of 7,8-dihydrofolate (H_2F) to 5,6,7,8-tetrahydrofolate (H_{1a}) using NADPH as a cofactor. The conversion requires the transfer of a hydride from C4 of the NADPH cofactor to C6 of the pterin ring of H_2F , accompanied by the protonation of dihydrofolate on N5. This reaction is essential in the de novo synthesis of purines, thymidine, and certain amino acids [9,10]. Given the important role of DHFR, which is ubiquitously expressed by all kingdoms of life, the enzyme may be an effective therapeutic target in cells with a rapid DNA turnover and therefore both in bacteria and the treatment of cancer [11,12].

Based on the straightforward synthesis of compounds **1a** and **1b**, which were readily prepared through a Groebke-Blackburn-Bienaymé (GBBR) multicomponent reaction (Scheme 1), and the preliminary bacteriological profiles, which combine suitable antibiotic potency and kinetics [6], compounds **1a** and **1b** are explored in this study with respect to their mechanism of action and possible synergistic effects when used in combination with other antibacterial agents.



Scheme 1. Multicomponent access to new trimethoprim (TMP) derivatives.

2. Results and Discussion

2.1. Antimicrobial Susceptibility of Planktonic Bacteria

The minimum inhibitory concentrations (MICs) of TMP, **1a** and **1b**, both alone and in combination with SMX and colistin, are shown in Table 1. The *E. coli* ATCC 25922 strain was susceptible to TMP, **1a** and **1b**, and the activity was enhanced when the compounds were combined with SMX. The *P. aeruginosa* PAO1 strain was resistant to TMP, **1a** and **1b**, but susceptible to colistin. On the contrary, *S. marcescens* was colistin-resistant, but susceptible to the combined treatment of the compounds with SMX. Finally, **1a** and **1b** were also tested in TMP-resistant strains (*E. coli* 220560529 and *S. epidermidis* 220560752) but no significant effect was observed, suggesting that these compounds should share the target with TMP (data not shown).

Table 1. Minimum inhibitory concentration (MIC, μM) of trimethoprim (TMP) and compounds **1a** and **1b** tested alone and in combination with sulfamethoxazole (SMX) and colistin against *Escherichia coli* ATCC 25922, *Pseudomonas aeruginosa* PAO1, and *Serratia marcescens* NIMA. Data for *P. aeruginosa* PAO1 and *E. coli* ATCC 25922 were already reported [6].

| Antimicrobial | MIC (μM) | | |
|-----------------|------------------------------|------------------------------|---------------------------|
| | <i>E. coli</i> ATCC 25922 | <i>P. aeruginosa</i> PAO1 | <i>S. marcescens</i> NIMA |
| TMP | 0.43 | >110.22 | 13.78 |
| TMP (SMX) | 0.11 (2.37) | 13.78 (315.86) | 0.86 (19.74) |
| 1a | 1.25 | >80.10 | 80.10 |
| 1a (SMX) | 0.63 (19.74) | 40.05 (1263.43) | 2.5 (78.96) |
| 1b | 1.02 | >65.50 | 16.37 |
| 1b (SMX) | 0.13 (3.95) | 32.75 (1263.43) | 1.02 (39.48) |
| Colistin | 0.43 | 1.73 | >886.23 |

2.2. Antimicrobial Susceptibility of Sessile Bacteria

Many microorganisms that cause infectious diseases normally grow attached to a surface or an interface, thus forming biofilms. These structured communities contain bacterial cells of one or more species, attached to a living or inert surface and immersed in a hydrated polymeric matrix [13]. Within the biofilm, bacteria grow as part of complex and dynamic systems that result in their ability to tolerate antimicrobials [14], leading to persistent infections. Thus, the efficacy of new antibiotics requires both conventional antimicrobial susceptibility tests against planktonic cells (e.g., MIC determinations) and tests against bacteria residing in biofilms. In this work, the activity of **1a** and **1b** was

measured under both conditions and then compared with the corresponding activity of TMP.

The minimum biofilm eradication concentration (MBEC) and biofilm prevention concentration (BPC) for TMP and compounds **1a** and **1b**, alone and in combination with SMX (1:20), are shown in Table 2. Antimicrobials that exhibited antibiofilm activity had higher MBECs than BPCs. This result reflects the fact that the MBEC is a measure of the antimicrobial activity on mature biofilms, while the BPC is the concentration at which biofilm formation is blocked by the antimicrobial. Compound **1b** was highly active in biofilm prevention, whereas neither TMP nor compounds **1a** and **1b** were able to fully eradicate *Staphylococcus aureus* biofilms (neither *S. aureus* ATCC 29213 nor *S. aureus* 8124825998).

Table 2. The minimum biofilm eradication concentration (MBEC, μM) and biofilm prevention concentration (BPC, μM) of TMP and the GBBR analogues **1a** and **1b** when tested alone and in combination with SMX (1:20) against *E. coli* ATCC 25922, *S. aureus* ATCC 29213, and *S. aureus* 8124825998.

| Antimicrobial | <i>E. coli</i> ATCC 25922 | | <i>S. aureus</i> ATCC 29213 | | <i>S. aureus</i> 8124825998 | |
|---------------|---------------------------|-----------------------|-----------------------------|-----------------------|-----------------------------|-----------------------|
| | MBEC (μM) | BPC (μM) | MBEC (μM) | BPC (μM) | MBEC (μM) | BPC (μM) |
| TMP | 275.56 | 275.56 | >2204.46 | 1102.23 | >2204.46 | >2204.46 |
| (SMX) | (6317.14) | (6317.14) | (50,537.15) | (25,268.58) | (50,537.15) | (50,537.15) |
| 1a | >1602.06 | 200.26 | >1602.06 | 801.03 | >1602.06 | >1602.06 |
| (SMX) | (50,537.15) | (6317.14) | (50,537.15) | (25,268.58) | (50,537.15) | (50,537.15) |
| 1b | 163.74 | 81.87 | >1309.91 | 163.74 | >1309.91 | 327.48 |
| (SMX) | (6317.14) | (3158.57) | (50,537.15) | (6317.14) | (50,537.15) | (12,634.29) |

2.3. Synergism Studies

Table 3 shows the results of TMP-SMX checkerboard assays in combination with colistin when tested in four clinical strains: *E. coli* 220560529, *P. aeruginosa* SJD 536, *P. aeruginosa* SJD VH023, and *P. aeruginosa* SJD 481. Synergistic effects between the two drugs were not found, as noted in the values of the fractional inhibitory concentration index (FIC_i), which is ≥ 0.5 and < 4 , in any of the studied strains.

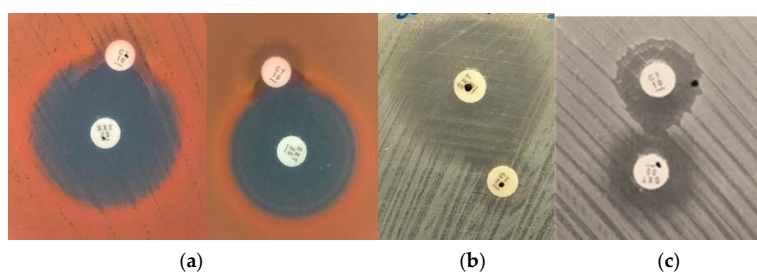
Table 3. Fractional inhibitory concentration index (FIC_i) of TMP-SMX (1:20) with colistin.

| Strains | FIC _i |
|-----------------------------|------------------|
| <i>E. coli</i> 220560529 | 2.0019 |
| <i>P. aeruginosa</i> SJD536 | 1 |
| <i>P. aeruginosa</i> VH023 | 1 |
| <i>P. aeruginosa</i> SJD481 | 1.003 |

By contrast, a strong synergism was observed with these drugs in TMP-susceptible/colistin-resistant *S. marcescens* (Table 4). This suggests that the susceptibility to TMP and TMP-like molecules in some gram-negative bacteria is due to limitations in TMP transport through the bacterial outer membrane. Colistin is unable to kill *S. marcescens* but it does adversely impact prodigiosin biosynthesis [15]. Effects on both the entry of antimicrobials as well as drug extrusion by efflux pumps have also been described [16]. Thus, as reported for antimicrobials such as linezolid and rifampin [17], colistin could be used to enhance bacterial susceptibility to TMP and TMP-like compounds. The use of very low concentrations of these drugs would limit their toxicity. It should be noted that in preliminary plate experiments, positive effects between colistin and TMP-SMX were observed in *E. coli* and *P. aeruginosa* (Figure 2), in agreement with the relatively low FIC_i (close to 1). In colistin-susceptible bacteria, however, the lethality of colistin masked any possible synergy.

Table 4. FIC_i of TMP and compounds **1a** and **1b** with SMX (1:20) when tested with colistin.

| Antimicrobial | FIC _i | | |
|-----------------|---------------------------|---------------------------|---------------------------|
| | <i>E. coli</i> ATCC 25922 | <i>P. aeruginosa</i> PAO1 | <i>S. marcescens</i> NIMA |
| TMP + SMX | 1.02 | 1.25 | 0.13 |
| 1a + SMX | 1.02 | 1.00 | 0.25 |
| 1b + SMX | 1.02 | 1.01 | 0.25 |

**Figure 2.** Interaction between colistin and TMP-SMX in (a) *S. marcescens* NIMA; (b) *E. coli* ATCC 25922, and (c) *P. aeruginosa* PAO1.

The effect of combining TMP, **1a** and **1b** with SMX and colistin in real-time were determined by plotting growth curves for *E. coli* ATCC 25922, *P. aeruginosa* PAO1, and *S. marcescens* NIMA using concentrations at which these strains were fully resistant (Figure 3). When TMP, **1a** and **1b** were used in combination with colistin, bacterial growth was nearly abolished, thus demonstrating synergism between these antibiotics. In the kinetics profile of *E. coli* (Figure 3a), although 0.11 μM colistin provoked a 10 h delay in growth, growth had resumed to the same level as the control at the end of the experiment. Following the addition of TMP + SMX (0.05 μM + 1.22 μM), however, growth was delayed for 20 h.

A similar effect was observed in *P. aeruginosa*, both with TMP and with compounds **1a** and **1b** (Figure 3b). At a colistin dose of 0.87 μM , the growth was delayed for 2 h and then reached the same level as the control. Similar curves were obtained with TMP + SMX (6.89 μM + 157.93 μM), whereas the growth delay was 4 h with **1a** + SMX (10.01 μM + 315.86 μM) and **1b** + SMX (8.19 μM + 315.86 μM). The addition of 0.87 μM colistin to **1a** + SMX and **1b** + SMX resulted in a delay of 10 h, whereas the addition of 0.87 μM colistin to TMP + SMX completely abolished the growth for 23 h after the start of the experiment. The results from the agar plates and the growth curves suggested an additive effect, even though it was not clearly reflected in the FIC_i values.

The effects of the antibiotics were also explored in *S. marcescens* (Figure 3c), which is intrinsically fully resistant to colistin. Thus, while colistin severely alters the bacterium's outer membrane, it does not affect bacterial viability, as the cytoplasmic membrane remains intact. The effect of colistin on the outer membrane of *Serratia* can be readily seen by transmission electron microscopy [18]. The growth curve of *S. marcescens* in the presence of TMP + SMX and colistin exhibited a longer delay (up to 10 h) in the start of detectable growth compared to the delay observed in the presence of TMP + SMX. Similar results were obtained with **1a**. Moreover, when testing **1b**, a complete abolition of growth was obtained in the presence of colistin.

The nearly complete abolition or prolonged delay of growth in the studied bacteria suggested that colistin alters the hydrophobic permeability barrier of the lipopolysaccharide outer membrane and thus facilitates the internalization of the DHFR inhibitors, which then inhibit the bacterial growth. The demonstration of these synergistic effects in gram-negative bacteria should renew the interest for the use of TMP and TMP-like molecules.

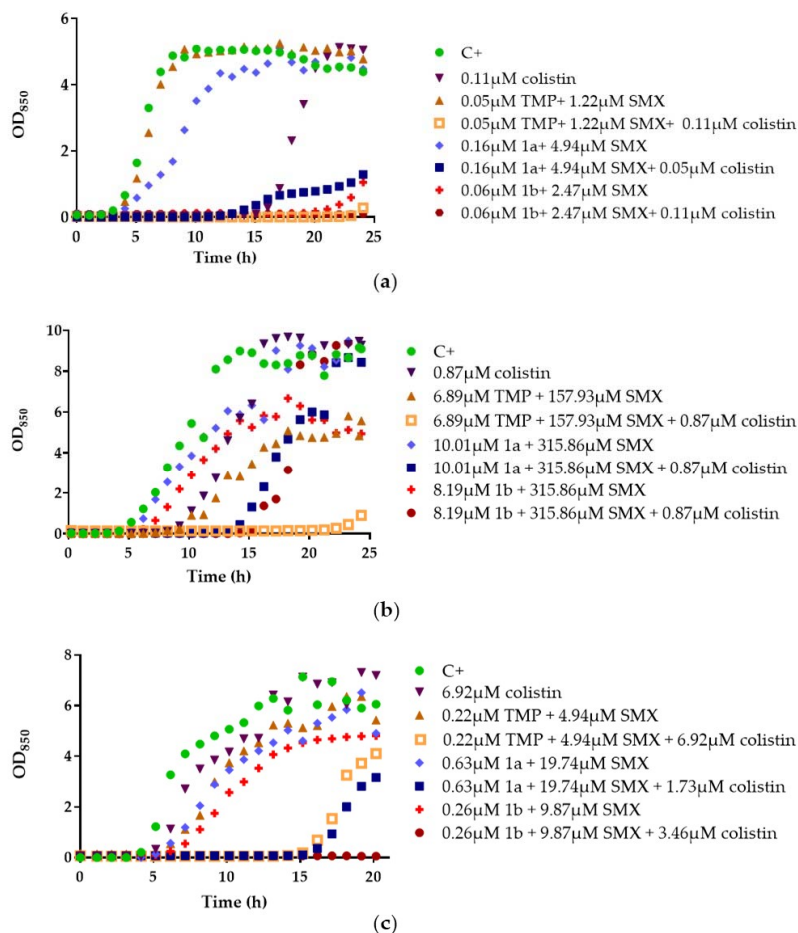


Figure 3. Effects of TMP, **1a** and **1b** when tested in combination with SMX (1:20) and in the presence of sublethal concentrations of colistin on the growth curve of (a) *E. coli* ATCC 25922, (b) *P. aeruginosa* PAO1, and (c) *S. marcescens* NIMA.

2.4. The Role of Efflux Pumps

The TMP analogues were tested in combination with SMX (1:20) in the presence of 20 μg/mL of the efflux pump inhibitor phenylalanine arginyl β-naphthylamide (PABN). At this point, it is worth noting that previous studies demonstrated that they have no detectable effect on bacterial growth when used at concentrations up to 40 μg/mL [19]. The MIC values are shown in Table 5. Lower MIC values were obtained in the presence of PABN compared to the assays performed in the absence of the efflux pump inhibitor.

A recent study demonstrated that colistin, even at low concentrations, has a direct effect on efflux pump functionality [16]. In the present study, the addition of 20 μg PABN/mL resulted in a 16-fold reduction in the MICs of TMP and its analogues (Table 5). These results are consistent with the critical role of efflux pumps in bacterial susceptibility to these antimicrobials.

Table 5. MIC values of TMP and compounds **1a** and **1b** in combination with SMX (1:20) as well as colistin in *P. aeruginosa* PAO1 in the presence or absence of the efflux pump inhibitor PAβN (20 µg/mL).

| Antimicrobial | MIC (µM) | |
|-----------------|---------------|-----------------|
| | With PAβN | Without PAβN |
| TMP (SMX) | 1.72 (39.48) | 27.56 (631.71) |
| 1a (SMX) | 5.01 (157.93) | 80.10 (2526.86) |
| 1b (SMX) | 2.05 (78.96) | 32.76 (1263.43) |
| Colistin | 1.73 | 1.73 |

This work examined possible synergisms between colistin and TMP, **1a** and **1b** in enhancing the antimicrobial activity, following the positive results in preliminary experiments on Petri dishes (Figure 2). The synergistic effects of colistin and all three TMP molecules were confirmed (Figure 3 and Table 4) and a possible mechanism involving bacterial efflux pumps was demonstrated. Our findings suggest that DHFR inhibitors can be used in combination with low concentrations of colistin or similar molecules as a new approach for the treatment of infections caused by multidrug-resistant variants of gram-negative bacteria. The synergism between colistin and the TMP molecules in *S. marcescens* further suggested that peptides with the ability to facilitate antibiotic penetration by altering the bacteria outer membrane and inhibiting bacterial efflux pumps can be used to sensitize bacteria to a wide range of otherwise ineffective antimicrobials.

2.5. Enzymatic Assays

Like TMP, compounds **1a** and **1b** are potent inhibitors of DHFR. Both analogues inhibited the activity of this enzyme by >80%. All three inhibitors were then tested in *E. coli* supplied with increased concentrations of the DHFR cofactor NADPH and the substrate H₂F. The reaction without inhibitors served as the reference (100% activity). In the reactions with TMP or its analogues, increasing concentrations of NADPH resulted in the increased enzyme activity (Figure 4). The enzyme activity was the highest at the highest tested concentration of NADPH (240 µM).

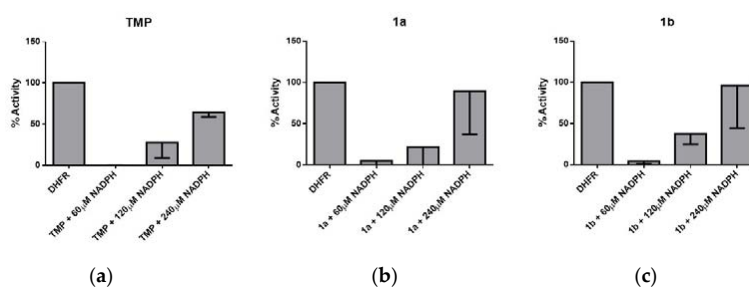


Figure 4. Activity (%) of *E. coli* dihydrofolate reductase (DHFR) after a 30-min incubation with substrate in the presence of the inhibitors (a) TMP, (b) **1a** and (c) **1b**, each at a concentration of 5 µM, and different concentrations of NADPH. The data are expressed as a percentage with respect to the control.

Similar results were obtained for the three antibiotics tested in the presence of increasing concentrations of H₂F (Figure 5) When the enzymatic assays were performed using a substrate concentration four times higher than the concentration used in the first assay (i.e., 50 µM H₂F), the inhibition was nearly reversed. Thus, as the concentrations of NADPH or H₂F were increased, the enzymatic activity was recovered as well, regardless of the presence of the antibiotics.

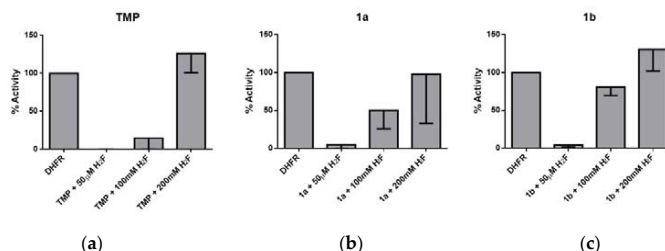


Figure 5. Percentage of activity of *E. coli* DHFR after a 30-min incubation. Each histogram represents the activity of DHFR in the presence of different concentrations of H₂F and 5 μM of the inhibitors (a) TMP, (b) **1a** and (c) **1b**. The data are expressed as a percentage with respect to the control.

To explore the molecular basis of these results, we examined the binding of **1a** to *E. coli* DHFR. According to the docking model, the heterocyclic ring of **1a** fills the pocket occupied by the nicotinamide ring of NADPH, whereas the trimethoxybenzene ring overlaps the same moiety present in TMP (Figure 6A). Accordingly, the binding of **1a** would compete with the substrate but would also affect the correct alignment of NADPH in its binding pocket.

This binding model is supported by the following experimental evidence. First, a comparison of the arrangements adopted by TMP in its interaction with human and *E. coli* DHFR showed the similar orientation of the diaminopyrimidine ring, which involves the formation of several hydrogen bonds with residues in the binding pocket (Asp27, Ile5, Ile94). By contrast, the position of the trimethoxybenzene ring is more variable and, in fact, it can adopt multiple arrangements, which often would sterically collide with NADPH when bound to the enzyme. Indeed, the most severe steric hindrance (PDB entry 2W9H; TMP, shown as blue sticks in Figure 6B) would occur in an X-ray structure that did not include NADPH. Furthermore, accommodation of compounds **1a** and **1b** was facilitated by the flexibility of the loops that shape the binding pocket. This was seen in the superposition of the X-ray structures 3DAU (*E. coli*) [20] and 4KM2 (*M. tuberculosis*) [21], which revealed the altered arrangement of loops Met20 and F-G (Figure 6C), as described in previous studies [22,23]. On the basis of this conformational flexibility, compound **1b** was docked using a structural model of *E. coli* DHFR built using the open structure of the enzyme (PDB entry 4KM2) as a template. The open structure enabled the proper accommodation of **1b** in the binding pocket of *E. coli* DHFR (Figure 6D), which would lead to steric hindrance with the nicotinamide ring of NADPH.

2.6. Cytotoxicity

At concentrations as high as 32 μg/mL, which was the maximal concentration considered in these assays, the cytotoxicity of TMP, as well as compounds **1a** and **1b** in HepG2 and L-929 cells, was almost negligible (Table 6). A drug is considered toxic when its cytotoxicity level exceeds 20% [24]. For all three compounds, the IC₅₀ (the drug concentration needed to inhibit cell growth by 50%) was >32 μg/mL.

Table 6. Cytotoxicity (%) of TMP, **1a** and **1b** in HepG2 and L-929 cells. The data are presented as the percentage of dead cells at maximal concentration tested of the compounds studied (32 μg/mL).

| Compound | Cytotoxicity (%) | |
|-----------|------------------|-------|
| | HepG2 | L-929 |
| | 32 μg/mL | |
| TMP | 0.35 | 0.8 |
| 1a | ND | 0 |
| 1b | 0.11 | 0 |

ND: Not determined.

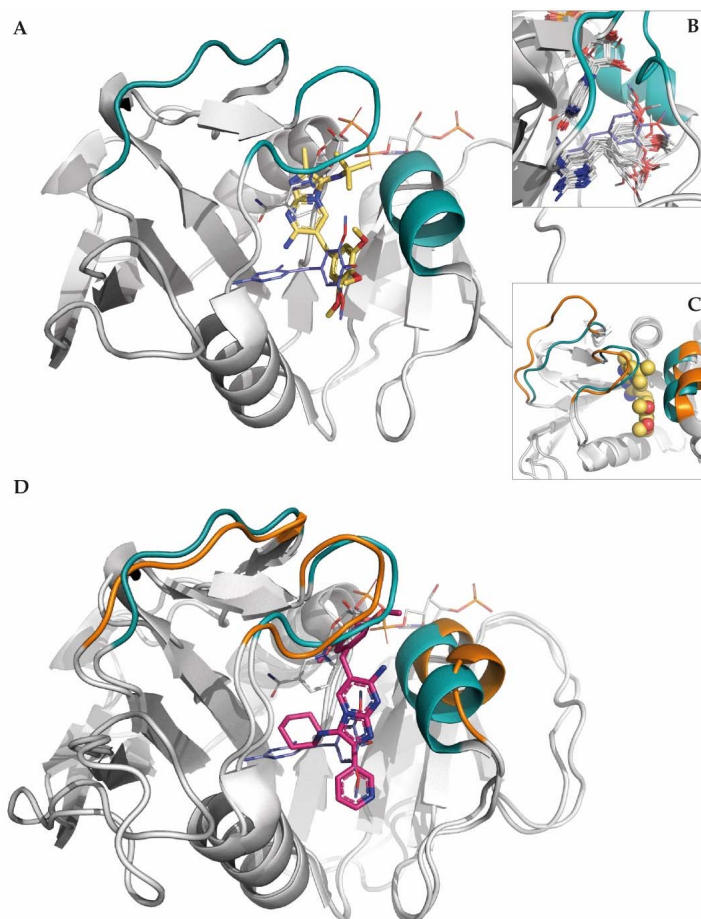


Figure 6. Binding mode of **1a** to the DHFR of *E. coli*. (A) The docked positions of **1a** and TMP are shown with their C atoms depicted as yellow sticks and in deep blue, respectively, and with the C atoms of NADPH in gray. (B) Superposition of the crystallographic poses of TMP (C atoms in gray). The crystallographic structure of TMP in PDB entry 2W9H, in which the trimethoxybenzene group sterically collides with the nicotinamide ring of NADPH, is shown in deep blue. (C) Loops Met20 and F-G, and helix 3 are highlighted to illustrate the differences in the 3D structures of PDB entries 3DAU (turquoise) and 4KM2 (orange). (D) The docked position of **1b** (C atoms in magenta) in a homology model of *E. coli* DHFR built using the open structure 4KM2 as a template. The position of TMP and NADPH is shown with their C atoms depicted as deep blue and gray, respectively.

3. Materials and Methods

3.1. Chemical Synthesis

Compounds **1a** and **1b** were prepared as previously reported [6], from the interaction of TMP with aldehydes and isocyanides in acetonitrile under $\text{Yb}(\text{OTf})_3$ catalysis. The compounds were purified by chromatography and stored at -20°C under an inert atmosphere. Stock solutions in DMSO were stable when kept in the cold. The integrity of these compounds and solutions thereof was confirmed by HPLC-MS (column: ZORBAX Extend-C18 3.5 μm 2.1 \times 50 mm, Agilent; mobile phase A: H_2O + 0.05% HCOOH ; mobile phase B:

ACN + 0.05% HCOOH; 10 min; 35 °C). There were no signs of decomposition at least 1 year after their chemical synthesis.

3.2. Antimicrobial Susceptibility of Planktonic Bacteria

The minimum inhibitory concentrations (MICs) of colistin, TMP, **1a**, and **1b** were determined using the microdilution method, according to EUCAST recommendations [25].

3.3. Antimicrobial Susceptibility of Sessile Bacteria

TMP and its analogues were tested against biofilms by determining the minimal biofilm eradication concentration (MBEC) and the biofilm prevention concentration (BPC). Bacterial viability within the biofilm was assessed using the dye resazurin, which is reduced by metabolically active bacteria to the fluorescent compound resorufin. Both collection strains, *E. coli* ATCC 25922 and *S. aureus* ATCC 29213, and methicillin-resistant *S. aureus* 8124825998 were tested. All three strains were grown in tryptic soy broth (TSB) with shaking at 200 rpm for 24 h at 37 °C. Bacterial biofilms were formed and treated as follows. Overnight suspensions of each strain were diluted 1/100 in TSB. One hundred µL of each of the adjusted cell suspensions were transferred to the wells of flat-bottomed 96-well microtiter plates (Guangzhou Jet Bio-Filtration Co., Ltd., Mianyang, China) and incubated at 37 °C for 24 h. Eight wells filled only with sterile TSB served as the negative controls. All wells were then gently rinsed with 100 µL of Ringer $\frac{1}{4}$ solution. The biofilms were exposed to several concentrations of the antimicrobials (leaving 8 wells without antimicrobials as a positive control) and incubated at 37 °C for 24 h. After the wells were again rinsed with 100 µL of Ringer $\frac{1}{4}$ solution, 100 µL of resazurin (0.0015%) was added to each well. The plates were then incubated for 3–5 h, after which cell fluorescence ($\lambda_{\text{ex}} = 530$; $\lambda_{\text{em}} = 590$) was measured using a scanning multi-well spectrophotometer (FLUOstar OPTIMA, BMG Labtech, Ortenberg, Germany). The MBEC was defined as the lowest concentration of antimicrobial activity that prevented bacterial regrowth from the treated biofilm.

3.4. Synergism Studies

The fractional inhibitory concentration (FIC) of TMP-SMX in combination with colistin was determined by the checkerboard method in four clinical bacterial strains: *E. coli* 220560529, *P. aeruginosa* SJD 536, *P. aeruginosa* SJD 481 (all three TMP resistant), and *P. aeruginosa* VH023. In addition, the FICs of colistin with TMP, **1a** and **1b**, and SMX (1:20) were determined in *E. coli* ATCC 25922, *P. aeruginosa* PAO1, and *S. marcescens* NIMA. The assays were performed in 96-well plates using serial dilutions of TMP and SMX (1:20). Serial dilutions of colistin starting from twice the previously determined MIC were prepared and added to plates inoculated with 5 µL of bacterial suspension. The plates were incubated overnight at 37 °C and read after at least 16 h of incubation.

The fractional inhibitory concentration index (FIC_i) was determined according to the formula $\text{FIC}_i = \text{FIC A} + \text{FIC B}$, where FIC A is the MIC of drug A (TMP + SMX) in combination/MIC of drug A alone and FIC B (colistin) is the MIC of drug B in combination/MIC of drug B alone. The combinations were defined as synergistic ($\text{FIC}_i \leq 0.5$), indifferent ($\text{FIC}_i > 0.5$ and < 4), or antagonistic ($\text{FIC}_i \geq 4$). An antimicrobial effect achieved at a drug concentration that was lower when the drug was used in combination with other drugs than alone was considered to be indicative of synergism between the tested antibiotics.

Additionally, the effect of TMP-SMX and the GBBR analogues in combination with sublethal concentrations of colistin was assessed in growth curves of *E. coli* ATCC 25922, *P. aeruginosa* PAO1, and *S. marcescens* NIMA. Exponential-phase cultures were adjusted to 5×10^9 CFU/mL in a final volume of 10 mL of TSB and the antimicrobials were added at sublethal concentrations. Growth was monitored using RTS-1C real-time cell growth loggers (Biosan SIA, Riga, Latvia) in cells incubated for 24 h at 37 °C with shaking at 2000 rpm. Growth was measured every 10 min as the optical density (OD 850 nm).

3.5. Efflux Pumps Effect

The efflux pump inhibitor phenyl-arginyl- β -naphthylamide (Pa β N) was purchased from Sigma-Aldrich Chemicals (Madrid, Spain). The MIC of the TMP analogues in combination with SMX in the presence of 20 μ g Pa β N/mL was determined in *P. aeruginosa* PAO1 using the microdilution method.

3.6. Dihydrofolate Reductase Assay

The DHFR assay is based on the reduction of 7,8-dihydrofolate to 5,6,7,8-tetrahydrofolate catalyzed by DHFR and using NADPH as a cofactor. Purified *E. coli* DHFR was kindly provided by E. Shakhnovich and J.V. Rodrigues (Harvard University, Cambridge, MA, USA). The DHFR assay kit (CS0340) was purchased from Sigma-Aldrich. The assay was performed in 96-well flat-bottom plates (Corning Costar 3606, NY, USA) with the protocol adjusted to accommodate a final reaction volume of 200 μ L. DHFR was diluted to a final concentration of 0.03 μ g/mL. The inhibitory effect of compounds **1a** and **1b** was tested, with TMP serving as the control. All three drugs were used at a concentration of 5 μ M, which was higher than the respective MICs (Table 1). To determine the effect of the concentration of the DHFR cofactor NADPH on inhibition, a dilution series of NADPH in assay buffer was carried out to obtain a concentration range between 60 μ M and 240 μ M. A dilution series of H₂F was similarly carried out in assay buffer to obtain a concentration range from 50 μ M to 200 μ M. In all assays, the enzyme was mixed with the different inhibitors and incubated for 30 min before the enzymatic reaction was initiated by the addition of NADPH and H₂F. The reaction was conducted at 37 °C and monitored by the decrease in absorbance at 340 nm (indicative of a decrease in the NADPH concentration). Measurements were performed every minute for 40 min [26] using a scanning multi-well spectrophotometer (FLUOstar OPTIMA, BMG Labtech, Germany). All measurements were performed in duplicate with three technical replicates.

3.7. Computational Chemistry

Docking simulations were carried out to explore the binding mode of TMP, **1a** and **1b** to *E. coli* DHFR, using the 2019–2 release of Glide [27,28]. The crystal structure of *E. coli* DHFR, retrieved from the Protein Data Bank (PDB code 3DAU [20]), includes methotrexate and NADPH. The protein structure of DHFR was thus prepared by deleting both of these compounds, by assigning bond orders, adding hydrogen atoms, and restrained energy minimization, using the Protein Preparation Wizard module in Maestro [29]. Compounds were prepared using LigPrep [30]. The binding site was enclosed in a grid defined with an inner box of 10 Å \times 10 Å \times 10 Å; GlideScore (SP) was used to evaluate the quality of the configurations [31]. Default settings were used for all remaining parameters. The results of the docking simulations were visually examined with the aid of PyMOL software [32]. Docking of **1b** was performed using a homology model of *E. coli* DHFR using the open structure from *M. tuberculosis* DHFR (PDB entry 4KM2) as a template.

3.8. Cytotoxicity

The cytotoxicity assay was carried out in the human hepatocellular carcinoma cell line Hep G2 ATCC and in murine L-929 fibroblasts (NCTC clone 929, ECACC 88102702), based on the experiments described by Vinuesa et al. [23]. The cells were obtained from Dr. Ricardo Pérez-Tomás (Cancer Cell Biology, University of Barcelona).

The cytotoxicity of TMP and compounds **1a** and **1b** was determined by measuring the intracellular reduction of resazurin sodium salt (Sigma-Aldrich, St. Louis, MO, USA). HepG2 and L-929 cells were grown in RPMI 1640 and MEM medium, respectively (Biochrom AG, Berlin, Germany), supplemented with 10% fetal bovine serum. Cells from pre-confluent cultures were harvested with trypsin-EDTA and maintained at 37 °C and 5% CO₂. HepG2 and L-929 cells (100 μ L each) were seeded in 96-well flat-bottomed microplates to obtain concentrations of 1.5×10^4 and 4×10^3 cells/well, respectively, and incubated at 37 °C for 24 h. Afterwards, the medium was replaced with 200 μ L of medium containing

the antimicrobials at concentrations ranging from 32 to 0.016 µg/mL and the microplates were incubated at 37 °C for 24 h. Twenty µL of resazurin was then added to each well and the plates were incubated under the same conditions. Fluorescence was measured at an excitation wavelength of 530 nm and an emission wavelength of 590 nm using a scanning multi-well spectrophotometer (FLUOstar OPTIMA, BMG Labtech, Germany). Cytotoxicity was calculated as follows:

$$\% \text{ Cytotoxicity} = 100 - \frac{(AT - ADB)}{(AC - AMB)} \times 100 \quad (1)$$

where AT is the absorbance of the treated cells, ADB the absorbance of the drug blank control, AC the absorbance of the untreated cells, and AMB the absorbance of the medium blank.

4. Conclusions

Two TMP derivatives (**1a** and **1b**) showed antibacterial activity against *E. coli*, *P. aeruginosa* and *S. marcescens* similar to that of TMP and acted synergistically with SMX. They resulted to be active in biofilm prevention, whereas neither TMP nor compounds **1a** and **1b** were able to fully eradicate *S. aureus* biofilms (neither *S. aureus* ATCC 29213 nor *S. aureus* 8124825998). On the other hand, at concentrations at which the products behave as good antibacterials, the cytotoxicity on HepG2 and L-929 cell lines was almost negligible. *P. aeruginosa* PAO1 was fully resistant to TMP and its derivatives as well as to the combination of TMP-SMX. Moreover, it can be suggested that blocking their efflux systems may influence the *P. aeruginosa* susceptibility to these antimicrobials. The combination of TMP, TMP-like molecules and SMX with colistin enhances their antimicrobial efficacy against *E. coli*, *P. aeruginosa* and *S. marcescens* by permeabilizing the cells.

Compounds **1a** and **1b**, like TMP, strongly inhibited the activity of the *E. coli* DHFR. The inhibition was reversed with increasing concentrations of NADPH and H₂F, suggesting that both molecules interact with the analogues during inhibition. As seen in the docking model, the heterocyclic ring of the compound **1a** fills the pocket occupied by the nicotinamide ring of NADPH. Thus, the binding of **1a** would compete with H₂F and would also prevent the correct recognition of NADPH.

As the search into new antimicrobial compounds is one of the main pathways to overcome bacterial resistance to antibiotics, it should be emphasized that all putative compounds should be tested in conditions in which the role of the outer membrane as a permeability barrier is inactivated. Their assay together with sublethal concentrations of colistin is proposed as one of the methods of election.

Author Contributions: M.P., O.G. and R.L. designed and performed the chemical section and analyzed the results. M.J., R.H. and M.V. designed and performed the biological experiments. L.C.-V. and F.J.L. performed the docking work. All authors have participated in scientific discussions, read and agreed to the published version of the manuscript.

Funding: This research was financially supported by the Marató TV3 Foundation (project BAR-NAPA); Ministerio de Ciencia e Innovación-Spain (PID2019-107991RB-I00), Generalitat de Catalunya (2017SGR1746), and the Consorci de Serveis Universitaris de Catalunya (project Molecular Recognition).

Institutional Review Board Statement: Not applicable.

Informed Consent Statement: Not applicable.

Data Availability Statement: Data is contained within the article.

Acknowledgments: We thank E. Shakhnovich and J.V. Rodrigues (Harvard University) for their kind supply of *E. coli*-DHFR.

Conflicts of Interest: The authors declare no conflict of interest.

References

1. Magiorakos, A.P.; Srinivasan, A.; Carey, R.B.; Carmeli, Y.; Falagas, M.E.; Giske, C.G.; Harbarth, S.; Hindler, J.F.; Kahlmeter, G.; Olsson-Liljequist, B.; et al. Multidrug-resistant, extensively drug-resistant and pandrug-resistant bacteria: An international expert proposal for interim standard definitions for acquired resistance. *Clin. Microbiol. Infect.* **2012**, *18*, 268–281. [CrossRef]
2. Toutain, P.L.; Ferran, A.A.; Bousquet-Melou, A.; Pelligand, L.; Lees, P. Veterinary medicine needs new green antimicrobial drugs. *Front. Microbiol.* **2016**, *7*, 1196. [CrossRef]
3. Wright, G.D. Resisting resistance: New chemical strategies for battling superbugs. *Chem. Biol.* **2000**, *7*, R127–R132. [CrossRef]
4. Góngora-Benítez, M.; Tulla-Puche, J.; Albericio, F. Handles for Fmoc solid-phase synthesis of protected peptides. *ACS Comb. Sci.* **2013**, *15*, 217–228. [CrossRef]
5. Deng, J.; Viel, J.H.; Kubyskhin, V.; Budisa, N.; Kuipers, O.P. Conjugation of synthetic polyproline moieties to lipid ii binding fragments of nisin yields active and stable antimicrobials. *Front. Microbiol.* **2020**, *11*, 1–9. [CrossRef]
6. Pedrola, M.; Jorba, M.; Jardas, E.; Jardi, F.; Ghashghaei, O.; Viñas, M.; Lavilla, R. Multicomponent reactions upon the known drug trimethoprim as a source of novel antimicrobial agents. *Front. Chem.* **2019**, *7*, 1–9. [CrossRef]
7. Sans-Serramitjana, E.; Fusté, E.; Martínez-Garriga, B.; Merlos, A.; Pastor, M.; Pedraz, J.L.; Esquisabel, A.; Bachiller, D.; Vinuesa, T.; Viñas, M. Killing effect of nanoencapsulated colistin sulfate on *Pseudomonas aeruginosa* from cystic fibrosis patients. *J. Cyst. Fibros.* **2016**, *15*, 611–618. [CrossRef] [PubMed]
8. Martín-Gómez, H.; Jorba, M.; Albericio, F.; Viñas, M.; Tulla-Puche, J. Chemical modification of microcin j25 reveals new insights on the stereospecific requirements for antimicrobial activity. *Int. J. Mol. Sci.* **2019**, *20*, 5152. [CrossRef]
9. Schweitzer, B.I.; Dicker, A.P.; Bertino, J.R. Dihydrofolate reductase as a therapeutic target. *FASEB J.* **1990**, *4*, 2441–2452. [CrossRef]
10. Srinivasan, B.; Skolnick, J. Insights into the slow-onset tight-binding inhibition of *Escherichia coli* dihydrofolate reductase: Detailed mechanistic characterization of pyrrolo [3,2-f] quinazoline-1,3-diamine and its derivatives as novel tight-binding inhibitors. *FEBS J.* **2015**, *282*, 1922–1938. [CrossRef]
11. Raimondi, M.V.; Randazzo, O.; La Franca, M.; Barone, G.; Vignoni, E.; Rossi, D.; Collina, S. DHFR inhibitors: Reading the past for discovering novel anticancer agents. *Molecules* **2019**, *24*, 1140. [CrossRef]
12. Wróbel, A.; Arciszewska, K.; Maliszewski, D.; Drozdowska, D. Trimethoprim and other nonclassical antifolates an excellent template for searching modifications of dihydrofolate reductase enzyme inhibitors. *J. Antibiot.* **2020**, *73*, 5–27. [CrossRef]
13. Costerton, J.W.; Stewart, P.S.; Greenberg, E.P. Bacterial biofilms: A common cause of persistent infections. *Science* **1999**, *284*, 1318–1322. [CrossRef]
14. Hall-Stoodley, L.; Costerton, J.W.; Stoodley, P. Bacterial biofilms: From the natural environment to infectious diseases. *Nat. Rev. Microbiol.* **2004**, *2*, 95–108. [CrossRef] [PubMed]
15. Lauferska, U.; Viñas, M.; Lorén, J.G.; Guinea, J. Enhancement by polymyxin B of proline-induced prodigiosin biosynthesis in non-proliferating cells of *Serratia marcescens*. *Microbiologica* **1983**, *6*, 155–162.
16. Armengol, E.; Domenech, O.; Fusté, E.; Pérez-Guillén, I.; Borrell, J.H.; Sierra, J.M.; Vinas, M. Efficacy of combinations of colistin with other antimicrobials involves membrane fluidity and efflux machinery. *Infect. Drug Resist.* **2019**, *12*, 2031. [CrossRef] [PubMed]
17. Armengol, E.; Asunción, T.; Viñas, M.; Sierra, J.M. When combined with colistin, an otherwise ineffective rifampicin–linezolid combination becomes active in *Escherichia coli*, *Pseudomonas aeruginosa*, and *Acinetobacter baumannii*. *Microorganisms* **2020**, *8*, 86. [CrossRef]
18. Rudilla, H.; Fusté, E.; Cajal, Y.; Rabanal, F.; Vinuesa, T.; Viñas, M. Synergistic antipseudomonal effects of synthetic peptide AMP38 and carbapenems. *Molecules* **2016**, *21*, 1223. [CrossRef] [PubMed]
19. Fusté, E.; López-Jiménez, L.; Segura, C.; Gainza, E.; Vinuesa, T.; Viñas, M. Carbapenem-resistance mechanisms of multidrug-resistant *Pseudomonas aeruginosa*. *J. Med. Microbiol.* **2013**, *62*, 1317–1325. [CrossRef]
20. Bennett, B.C.; Wan, Q.; Ahmad, M.F.; Langan, P.; Dealwis, C.G. X-ray structure of the ternary MTX NADPH complex of the anthrax dihydrofolate reductase: A pharmacophore for dual-site inhibitor design. *J. Struct. Biol.* **2009**, *166*, 162–171. [CrossRef]
21. Dias, M.V.B.; Tyrakis, P.; Domingues, R.R.; Leme, A.F.P.; Blundell, T.L. Mycobacterium tuberculosis dihydrofolate reductase reveals two conformational states and a possible low affinity mechanism to antifolate drugs. *Structure* **2014**, *22*, 94–103. [CrossRef] [PubMed]
22. Bystroff, C.; Kraut, J. Crystal structure of unliganded *Escherichia coli* dihydrofolate reductase. Ligand-induced conformational changes and cooperativity in binding. *Biochemistry* **1991**, *30*, 2227–2239. [CrossRef] [PubMed]
23. Sawaya, M.R.; Kraut, J. Loop and subdomain movements in the mechanism of *Escherichia coli* dihydrofolate reductase: Crystallographic evidence. *Biochemistry* **1997**, *36*, 586–603. [CrossRef] [PubMed]
24. Vinuesa, T.; Herráez, R.; Oliver, L.; Elizondo, E.; Acarregui, A.; Esquisabel, A.; Pedraz, J.L.; Ventosa, N.; Veciana, J.; Viñas, M. Benzimidazole nanoformulates: A chance to improve therapeutics for Chagas disease. *Am. J. Trop. Med. Hyg.* **2017**, *97*, 1469–1476. [CrossRef] [PubMed]
25. EUCAST Reading Guide for Broth Microdilution. Available online: https://www.eucast.org/fileadmin/src/media/PDFs/EUCAST_files/MIC_testing/Reading_guide_BMD_v_3.0_2021.pdf (accessed on 9 April 2021).
26. Phetsang, W.; Pelington, R.; Butler, M.S.; Kc, S.; Pitt, M.E.; Kaeslin, G.; Cooper, M.A.; Blaskovich, M.A.T. Fluorescent Trimethoprim conjugate probes to assess drug accumulation in wild type and mutant *Escherichia coli*. *ACS Infect. Dis.* **2016**, *2*, 688–701. [CrossRef] [PubMed]

Outer membrane: a key obstacle for new antimicrobial agents

27. *Schrödinger Release 2019-2: Glide*; Schrödinger LLC: New York, NY, USA, 2019.
28. Friesner, R.A.; Banks, J.L.; Murphy, R.B.; Halgren, T.A.; Klicic, J.J.; Mainz, D.T.; Repasky, M.P.; Knoll, E.H.; Shelley, M.; Perry, J.K.; et al. Glide: A New approach for rapid, accurate docking and scoring. 1. Method and assessment of docking accuracy. *J. Med. Chem.* **2004**, *47*, 1739–1749. [[CrossRef](#)] [[PubMed](#)]
29. *Schrödinger Release 2019-3: Maestro*; Schrödinger LLC: New York, NY, USA, 2019.
30. *Schrödinger Release 2016-3: LigPrep*; Schrödinger LLC: New York, NY, USA, 2016.
31. Friesner, R.A.; Murphy, R.B.; Repasky, M.P.; Frye, L.L.; Greenwood, J.R.; Halgren, T.A.; Sanschagrin, P.C.; Mainz, D.T. Extra precision Glide: Docking and scoring incorporating a model of hydrophobic enclosure for protein-ligand complexes. *J. Med. Chem.* **2006**, *49*, 6177–6196. [[CrossRef](#)] [[PubMed](#)]
32. *The PyMOL Molecular Graphics System*; Version 2.0; Schrödinger LLC: New York, NY, USA, 2016.

4. DISCUSSION

Being infections caused by antibiotic resistant bacteria one of the major challenges worldwide, it has become necessary to design and investigate new approaches to tackle these infections. Modification of existing antibiotic compounds as well as combination of the latterly synthesized drugs and/or last resort antibiotics and considering their potential in antimicrobial therapeutics have been seen as a feasible option.

The studies were carried out in collaboration with Prof. Fernando Albericio and Prof. Rodolfo Lavilla, from Dept. of Organic Chemistry at University of KwaZulu-Natal (South-Africa) and Dept. of Pharmacology, Toxicology and Medicinal Chemistry at the University of Barcelona, respectively.

Experimental work done with Microcin J25, consisted basically of a treatment with harsh basic conditions (0.5 M NaOH) applied to the lasso peptide MccJ25 resulting in a new peptide with altered topology. The effect of the chemical modification on the structure of the peptide and its biological activity was investigated and compared with the natural peptide. The unmodified peptide was referred to as **native MccJ25** and the hydrolysed peptide as **new compound**.

As it had previously been described^{44,50,120}, the **native MccJ25** showed bactericidal activity against Gram-negative pathogens such as *Escherichia coli* and *Salmonella*, being two of them MDR strains (Article 1, Table 1). On the contrary, the **new compound** showed no activity,

presenting MIC values over 128 μ g/ml against the tested strains. The loss of the activity of the **new compound** could be due to the relevant structure modifications. Therefore, it was investigated whether the loss of the activity had been caused by a loss in the ability to penetrate the bacteria or, once inside the cell, the **new compound** had lost the ability to inhibit its target.

To understand the causes of the differences in the biological activity of the **new compound** with respect to the **native MccJ25**, some chemical assays were performed by our collaborators. They noticed that MccJ25 was not completely chemically stable as it was sensitive to basic conditions, as the chemical treatment carried out caused changes in topology and generated another peptide. It could be confirmed that the **new compound** showed the lasso topology, and its structure was nearly the same as that of the **native MccJ25**. Moreover, it could be affirmed that there was a difference between the two peptides involving the residues 10-12 in the loop region which are included in the β -hairpin. The results pointed to the epimerization at the Val11 residue, which adopted a new orientation.

As pointed out before, colistin is a cationic antimicrobial peptide that acts disrupting the bacterial outer membrane facilitating the entrance of other antibiotics. Thus, a combination of colistin with the microcins was explored. When combined with colistin, the **new compound** showed antimicrobial activity, which might suggest that colistin facilitates its entrance across the membrane. MccJ25 interacts with the FhuA outer

membrane receptor to enter the periplasmic space and then with the SbmA inner membrane protein⁵⁵. The findings of the new chemical properties of the modified compound coupled with its synergism with colistin suggested that Val11 is involved in the FhuA binding¹²¹. Therefore, the changes made during hydrolysis treatment, would have caused its inability to enter the cell, preventing the interaction with FhuA but retaining its ability to inhibit the growth of bacteria. Consequently, when colistin disrupted the outer membrane, it allowed the **new compound** to penetrate to the cell and reach its target. Further evidence that the residues Val11 to Pro16 are needed for the MccJ25 uptake arose from the findings of Pavlova *et al.*⁴⁸.

Additionally, an alteration in the orientation of Ile13 has also been seen in the **new compound**. It has been reported that the Ile13 residue in the β -hairpin loop is required for the interaction with FhuA but not for the interaction with the inner membrane protein SbmA¹²².

With the aim to understand the SAR (structure activity relationship) of MccJ25, and find new molecules with enhanced properties, several groups^{48,122} have generated synthetic peptides derived from the microcin sequence by replacing one or various residues. Some have managed to produce peptides with significant antimicrobial activity, although in all cases they have resulted to be less effective than MccJ25.

As a further matter, it had also been observed that the **native MccJ25** did not show activity against other strains of *Salmonella* and *E. coli*. It

was considered that they could have acquired some mechanism of resistance that had allowed them to survive to the microcin activity. When combining the **native MccJ25** with colistin against these resistant strains, no activity differences were observed. Therefore, the mechanism of resistance would not be related to permeability across the cell membrane, as if this were the case, when using colistin, the **native MccJ25** should be able to enter and reach the cell target. These results suggested that the mechanism of resistance of these strains could be related to the intracellular target (RNA Polymerase), as it has been observed that mutations in the *rpoC* gene, which encodes the β 'subunit of RNAP, lead to resistance to MccJ25^{123,124}.

Biofilms are communities of surface-adherent microorganisms that play a significant role in the persistence of bacterial infections, as bacteria that form the biofilm are 10-1000 times more resistant to antibiotics than planktonic bacteria. As several authors have pointed out¹²⁵⁻¹²⁸, bacterial biofilms are one of the major clinical problems, and the eradication of biofilms presents a challenge for antimicrobial chemotherapy.

Many strains of *Salmonella* and *E. coli* are capable of forming biofilms, and this ability has been involved in their undesired persistence in the environment and in industrial, veterinary and medical settings^{129,130}. Given the critical challenges caused by biofilms, the evaluation of the capability of the **native MccJ25** and the **new compound** to eradicate biofilms was seen as interesting. However, it could be confirmed that both microcins had no activity against a stable biofilm of *E. coli* and *S.*

enterica species. For this reason, it has been assumed that neither the **native MccJ25** nor the **new compound** can be regarded as antibiofilm agents.

In terms of cell toxicity, neither of the two compounds displayed cytotoxicity at the highest concentration tested. These results are consistent with other studies done on cancer cell lines where it was also observed that MccJ25 and derived peptides showed very low toxicity¹³¹. In this context, it is relevant to note that low cytotoxicity is attractive to consider an antimicrobial as interesting¹³.

As multidrug-resistant infections have emerged as a challenge in microbiological research and the approaches to fight MDR bacteria are becoming less effective, new strategies are being sought to address this issue. Thus, the combination of microcins with “door-opening molecules” such as colistin or other antimicrobial peptides capable of increasing antimicrobial permeability, could be considered as a promising strategy to fight multidrug-resistant infections.

Being Trimethoprim a first-line antibiotic and due to the emergence and dispersion of antimicrobial resistance and the consequent inefficacy of the co-therapy with Trimethoprim-Sulfamethoxazole against some bacterial infections, it was considered as an optimal antibiotic to be studied. In the context of finding novel antimicrobial options, new Trimethoprim derivatives were explored expecting higher antimicrobial activity, lower levels of cytotoxicity, or new mechanisms of action.

To study the SAR of the new compounds, the chemical alterations previously done should be carefully observed. In this work, the TMP modifications were done at the 2,4-diaminopyrimidine moiety through a multicomponent reaction¹³² called Groebke-Blackburn-Bienaymé reaction (GBBR)¹¹⁸ (Article 2, Scheme 1). This part of the molecule has never been changed before because it is involved in the recognition of the substrate by the DHFR active site. As this core can be decorated with up to four diversity points, the development of the TMP-like molecules was by interaction of the original TMP molecule with aldehydes and isocyanides resulting in a library of 15 analogues. The reactions lead to a great degree of chemical diversity including mono-GBBR derivatives **4**, doubly substituted-GBBR derivatives **5** and derivatives **6** and **7** which were obtained from substitutions in compounds **4** and **5**.

The MIC values showed that, even though TMP was the most potent compound, the analogues **4c**, **4f**, **4h**, **4i**, **4j** and **6b** showed a great activity against *E. coli* ATCC 25922. Some interesting activities were also

detected against *S. aureus* ATCC 29213. It was seen that the reduction of the size of R¹ substitutions provided a better antimicrobial activity.

Some previous studies about TMP-derivatives modified at the trimethoxybenzyl residue showed that some derivatives had an excellent *in vitro* antibacterial activity against *S. aureus* and *E. coli*^{133–135} as seen in the explored TMP analogues. Moreover, some of the new derivatives (**4b**, **5a**, **5b** and **7a**) lacked activity against the strains tested. That confirmed large activity differences between the new TMP-like compounds depending on their chemical modifications and may indicate the unsuitability to bind to their enzyme target.

Additionally, previous studies had shown that TMP derivatives possessed significant antibacterial activity. Several classes of antifolates such as diaminoquinazoline, diaminopyrimidine, diaminopteridine and diaminotriazines have been examined^{135,136}.

When combining the TMP-like compounds with Sulfamethoxazole, high synergistic effects were detected in almost all analogues as seen in the case of TMP.

Concerning the clinical strains tested, some derivatives showed great antibacterial activity against them and high synergistic effect when combined with SMX. Some of the compounds (**4i**, **4h** and **4f**) had similar activities to TMP (Article 2, Table 2). It is important to notice that they were clinical isolates of Methicillin resistant *Staphylococcus aureus*

(MRSA) from Cystic Fibrosis patients. As MRSA infections have become a public health challenge^{137,138}, it is necessary to find new treatments to fight them. In this context, Wyatt *et al.* explored some anti-MRSA DHFR inhibitors with similar interesting activity¹³⁹.

P. aeruginosa PAO1 was fully resistant to TMP and all its derivatives. The combination of TMP and its analogues with SMX also resulted in almost no activity against the tested *P. aeruginosa* strain. These results are consistent with previous studies in which it was reported that the activity of TMP and SMX against *P. aeruginosa* is limited. Several authors have indicated that *P. aeruginosa* efflux pumps play a key role in its antimicrobial resistance, pointing MexAB-OprM and MexCD-OprJ as the responsible efflux systems for Trimethoprim and Sulfamethoxazole extrusion¹⁴⁰⁻¹⁴². Efflux pumps contribute to TMP-SMX resistance in other species such as in *Stenotrophomonas maltophilia*¹⁴³. Moreover, it was detected that the addition of the efflux pump inhibitor PA β N resulted in a strong reduction in the MIC values of TMP and its derivatives against *P. aeruginosa* (Article 3, Table 5). Thus, blocking efflux systems influences bacterial susceptibility to these antimicrobials.

To understand the effect of the antibiotics over time, it is appropriate to study bacterial growth curves. Examining the kinetic profile of the bacteria in the presence of the antimicrobial compounds may give relevant information. When analysing the growth curves of *E. coli* ATCC 25922 and *S. aureus* ATCC 29213 in the presence of chosen compounds with SMX, it had been seen that even subinhibitory concentrations (1/2

MIC or 1/4 MIC) were able to inhibit the bacterial growth or cause a significant delay in respect to the control. All the explored compounds showed substantial reductions in the bacterial growth rate, being **4i** the one which displayed the best results against both strains (Article 2, Figure 4; pg. 29-32 Supplementary material).

In the last part of our studies, all the experiments focused on two of the most potent TMP-like molecules previously investigated (Article 2) comparing them with TMP. From now on, the molecules **4f** and **4i** will be referred to as **1a** and **1b**. Moreover, *Serratia marcescens* NIMA, which is intrinsically resistant to colistin, was included in the last part of the experimental work. The analogues **1a** and **1b** showed similar effect to TMP against this strain.

The ability of the new compounds **1a** and **1b** in combination with SMX to prevent the biofilm formation and to eradicate mature biofilms was investigated. Although compound **1b** was highly active in biofilm prevention, none of the compounds were able to fully eradicate *Staphylococcus aureus* biofilms (neither *S. aureus* ATCC 29213 nor *S. aureus* 8124825998).

Apart from the modifications of existing compounds, another option seen as feasible to tackle antibiotic resistance has been the use of combinations of drugs. Thus, the combination of sublethal concentrations of colistin with the TMP-like compounds was explored. As mentioned above, colistin acts by disrupting the Gram-negative

outer membrane leading to a bacterial permeabilization that permits the desired molecules to reach their target. Moreover, it has been recently demonstrated that low doses of colistin may affect the efflux pumps functionality¹⁴⁴.

When tested in four clinical strains (*Escherichia coli* 220560529, *P. aeruginosa* SJD536, *P. aeruginosa* VH023, and *P. aeruginosa* SJD481) synergistic effects between colistin and TMP/SMX were not detected (FIC_i ≥ 0.5 and < 4). Strikingly, a strong synergism was observed between colistin and TMP-like compounds in TMP-susceptible/colistin-resistant *S. marcescens*. This may suggest that the transport of these compounds through the Gram-negative bacterial outer membrane is a limitation.

Noteworthy, some positive effects were observed between colistin and TMP-SMX in preliminary plate experiments in *E. coli*, *P. aeruginosa* and *S. marcescens*. These findings were in agreement with the relatively low FIC_i detected on those strains, although in the colistin-susceptible bacteria, the lethality of colistin masked possible synergisms when using the checkerboard method. In other words, the higher toxicity of colistin in this scenario may kill a significant fraction of the population and TMP-SMX the rest. Therefore, the MIC values of the combined antimicrobials decrease slightly but not enough to be considered as synergistic.

Strong synergism was detected when testing the effects of combinations between sublethal concentrations of TMP-like compounds, SMX, and colistin in real-time against the *E. coli*, *P. aeruginosa* and *S. marcescens* strains tested. It must be emphasized that in some cases bacterial growth was nearly abolished (Article 3, Figure 3). Remarkably, in the case of *S. marcescens*, its inner membrane remains intact while its outer membrane, the efflux pump drug extrusion and the production of prodigiosin are severely affected by colistin¹⁴⁵. Thus, the alterations previously seen by transmission electron microscopy (TEM) on its outer membrane¹⁴⁶ do not affect the bacterial viability of *Serratia*. In fact, the integrity of the outer membrane is not only determinant in the degree of susceptibility of Gram-negative bacteria to antibiotics but also in the susceptibility/resistance response. Thus, in *Serratia* (fully resistant to colistin and susceptible to TMP and TMP-like molecules) the induction of injuries in the outer membrane, which has no effect on bacterial viability, causes an increase in the susceptibility of these molecules. Actually, this effect may be due to the dysfunctionality of efflux pumps that may not be enough to generate resistance but may diminish the intracellular concentration of antimicrobial compounds. As our group has pointed out before¹⁴⁴ the outer membrane integrity is needed for a correct functionality of efflux pumps.

It is worth to notice that the nearly complete abolition or prolonged delay of growth in the three studied bacteria indicated an alteration of the hydrophobic permeability barrier of the lipopolysaccharide outer

membrane. Therefore, it is clear that sublethal doses of colistin may facilitate internalization of the DHFR inhibitors which, once inside the cell, are able to inhibit the bacterial growth. As Armengol *et al.* pointed out for other antimicrobials such as linezolid and rifampin¹¹¹, sublethal concentrations of colistin could be used as an enhancer of bacterial susceptibility to TMP and TMP-like compounds. The use of very low concentrations of these three drugs would prevent colistin toxicity.

The interest for the combination of antifolates with colistin to enhance the permeabilization of the outer membrane of Gram-negative bacteria has led to its previous exploration as an option to fight against MDR bacteria. A strong synergistic effect of colistin in combination with TMP/SMX has been observed both *in vitro* and *in vivo* (in a *Galleria mellonella* model) against carbapenem-resistant *A. baumannii* isolates (CRAB)^{147,148} and against carbapenem-resistant *Klebsiella pneumoniae* (CRKN)¹⁴⁹. Similarly, other groups evaluated the effect of these drugs against colistin susceptible and resistant strains of *A. baumannii*, *P. aeruginosa*, and *K. pneumoniae*. They reported an interesting synergy between TMP-SMX and colistin against a colistin-resistant *P. aeruginosa* strain, suggesting that colistin resistance is favourable to the antimicrobial activity of these combinations¹⁵⁰.

With the aim to explore the mechanism of action of the TMP-like molecules and compare them with the one of TMP, an enzymatic assay was performed. It was detected that, like TMP, compounds **1a** and **1b** inhibited the activity of the DHFR enzyme by > 80%. To detect whether

the new molecules had the same active site as TMP and thus, interacted with DHFR in the same place, different concentrations of the DHFR cofactor NADPH and the substrate H₂F were added to check if they displaced the inhibitors. Surprisingly, the increase in the concentrations of both NADPH and H₂F resulted in a reversion of the inhibition. To further understand these enzymatic results, a molecular approach with compound **1a** was performed by Prof. Javier Luque. The docking model showed that the heterocyclic ring of the compound **1a** fills the pocket occupied by the nicotinamide ring of NADPH. On the other hand, the trimethoxybenzene ring overlaps the same moiety present in TMP. Therefore, it could be suggested that the binding of **1a** would compete with the H₂F but would also prevent the correct recognition of NADPH. These results may corroborate the enzymatic findings since the **1a** compound interacts with the H₂F binding site of the *E. coli* DHFR while avoiding the recognition of the cofactor. Thus, when increasing the concentrations of NADPH and H₂F, in both cases the inhibition is reversed because **1a** interacts with both.

Some research groups have reported the characterization of the catalytic mechanism of action of the *E. coli* DHFR enzyme. They emphasized that a flexible loop centred on residue Met20 was where the co-factor bound, and the catalysis occurred¹⁵¹. Moreover, they pointed out that DHFR enzymes can be effectively targeted while not interfering with the human DHFR due to clear differences between them¹⁵².

As seen above, a crucial condition for an antibiotic candidate is the ability to kill bacteria without damaging host cells. It was seen that neither of the two TMP-like compounds was toxic to the tested cell lines. Hence, the changes made in the TMP analogues do not increase the toxicity of the molecules, making them suitable candidates to be used as an antibiotic.

In summary, the new TMP-like compounds may open new possibilities to fight bacterial infections. The demonstration of the synergistic effect of the combinations of colistin with antifolates in Gram-negative bacteria should renew interest in the use of TMP and TMP-like molecules.

5. CONCLUSIONS

1. The chemical modification of MccJ25 during the hydrolytic treatment resulted in a new peptide. The new compound lost its antimicrobial activity on originally susceptible strains because it failed to cross the bacterial outer membrane as it could not be recognized by FhuA.
2. The new MccJ25 compound acted synergistically with sublethal concentrations of colistin as the polymyxin facilitated the microcin entrance across the membrane. Moreover, the chemical modifications did not affect the interaction with the target and, once inside the cell, the new compound retained its ability to inhibit the growth of bacteria.
3. Neither the native MccJ25 nor the new compound can be regarded as antibiofilm agents just as neither of the two compounds can be considered as cytotoxic.
4. Some of the new TMP derivatives showed antibacterial activity against *Escherichia coli* and *Staphylococcus aureus* similar to that of TMP. Almost all the new TMP-like compounds acted synergistically with SMX; even against methicillin resistant *S. aureus*.
5. TMP derivatives were active in biofilm prevention whereas neither TMP nor compounds 1a and 1b were able to fully

eradicate *S. aureus* biofilms (neither *S. aureus* ATCC 29213 nor *S. aureus* 8124825998). On the other hand, at concentrations at which the products behave as good antibacterials, the cytotoxicity on HepG2 and L-929 cell lines was almost negligible.

6. *Pseudomonas aeruginosa* PAO1 was fully resistant to TMP and all its derivatives as well as to the combination of TMP-SMX. Moreover, it can be suggested that blocking their efflux systems may influence in *P. aeruginosa* susceptibility to these antimicrobials.
7. Being able to cross the outer membrane is crucial for antibiotics to kill gram-negative bacteria. The combination of TMP, TMP-like molecules and SMX with colistin enhances their antimicrobial efficacy against *E. coli*, *P. aeruginosa* and *Serratia marcescens* by permeabilizing the cells.
8. Compounds 1a and 1b, like TMP, strongly inhibited the activity of the *E. coli* DHFR. The inhibition was reversed with increasing concentrations of NADPH and H₂F suggesting that both molecules interact with the analogues during inhibition.
9. As seen in the docking model, the heterocyclic ring of the compound 1a fills the pocket occupied by the nicotinamide ring

of NADPH. Thus, the binding of **1a** would compete with the H₂F and would also prevent the correct recognition of NADPH.

10. As the search of new antimicrobial compounds is one of the main pathways to overtake bacterial resistance to antibiotics, it should be emphasized that all putative compounds should be tested in conditions in which outer membrane role as permeability barrier is inactivated. Their assay together with sublethal concentrations of colistin is proposed as one of the methods of election.

6.REFERENCES

1. Ruiz, N., Kahne, D. & Silhavy, T. J. Advances in understanding bacterial outer-membrane biogenesis. *Nat. Rev. Microbiol.* **4**, 57–66 (2006).
2. Christiansen, G. *General microbiology, seventh edition. FEBS Letters* vol. 356 (1994).
3. Popescu, A. & Doyle, R. J. The Gram Stain after More than a Century. *Biotech. Histochem.* **71**, 145–151 (1996).
4. Silhavy, T. J., Kahne, D. & Walker, S. The Bacterial Cell Envelope. *Cold Spring Harb. Perspect. Biol.* **2**, 1–16 (2010).
5. Swoboda, J. G., Campbell, J., Meredith, T. C. & Walker, S. Wall teichoic acid function, biosynthesis, and inhibition. *ChemBioChem* **11**, 35–45 (2010).
6. Wu, E. L. *et al.* Molecular dynamics and NMR spectroscopy studies of E. coli lipopolysaccharide structure and dynamics. *Biophys. J.* **105**, 1444–1455 (2013).
7. Nikaido, H. Outer Membrane, Gram-Negative Bacteria. in *Encyclopedia of Microbiology* 439–452 (Elsevier Inc, 2009) doi:10.1016/B978-012373944-5.00050-X.
8. Blanco, P. *et al.* Bacterial Multidrug Efflux Pumps: Much More Than Antibiotic Resistance Determinants. *Microorganisms* **4**, 14 (2016).
9. Du, D. *et al.* Multidrug efflux pumps: structure, function and regulation. *Nat. Rev. Microbiol.* **16**, 523–539 (2018).
10. Li, X. Z., Plésiat, P. & Nikaido, H. The challenge of efflux-mediated antibiotic resistance in Gram-negative bacteria. *Clin. Microbiol. Rev.* **28**,

- 337–418 (2015).
11. Shi, X. *et al.* In situ structure and assembly of the multidrug efflux pump AcrAB-TolC. *Nat. Commun.* **10**, 4–9 (2019).
 12. Lewis, K. The Science of Antibiotic Discovery. *Cell* **181**, 29–45 (2020).
 13. Singh, S. B., Young, K. & Silver, L. L. What is an “ ideal ” antibiotic ? Discovery challenges and path forward. *Biochem. Pharmacol.* **133**, 63–73 (2017).
 14. Silver, L. L. A Gestalt approach to Gram-negative entry. *Bioorganic Med. Chem.* **24**, 6379–6389 (2016).
 15. Brunel, J. Antibiosis from Pasteur to Fleming. *J. Hist. Med. Allied Sci.* **6**, 287–301 (1951).
 16. Vuillemin, P. Antibiose et symbiose. *Compte Rendu la Assoc. Française pour l'Avancement des Sci.* **2**, 525–543 (1889).
 17. Kohanski, M. A., Dwyer, D. J. & Collins, J. J. How antibiotics kill bacteria: From targets to networks. *Nat. Rev. Microbiol.* **8**, 423–435 (2010).
 18. Lewis, K. Platforms for antibiotic discovery. *Nat. Rev. Drug Discov.* **12**, 371–387 (2013).
 19. Wright, G. D. Q&A: Antibiotic resistance: Where does it come from and what can we do about it? *BMC Biol.* **8**, (2010).
 20. Hutchings, M., Truman, A. & Wilkinson, B. Antibiotics: past, present and future. *Curr. Opin. Microbiol.* **51**, 72–80 (2019).

21. Gould, K. Antibiotics: From prehistory to the present day. *J. Antimicrob. Chemother.* **71**, 572–575 (2016).
22. Tulchinsky, T. H. & Varavikova, E. A. *The New Public Health.* (2015).
23. Fracastoro, G. & Busacchi, V. *Il contagio, le malattie contagiose e la loro cura.* (1950).
24. Bentley, R. Bartolomeo Gosio, 1863-1944: An Appreciation. **48**, (2001).
25. Durand, G. A., Raoult, D. & Dubourg, G. Antibiotic discovery: history, methods and perspectives. *Int. J. Antimicrob. Agents* **53**, 371–382 (2019).
26. Aminov, R. History of antimicrobial drug discovery: Major classes and health impact. *Biochem. Pharmacol.* **133**, 4–19 (2017).
27. da Cunha, B. R., Fonseca, L. P. & Calado, C. R. C. Antibiotic discovery: Where have we come from, where do we go? *Antibiotics* **8**, (2019).
28. Fleming, A. Alexander Fleming - Nobel Lecture. Available from: <https://www.nobelprize.org/prizes/medicine/1945/fleming/lecture/> (1945).
29. Sköld, O. Sulfonamide resistance: Mechanisms and trends. *Drug Resist. Updat.* **3**, 155–160 (2000).
30. Waksman, S. A., Schatz, A. & Reynolds, D. M. Production of antibiotic substances by actinomycetes. *Ann. N. Y. Acad. Sci.* **1213**, 112–124 (2010).
31. Villa, T. G. & Viñas, M. *New weapons to control bacterial growth.* (2016). doi:10.1007/978-3-319-28368-5.

32. Gratia, A. Sur un remarquable exemple d'antagonisme entre deux souches de colibacille. *Compt. Rend. Soc. Biol.* **93**, 1040–1042 (1925).
33. Fredericq, P. & Levine, M. Antibiotic interrelationships among the enteric group of bacteria. *J. Bacteriol.* **54**, 27 (1947).
34. Yang, S. C., Lin, C. H., Sung, C. T. & Fang, J. Y. Antibacterial activities of bacteriocins: Application in foods and pharmaceuticals. *Front. Microbiol.* **5**, 1–10 (2014).
35. Simons, A., Alhanout, K. & Duval, R. E. Bacteriocins, antimicrobial peptides from bacterial origin: Overview of their biology and their impact against multidrug-resistant bacteria. *Microorganisms* **8** (2020).
36. Baquero, F., Lanza, V. F., Baquero, M. R., del Campo, R. & Bravo-Vázquez, D. A. Microcins in Enterobacteriaceae: Peptide Antimicrobials in the Eco-Active Intestinal Chemosphere. *Front. Microbiol.* **10**, 1–25 (2019).
37. Dactibase. Available from: <http://bactibase.hammamilab.org/main.php>.
38. Baquero, F. & Moreno, F. The microcins. *FEMS Microbiol. Lett.* **23**, 117–124 (1984).
39. Baquero, F. Metagenomic epidemiology: A public health need for the control of antimicrobial resistance. *Clin. Microbiol. Infect.* **18**, 67–73 (2012).
40. Aguilar, A., Perez-Diaz, J. C., Baquero, F. & Asensio, C. Microcin 15m from *Escherichia coli*: Mechanism of antibiotic action. *Antimicrob. Agents Chemother.* **21**, 381–386 (1982).

41. Telhig, S., Ben Said, L., Zirah, S., Fliss, I. & Rebuffat, S. Bacteriocins to Thwart Bacterial Resistance in Gram Negative Bacteria. *Front. Microbiol.* **11**, (2020).
42. Arnison, P. G. *et al.* Ribosomally synthesized and post-translationally modified peptide natural products: Overview and recommendations for a universal nomenclature. *Nat. Prod. Rep.* **30**, 108–160 (2013).
43. Duquesne, S., Destoumieux-Garzón, D., Peduzzi, J. & Rebuffat, S. Microcins, gene-encoded antibacterial peptides from enterobacteria. *Nat. Prod. Rep.* **24**, 708–734 (2007).
44. Salomón, R. A. & Fariás, R. N. Microcin 25, a novel antimicrobial peptide produced by *Escherichia coli*. *J. Bacteriol.* **174**, 7428–7435 (1992).
45. Salomon, R. A. & Farias, R. N. The *fhuA* protein is involved in microcin 25 uptake. *J. Bacteriol.* **175**, 7741–7742 (1993).
46. Solbiati, J. O., Ciaccio, M., Parías, R. N. & Salomón, R. A. Genetic analysis of plasmid determinants for microcin J25 production and immunity. *J. Bacteriol.* **178**, 3661–3663 (1996).
47. Solbiati, J. O. *et al.* Sequence analysis of the four plasmid genes required to produce the circular peptide antibiotic microcin J25. *J. Bacteriol.* **181**, 2659–2662 (1999).
48. Pavlova, O., Mukhopadhyay, J., Sineva, E., Ebright, R. H. & Severinov, K. Systematic structure-activity analysis of microcin J25. *J. Biol. Chem.* **283**, 25589–25595 (2008).
49. Smits, S. H. J. & Schmitt, L. Self-immunity to antibacterial peptides by

- ABC transporters. **594**, 3920–3942 (2020).
50. Hammami, R. *et al.* Lasso-inspired peptides with distinct antibacterial mechanisms. *Amino Acids* **47**, 417–428 (2015).
51. Bellomio, A., Vincent, P. A., Arcuri, B. F. De, Morero, R. D. & Fari, R. N. The microcin J25 β -hairpin region is important for antibiotic uptake but not for RNA polymerase and respiration inhibition. **325**, 1454–1458 (2004).
52. Semenova, E., Yuzenkova, Y., Peduzzi, J., Rebuffat, S. & Severinov, K. Structure-activity analysis of microcin J25: Distinct parts of the threaded lasso molecule are responsible for interaction with bacterial RNA polymerase. *J. Bacteriol.* **187**, 3859–3863 (2005).
53. Blond, A. *et al.* The cyclic structure of microcin J25, a 21-residue peptide antibiotic from *Escherichia coli*. *Eur. J. Biochem.* **259**, 747–756 (1999).
54. Martin-Gómez, H., Jorba, M., Albericio, F., Viñas, M. & Tulla-Puche, J. Chemical modification of microcin j25 reveals new insights on the stereospecific requirements for antimicrobial activity. *Int. J. Mol. Sci.* **20** (2019).
55. Mathavan, I. *et al.* Structural basis for hijacking siderophore receptors by antimicrobial lasso peptides. *Nat. Chem. Biol.* **10**, 340–342 (2014).
56. Salomon, R. A. & Farias, R. N. The peptide antibiotic microcin 25 is imported through the tonB pathway and the sbmA protein. *J. Bacteriol.* **177**, 3323–3325 (1995).
57. Mathavan, I. & Beis, K. The role of bacterial membrane proteins in the

- internalization of microcin MccJ25 and MccB17. *Biochem. Soc. Trans.* **40**, 1539–1543 (2012).
58. Hickman, S. J., Cooper, R. E. M., Bellucci, L., Paci, E. & Brockwell, D. J. Gating of TonB-dependent transporters by substrate-specific forced remodelling. *Nat. Commun.* **8**, 1–12 (2017).
59. Bae, B., Feklistov, A., Lass-napiorkowska, A., Landick, R. & Darst, S. A. Structure of a bacterial RNA polymerase holoenzyme open promoter complex. *Elife* 1–23 (2015).
60. Vassylyev, D. G. *et al.* Crystal structure of a bacterial RNA polymerase holoenzyme at resolution. *Nature* **417**, 0–7 (2002).
61. Finn, R. D., Orlova, E. V, Gowen, B., Buck, M. & Heel, M. Van. Escherichia coli RNA polymerase core and holoenzyme structures. **19**, 6833–6844 (2000).
62. Zhang, G. *et al.* Crystal Structure of Thermus aquaticus resolution core RNA Polymerase at 3 . 3 Å. **98**, 811–824 (1999).
63. Mukhopadhyay, J., Sineva, E., Knight, J., Levy, R. M. & Ebright, R. H. Antibacterial peptide Microcin J25 inhibits transcription by binding within and obstructing the RNA polymerase secondary channel. *Mol. Cell* **14**, 739–751 (2004).
64. Campbell, E. A. *et al.* Structural Mechanism for Rifampicin Inhibition of Bacterial RNA Polymerase. **104**, 901–912 (2001).
65. Bellomio, A., Vincent, P. A., Arcuri, B. F. De, Fari, R. N. & Morero, R. D. Microcin J25 Has Dual and Independent Mechanisms of Action in

- Escherichia coli : RNA Polymerase Inhibition and Increased Superoxide Production . **189**, 4180–4186 (2007).
66. Galván, A. E. *et al.* Cytochromes bd-I and bo3 are essential for the bactericidal effect of microcin J25 on Escherichia coli cells. *Biochim. Biophys. Acta - Bioenerg.* **1859**, 110–118 (2018).
67. Estrada, A., Wright, D. L. & Anderson, A. C. Antibacterial antifolates: From development through resistance to the next generation. *Cold Spring Harb. Perspect. Med.* **6**, 1–9 (2016).
68. Bertacine Dias, M. V., Santos, J. C., Libreros-Zúñiga, G. A., Ribeiro, J. A. & Chavez-Pacheco, S. M. Folate biosynthesis pathway: Mechanisms and insights into drug design for infectious diseases. *Future Med. Chem.* **10**, 935–959 (2018).
69. Bermingham, A. & Derrick, J. P. The folic acid biosynthesis pathway in bacteria: Evaluation of potential for antibacterial drug discovery. *BioEssays* **24**, 637–648 (2002).
70. Fischer, M., Thöny, B. & Leimkühler, S. The biosynthesis of folate and pterins and their enzymology. *Compr. Nat. Prod. II Chem. Biol.* **7**, 599–648 (2010).
71. Pedrola, M. *et al.* Multicomponent Reactions Upon the Known Drug Trimethoprim as a Source of Novel Antimicrobial Agents. *Front. Chem.* **7**, 27–31 (2019).
72. Gertrude Belle Elion (1918-99) Trudy Elion was one of only half a dozen. **398**, 27709 (1999).

-
73. Huovinen, P. Resistance to Trimethoprim-Sulfamethoxazole. **32**, (2001).
74. National Centre for Biotechnology Information. PubChem Compound Summary for CID 5578, Trimethoprim. <https://pubchem.ncbi.nlm.nih.gov/compound/5578> (2021).
75. WHO. *21th World Health Organization Model List of Essential Medicines*. (2019).
76. Schweitzer, B. I., Dicker, A. P. & Bertino, J. R. Dihydrofolate reductase as a therapeutic target. *FASEB J.* **4**, 2441–2452 (1990).
77. Srinivasan, B. & Skolnick, J. Insights into the slow-onset tight-binding inhibition of *Escherichia coli* dihydrofolate reductase: Detailed mechanistic characterization of pyrrolo [3,2-f] quinazoline-1,3-diamine and its derivatives as novel tight-binding inhibitors. *FEBS J.* **282**, 1922–1938 (2015).
78. Wróbel, A., Arciszewska, K., Maliszewski, D. & Drozdowska, D. Trimethoprim and other nonclassical antifolates an excellent template for searching modifications of dihydrofolate reductase enzyme inhibitors. *J. Antibiot. (Tokyo)*. **73**, 5–27 (2020).
79. Liu, C. T. *et al.* Functional significance of evolving protein sequence in dihydrofolate reductase from bacteria to humans. *Proc. Natl. Acad. Sci. U. S. A.* **110**, 10159–10164 (2013).
80. Shrimpton, P. & Allemann, R. K. Role of water in the catalytic cycle of *E. coli* dihydrofolate reductase. *Protein Sci.* **11**, 1442–1451 (2002).
81. Rod, T. H. & Brooks, C. L. How dihydrofolate reductase facilitates

- protonation of dihydrofolate. *J. Am. Chem. Soc.* **125**, 8718–8719 (2003).
82. Boehr, D. D., McElheny, D., Dyson, H. J. & Wrightt, P. E. The dynamic energy landscape of dihydrofolate reductase catalysis. *Science (80-.)*. **313**, 1638–1642 (2006).
83. Cao, H., Gao, M., Zhou, H. & Skolnick, J. The crystal structure of a tetrahydrofolate-bound dihydrofolate reductase reveals the origin of slow product release. *Commun. Biol.* **1**, 1–10 (2018).
84. Mathews, C. K., Spencer, A. J. & Van Holde, K. E. *Bioquímica*. (2013).
85. National Centre for Biotechnology Information. PubChem Compound Summary for CID 5329, Sulfamethoxazole. <https://pubchem.ncbi.nlm.nih.gov/compound/5329#section=2D-Structure> (2021).
86. El-Sayed Ahmed, M. A. E. G. *et al.* Colistin and its role in the Era of antibiotic resistance: an extended review (2000–2019). *Emerg. Microbes Infect.* **9**, 868–885 (2020).
87. Hamel, M., Rolain, J. M. & Baron, S. A. The history of colistin resistance mechanisms in bacteria: Progress and challenges. *Microorganisms* **9**, 1–18 (2021).
88. Baron, S., Hadjadj, L., Rolain, J. M. & Olaitan, A. O. Molecular mechanisms of polymyxin resistance: knowns and unknowns. *Int. J. Antimicrob. Agents* **48**, 583–591 (2016).
89. Karaiskos, I., Souli, M., Galani, I. & Giamarellou, H. Colistin: still a lifesaver for the 21st century? *Expert Opin. Drug Metab. Toxicol.* **13**, 59–

- 71 (2017).
90. Poirel, L., Aurélie, J. & Nordmann, P. Polymyxins: Antibacterial Activity, Susceptibility Testing, and Resistance Mechanisms Encoded by Plasmids or Chromosomes Laurent Poirel^{a,b,c}, Aurélie Jayola^{a,b,c} and Patrice Nordmann. *Clin. Microbiol. Rev.* **30**, 557–596 (2017).
 91. Colistin | C52H98N16O13 - PubChem. <https://pubchem.ncbi.nlm.nih.gov/compound/Colistin#section=Structures>.
 92. Upert, G., Luther, A., Obrecht, D. & Ermert, P. Emerging peptide antibiotics with therapeutic potential. *Med. Drug Discov.* **9**, (2021).
 93. Pendleton, J. N., Gorman, S. P. & Gilmore, B. F. Clinical relevance of the ESKAPE pathogens. *Expert Rev. Anti. Infect. Ther.* **11**, 297–308 (2013).
 94. Centers for Disease Control and Prevention. About Antibiotic Resistance | Antibiotic/Antimicrobial Resistance | CDC. <https://www.cdc.gov/drugresistance/about.html>.
 95. Munita, J. M. & Arias, C. A. Mechanisms of antibiotic resistance. *Virulence Mech. Bact. Pathog.* 481–511 (2016).
 96. Magiorakos, A. *et al.* Bacteria: an International Expert Proposal for Interim Standard Definitions for Acquired Resistance. (2011).
 97. Mulani, M. S., Kamble, E. E., Kumkar, S. N., Tawre, M. S. & Pardesi, K. R. Emerging strategies to combat ESKAPE pathogens in the era of antimicrobial resistance: A review. *Front. Microbiol.* **10**, (2019).
 98. WHO. *2020 antibacterial agents in clinical and preclinical development.*

- (2021).
99. O'Neill, J. *Tackling drug-resistant infections globally. Final report and recommendations.* (2016) doi:10.4103/2045-080x.186181.
 100. Magiorakos, A. P. *et al.* Multidrug-resistant, extensively drug-resistant and pandrug-resistant bacteria: An international expert proposal for interim standard definitions for acquired resistance. *Clin. Microbiol. Infect.* **18**, 268–281 (2012).
 101. Tacconelli, E. *et al.* Discovery, research, and development of new antibiotics: the WHO priority list of antibiotic-resistant bacteria and tuberculosis. *Lancet Infect. Dis.* **18**, 318–327 (2018).
 102. WHO. *Prioritization of pathogens to guide discovery, research and development of new antibiotics for drug resistant bacterial infections, including tuberculosis.* (2017).
 103. Rice, L. B. Federal funding for the study of antimicrobial resistance in nosocomial pathogens: No ESKAPE. *J. Infect. Dis.* **197**, 1079–1081 (2008).
 104. Ryan, K. J. & Ray, C. G. *Sherris Medical Microbiology.* (2003).
 105. Allen, H. K. *et al.* Call of the wild: Antibiotic resistance genes in natural environments. *Nat. Rev. Microbiol.* **8**, 251–259 (2010).
 106. The Pew Charitable Trusts. Tracking the Global Pipeline of Antibiotics in Development . Available from: <https://www.pewtrusts.org/en/research-and-analysis/issue-briefs/2021/03/tracking-the-global-pipeline-of-antibiotics-in-development>.

107. O'Rourke, A. *et al.* Mechanism-of-action classification of antibiotics by global transcriptome profiling. *Antimicrob. Agents Chemother.* **64**, 1–15 (2020).
108. Wright, P. M., Seiple, I. B. & Myers, A. G. The Evolving Role of Chemical Synthesis in Antibacterial Drug Discovery. *Angew. Chemie Int. Ed.* **53**, 8840–8869 (2014).
109. Tyers, M. & Wright, G. D. Drug combinations: a strategy to extend the life of antibiotics in the 21st century. *Nat. Rev. Microbiol.* **17**, 141–155 (2019).
110. Li, Q. *et al.* Outer-membrane-acting peptides and lipid II-targeting antibiotics cooperatively kill Gram-negative pathogens. *Commun. Biol.* **4**, 1–11 (2021).
111. Armengol, E., Asunción, T., Viñas, M. & Sierra, J. M. When Combined with Colistin, an Otherwise Ineffective Rifampicin–Linezolid Combination Becomes Active in *Escherichia coli*, *Pseudomonas aeruginosa*, and *Acinetobacter baumannii*. *Microorganisms* **8**, 86 (2020).
112. Kortright, K. E., Chan, B. K., Koff, J. L. & Turner, P. E. Review Phage Therapy: A Renewed Approach to Combat Antibiotic-Resistant Bacteria. *Cell Host Microbe* **25**, 219–232 (2019).
113. Sierra, J. M. & Viñas, M. Future prospects for Antimicrobial peptide development: peptidomimetics and antimicrobial combinations. *Expert Opin. Drug Discov.* **00**, 1–4 (2021).
114. Sans-Serramitjana, E. *et al.* Free and Nanoencapsulated Tobramycin: Effects on Planktonic and Biofilm Forms of *Pseudomonas*.

- Microorganisms* **5**, 35 (2017).
115. Pang, Z., Raudonis, R., Glick, B. R., Lin, T. & Cheng, Z. Antibiotic resistance in *Pseudomonas aeruginosa*: mechanisms and alternative therapeutic strategies. *Biotechnol. Adv.* **37**, 177–192 (2019).
116. Theuretzbacher, U. & Outterson, K. The global preclinical antibacterial pipeline. *Nat. Rev. Microbiol.* **18**, 275–285 (2020).
117. Theuretzbacher, U. & Piddock, L. J. V. Review Non-traditional Antibacterial Therapeutic Options and Challenges. *Cell Host Microbe* **26**, 61–72 (2019).
118. Shaaban, S. & Abdel-Wahab, B. F. Groebke–Blackburn–Bienaymé multicomponent reaction: emerging chemistry for drug discovery. *Mol. Divers.* **20**, 233–254 (2016).
119. Assis, L. M., Nedeljković, M. & Dessen, A. New strategies for targeting and treatment of multi-drug resistant *Staphylococcus aureus*. *Drug Resist. Updat.* **31**, 1–14 (2017).
120. Bosák, J., Hrala, M., Micenková, L. & Šmajš, D. Non-antibiotic antibacterial peptides and proteins of *Escherichia coli*: efficacy and potency of bacteriocins. *Expert Rev. Anti. Infect. Ther.* **19**, 309–322 (2021).
121. Semenova, E., Yuzenkova, Y., Peduzzi, J., Rebuffat, S. & Severinov, K. Structure-activity analysis of microcin J25: Distinct parts of the threaded lasso molecule are responsible for interaction with bacterial RNA polymerase. *J. Bacteriol.* **187**, 3859–3863 (2005).
122. Socias, S. B., Severinov, K. & Salomon, R. A. The Ile13 residue of

- microcin J25 is essential for recognition by the receptor FhuA, but not by the inner membrane transporter SbmA. *FEMS Microbiol. Lett.* **301**, 124–129 (2009).
123. Delgado, M. A., Rintoul, M. R., Fariás, R. N. & Salomón, R. A. Escherichia coli RNA polymerase is the target of the cyclopeptide antibiotic microcin J25. *J. Bacteriol.* **183**, 4543–4550 (2001).
124. Yuzenkova, J. *et al.* Mutations of bacterial RN A polymerase leading to resistance to microcin J25. *J. Biol. Chem.* **277**, 50867–50875 (2002).
125. Rabin, N. *et al.* Biofilm formation mechanisms and targets for developing antibiofilm agents. *Future Med. Chem.* **7**, 493–512 (2015).
126. Sharma, D., Misba, L. & Khan, A. U. Antibiotics versus biofilm: An emerging battleground in microbial communities. *Antimicrob. Resist. Infect. Control* **8**, 1–10 (2019).
127. Verderosa, A. D., Totsika, M. & Fairfull-Smith, K. E. Bacterial Biofilm Eradication Agents: A Current Review. *Front. Chem.* **7**, 1–17 (2019).
128. Hall-Stoodley, L., Costerton, J. W. & Stoodley, P. Bacterial biofilms: From the natural environment to infectious diseases. *Nat. Rev. Microbiol.* **2**, 95–108 (2004).
129. Baugh, S., Ekanayaka, A. S., Piddock, L. J. V & Webber, M. A. Loss of or inhibition of all multidrug resistance efflux pumps of Salmonella enterica serovar Typhimurium results in impaired ability to form a biofilm. 2409–2417 (2012).
130. Lüthje, P. & Brauner, A. Virulence Factors of Uropathogenic E. coli and

- Their Interaction with the Host. *Adv. Microb. Physiol.* **65**, 337–372 (2014).
131. Soudy, R., Wang, L. & Kaur, K. Synthetic peptides derived from the sequence of a lasso peptide microcin J25 show antibacterial activity. *Bioorganic Med. Chem.* **20**, 1794–1800 (2012).
132. Insuasty, D., Castillo, J., Becerra, D., Rojas, H. & Abonia, R. Synthesis of biologically active molecules through multicomponent reactions. *Molecules* **25**, (2020).
133. Rashid, U. *et al.* Design, synthesis, antibacterial activity and docking study of some new trimethoprim derivatives. *Bioorganic Med. Chem. Lett.* **26**, 5749–5753 (2016).
134. Zhou, W., Scocchera, E. W., Wright, D. L. & Anderson, A. C. Antifolates as Effective Antimicrobial Agents: New Generations of Trimethoprim Analogs. *Med. Chem. Commun.* **4**, 908–915 (2013).
135. Wróbel, A., Maliszewski, D., Baradyn, M. & Drozdowska, D. Trimethoprim: An old antibacterial drug as a template to search for new targets. Synthesis, biological activity and molecular modeling study of novel trimethoprim analogs. *Molecules* **25**, (2020).
136. Srinivasan, B., Tonddast-Navaei, S. & Skolnick, J. Ligand binding studies, preliminary structure–activity relationship and detailed mechanistic characterization of 1-phenyl-6,6-dimethyl-1,3,5-triazine-2,4-diamine derivatives as inhibitors of *Escherichia coli* dihydrofolate reductase. *Eur. J. Med. Chem.* **103**, 600–614 (2015).
137. Dolce, D. *et al.* Methicillin-resistant *Staphylococcus aureus* eradication in cystic fibrosis patients: A randomized multicenter study. *PLoS One*

- 14, 1–15 (2019).
138. Liu, W. *et al.* Microbial Pathogenesis Emerging resistance mechanisms for 4 types of common anti-MRSA antibiotics in *Staphylococcus aureus* : A comprehensive review. *Microb. Pathog.* **156**, 104915 (2021).
139. Wyatt, E. E. *et al.* Identification of an anti-MRSA dihydrofolate reductase inhibitor from a diversity-oriented synthesis. *Chem. Commun.* 4962–4964 (2008).
140. Köhler, T. *et al.* Multidrug efflux in intrinsic resistance to trimethoprim and sulfamethoxazole in *Pseudomonas aeruginosa*. *Antimicrob. Agents Chemother.* **40**, 2288–2290 (1996).
141. Terzi, H. A., Kulah, C. & Ciftci, İ. H. The effects of active efflux pumps on antibiotic resistance in *Pseudomonas aeruginosa*. *World J. Microbiol. Biotechnol.* **30**, 2681–2687 (2014).
142. Dreier, J. & Ruggerone, P. Interaction of antibacterial compounds with RND efflux pumps in *Pseudomonas aeruginosa*. *Front. Microbiol.* **6**, 1–21 (2015).
143. Sánchez, M. B. & Martínez, J. L. The efflux pump SmeDEF contributes to trimethoprim-sulfamethoxazole resistance in *Stenotrophomonas maltophilia*. *Antimicrob. Agents Chemother.* **59**, 4347–4348 (2015).
144. Armengol, E. *et al.* Efficacy of combinations of colistin with other antimicrobials involves membrane fluidity and efflux machinery. *Infect. Drug Resist.* **Volume 12**, 2031–2038 (2019).
145. Lauferska, U., Viñas M., Lorén, J. G. Enhancement by polymyxin B of

- proline-induced prodigiosin biosynthesis in non-proliferating cells of *Serratia marcescens*. *Microbiologica* (1983).
146. Rudilla, H. *et al.* Synergistic antipseudomonal effects of synthetic peptide AMP38 and carbapenems. *Molecules* **21**, 1–12 (2016).
147. Khalil, M. A. F., Moawad, S. S. & Hefzy, E. M. In vivo activity of co-trimoxazole combined with colistin against *Acinetobacter baumannii* producing oxa-23 in a galleria mellonella model. *J. Med. Microbiol.* **68**, 52–59 (2019).
148. Nepka, M. *et al.* In vitro bactericidal activity of trimethoprim-sulfamethoxazole alone and in combination with colistin against carbapenem-resistant *Acinetobacter baumannii* clinical isolates. *Antimicrob. Agents Chemother.* **60**, 6903–6906 (2016).
149. Su, J. *et al.* In vitro bactericidal activity of trimethoprim-sulfamethoxazole/colistin combination against carbapenem-resistant *Klebsiella pneumoniae* clinical isolates. *Microb. Drug Resist.* **25**, 152–156 (2019).
150. Vidailiac, C., Benichou, L. & Duval, R. E. In vitro synergy of colistin combinations against colistin-resistant *Acinetobacter baumannii*, *Pseudomonas aeruginosa*, and *Klebsiella pneumoniae* isolates. *Antimicrob. Agents Chemother.* **56**, 4856–4861 (2012).
151. Schnell, J. R., Dyson, H. J. & Wright, P. E. Structure, dynamics, and catalytic function of dihydrofolate reductase. *Annu. Rev. Biophys. Biomol. Struct.* **33**, 119–140 (2004).
152. Bourne, C. R. Utility of the biosynthetic folate pathway for targets in

antimicrobial discovery. *Antibiotics* **3**, 1–28 (2014).

7. ANNEXES

7.1. ANNEX I

The experimental data presented in the following published articles was obtained as part of the PhD thesis of my colleague Dr. Sans Serramitjana. At the beginning of my PhD, I had the opportunity to collaborate with her on what was the end of her experimental stage (January- June 2017).

We explored the antimicrobial activity of nanoencapsulated tobramycin, both in solid lipid nanoparticles (SLN) and in nanostructured lipid carriers (NLC), against clinical isolates of *P. aeruginosa* obtained from CF patients. The efficacy of these formulations was investigated both in planktonic and in sessile bacteria (Annex I, Article I).

Moreover, the time-dependent viability of *P. aeruginosa* biofilms treated with both free and nanoencapsulated colistin was also determined (Annex I, Article II).

7.1.1. ARTICLE I



Article

Free and Nanoencapsulated Tobramycin: Effects on Planktonic and Biofilm Forms of *Pseudomonas*

Eulalia Sans-Serramitjana ¹, Marta Jorba ¹, Ester Fusté ^{1,2}, José Luis Pedraz ³, Teresa Vinuesa ¹ and Miguel Viñas ^{1,*}

¹ Laboratory of Molecular Microbiology and Antimicrobials, Department of Pathology and Experimental Therapeutics, Faculty of Medicine & Health Sciences, University of Barcelona, 08007 Barcelona, Spain; eulalia.bio.87@gmail.com (E.S.-S.); m.jorba.pedrosa@gmail.com (M.J.); esterfustedominguez@ub.edu (E.F.); tvinuesa@ub.edu (T.V.); esterfustedominguez@ub.edu (E.F.); tvinuesa@ub.edu (T.V.)

² School of Nursing, Faculty of Medicine & Health Sciences, University of Barcelona, 08007 Barcelona, Spain

³ Laboratory of Pharmaceuticals, University of the Basque Country and Biomedical Research Networking Center in Bioengineering, Biomaterials and Nanomedicine (CIBER-BBN), 48940 Lejona, Spain; joseluis.pedraz@ehu.es

* Correspondence: mvinyas@ub.edu; Tel.: +34-934-024-265

Received: 16 April 2017; Accepted: 19 June 2017; Published: 26 June 2017

Abstract: Cystic fibrosis (CF) is a genetic disorder in which frequent pulmonary infections develop secondarily. One of the major pulmonary pathogens colonizing the respiratory tract of CF patients and causing chronic airway infections is *Pseudomonas aeruginosa*. Although tobramycin was initially effective against *P. aeruginosa*, tobramycin-resistant strains have emerged. Among the strategies for overcoming resistance to tobramycin and other antibiotics is encapsulation of the drugs in nanoparticles. In this study, we explored the antimicrobial activity of nanoencapsulated tobramycin, both in solid lipid nanoparticles (SLN) and in nanostructured lipid carriers (NLC), against clinical isolates of *P. aeruginosa* obtained from CF patients. We also investigated the efficacy of these formulations in biofilm eradication. In both experiments, the activities of SLN and NLC were compared with that of free tobramycin. The susceptibility of planktonic bacteria was determined using the broth microdilution method and by plotting bacterial growth. The minimal biofilm eradication concentration (MBEC) was determined to assess the efficacy of the different tobramycin formulations against biofilms. The activity of tobramycin-loaded SLN was less than that of either tobramycin-loaded NLC or free tobramycin. The minimum inhibitory concentration (MIC) and MBEC of nanoencapsulated tobramycin were slightly lower (1–2 logs) than the corresponding values of the free drug when determined in tobramycin-susceptible isolates. However, in tobramycin-resistant strains, the MIC and MBEC did not differ between either encapsulated form and free tobramycin. Our results demonstrate the efficacy of nanoencapsulated formulations in killing susceptible *P. aeruginosa* from CF and from other patients.

Keywords: tobramycin; lipid nanoparticles; antibacterial and antibiofilm effects; *P. aeruginosa*; cystic fibrosis

1. Introduction

Cystic fibrosis (CF) is the most common genetic disorder in the Caucasian population and it is characterized by a high morbidity and mortality. The CF lung is compromised by the production of viscous mucus secretions, resulting in a debilitated mucociliary clearance that promotes bacterial infection and inflammation [1]. *Pseudomonas aeruginosa* is the predominant opportunistic pathogen infecting the respiratory tract of CF patients. Once chronic lung colonization occurs, *P. aeruginosa* changes phenotypically to produce alginate, which allows the bacterium to become established within

mucoid biofilms and thus highly resistant to multiple antimicrobials [2,3]. Indeed, the emergence of multidrug-resistant phenotypes and treatment failure were shown to correlate with the reduced permeability of the outer membrane of *P. aeruginosa* to most antimicrobials and the acquisition of genes, encoding antimicrobial resistance [4,5].

Tobramycin is a hydrophilic, cationic antibiotic administered as an aerosol in the treatment of *P. aeruginosa* lung infections in CF patients [6]. Like other aminoglycosides, tobramycin targets the bacterial ribosome, such that bacterial resistance, although rare, mainly involves impermeability and the acquisition of aminoglycoside-modifying enzymes, encoded either on a plasmid or within the genome by transposable elements [7]. However—despite their chemical stability, fast bactericidal effect, synergy with β -lactam antibiotics, and low incidence of resistance—aminoglycosides are of limited utility because of their nephrotoxicity [8,9]. While tobramycin is less nephrotoxic than gentamicin and other aminoglycosides and has been successfully used against *P. aeruginosa* [10], planktonic bacteria are much more sensitive than bacteria in biofilms, the growth form occurring in the lower respiratory tract of CF patients. The reduced efficacy of tobramycin and other antimicrobials is due to poor mucus penetration, the resilience of the extracellular matrix of the biofilm, and inactivation of the drug through various binding interactions in the infected CF lung [11]. The mechanisms of tobramycin resistance are, to our knowledge, not fully understood. The relationship between mucoidity and tobramycin resistance has been explored; the main conclusion is that mucoidity per se has no effect on resistance [12]. However, the study also distinguished between the roles of mucoidity and biofilm formation in the ability of *P. aeruginosa* to resist antibiotic treatment. While biofilm formation expectantly increased resistance of PAO1 to tobramycin, uncontrolled alginate production did not. Thus, one should speculate that other mechanisms than external matrix have to be involved in the resistance caused by biofilm. It has been shown that iron regulation clearly affects susceptibility, but also gene expression differences.

Nanoformulations such as lipid nanoparticles could improve the delivery of tobramycin and thus enhance its activity. Lipid nanoparticles with a solid matrix are available as solid lipid nanoparticles (SLN) and as newer-generation lipid nanostructured lipid carriers (NLC). SLN are composed of solid lipids. NLC are prepared from a blend of a solid lipid with a liquid lipid. Both are stabilized by surfactants and are able to incorporate lipophilic and hydrophilic drugs [13].

Among the key benefits of lipid nanoparticles in the pulmonary delivery of antibiotics are the improved bioavailability and rapid distribution of the drug; precise targeting of the site of infection; the need for a lower dose; longer administration intervals, thereby reducing the risk of serious dose-related side effects; and the scaling-up feasibility of nanoparticle production [14]. The specific advantages of SLN and NLC over other delivery systems include their higher stability compared to liposomes, both in vitro and in vivo [13,15], as well as their better biocompatibilities and lower potential toxicity (both acute and chronic) compared to polymeric nanoparticles and other synthetic formulations [15,16]. Moreover, the use of nanoparticles could overcome pre-existing drug resistance mechanisms, including those involving the decreased uptake and increased efflux of the drug, to achieve better biofilm penetration. Previous studies testing the effectiveness of aminoglycosides against clinical isolates of *P. aeruginosa* reported better results with compounds loaded in nanoformulations than with the free drug [17–19].

Based on these findings and our own results demonstrating the antimicrobial activity of colistin loaded into lipid nanoparticles [20,21], in this work we explored the activity of nanoencapsulated (both SLN and NLC) tobramycin versus that of the free drug against *P. aeruginosa* clinical isolates obtained from CF patients. We then investigated the efficacy of these novel formulations in the eradication of *P. aeruginosa* biofilms. The main purpose was to demonstrate that after their inclusion in nanoparticles tobramycin was able to conserve its antimicrobial activity. Even when antimicrobial action is not higher, the nanoparticles are of interest since pharmacology has demonstrated a better distribution in the respiratory tree of molecules in lipid nanoparticles. Moreover, we have reported that in vivo

nanoparticles spread homogenously through the lung and there is no migration of lipid nanoparticles to other organs, such as liver, spleen, or kidneys [21].

2. Materials and Methods

2.1. Bacterial Isolates

The 34 clinical isolates of *P. aeruginosa* (17 non-mucoid and 17 mucoid) included in this study were obtained from the sputum samples and pharyngeal exudates of CF patients seen at the University Hospital Vall d'Hebrón and University Hospital Sant Joan de Déu (Barcelona, Spain) between January and April 2012. The patients (59% female, 41% male) ranged in age from 9 to 50 years (mean: 27 years). *P. aeruginosa* strains ATCC 27853 and PAO1 served as the control strains in the drug susceptibility assays and biofilm studies, respectively. Two CF clinical isolates, *P. aeruginosa* strain 362VH (tobramycin-resistant) and strain 056SJD (tobramycin-susceptible), were used to evaluate the ability of free and nanoencapsulated tobramycin to inhibit bacterial growth and eradicate bacterial biofilms. Table 1 summarizes the isolates used and their main characteristics.

Table 1. Bacterial strains used in this research. Strains SJD were isolated in Sant Joan de Déu Hospital and those being VH in the Hospital of Vall d'Hebrón. Abbreviations: Piper/Tz: Piperacillin/Tazobactam; Caz: Ceftazidime; Azt: Aztreonam; Imp: Imipenem; Mero: Meropenem; Gnt: Gentamicin; Tobra: Tobramycin; Amk: Amikacin; Col: Colistin; Cpfx: Ciprofloxacin. S: Susceptible; R: Resistant; I: Intermediate.

| Source | Patient | | Characteristics | | | | | Antibiotics | | | | | | | |
|--------------|---------|--------|-----------------|--------|-----------|----------|-----|-------------|-----|------|-----|-------|-----|-----|------|
| | Strain | Age | Gender | Mucoid | Hemolysis | PIPER/TZ | CAZ | AZT | IMP | MERO | GNT | TOBRA | AMK | COL | CPEX |
| PA 056 SJD | 14 | Male | - | β | R | S | R | I | R | S | S | S | S | S | R |
| PA 086 SJD | 13 | Female | + | β | S | S | S | S | S | R | R | R | S | S | S |
| PA 571.1 SJD | 10 | Male | + | - | S | S | S | S | S | S | S | S | S | S | S |
| PA 571.2 SJD | 10 | Male | + | - | S | S | S | S | S | S | S | S | S | S | S |
| PA 288 SJD | 13 | Male | - | - | S | S | R | R | R | I | S | S | S | S | S |
| PA 596 SJD | 9 | Male | - | β | S | S | S | S | S | S | S | S | S | S | S |
| PA 666 SJD | 13 | Male | - | β | S | S | S | S | S | S | S | S | S | S | R |
| PA 686 SJD | 13 | Male | - | β | S | S | S | S | S | S | S | S | S | S | S |
| PA 744 SJD | 14 | Female | - | - | S | S | S | S | S | S | S | S | S | S | S |
| PA 668 SJD | 2 | Female | - | - | S | S | S | S | S | S | S | S | S | S | S |
| PA 721 SJD | 7 | Female | - | β | S | S | S | S | S | S | S | S | S | S | S |
| PA 122 SJD | 11 | Male | + | β | S | S | S | S | S | S | S | S | S | S | S |
| PA 788 SJD | 7 | Female | - | β | S | S | S | S | S | R | S | S | S | S | S |
| PA 768 SJD | 14 | Male | - | β | S | S | R | I | R | S | S | S | S | S | R |
| 594 SJD | 9 | Male | + | β | S | S | S | S | S | S | S | S | S | S | S |
| 2881M SJD | 13 | Male | + | - | S | I | R | R | R | S | S | S | S | S | R |
| 610M SJD | 13 | Male | + | - | S | S | R | R | R | S | S | S | S | S | R |
| 610 SJD | 13 | Male | - | β | S | S | R | I | R | S | S | S | S | S | R |
| 805 SJD | 15 | Female | - | β | S | S | S | S | S | R | S | S | S | S | S |
| 555.1 SJD | 7 | Female | + | - | S | S | S | S | S | S | S | S | S | S | S |
| PA 417 VH | 17 | Female | - | β | R | R | R | S | S | S | S | S | S | S | R |
| PA 362 VH | 36 | Male | + | β | S | S | S | S | S | R | S | S | S | S | S |
| PA 684 VH | 32 | Male | - | - | S | S | I | R | R | S | I | S | S | S | I |
| PA 103 VH | 29 | Female | + | - | R | S | S | S | S | R | S | R | S | S | S |
| 023 VH | 15 | Male | + | - | S | R | I | R | R | R | R | R | S | S | S |
| 852 VH | 17 | Male | - | - | S | S | S | S | S | S | S | S | S | S | S |
| 153 VH | 17 | Female | + | - | S | S | S | S | S | S | S | S | S | S | R |
| 516 VH | 20 | Female | + | - | S | S | S | S | S | S | S | S | S | S | S |
| 547 VH | 15 | Male | + | - | R | R | R | R | R | R | R | R | S | S | R |
| 861 VH | 23 | Male | + | β | S | S | S | S | S | S | S | S | S | S | S |
| 639 VH | 18 | Male | + | - | S | S | S | S | S | S | S | S | S | S | R |
| 897 VH | 26 | Female | - | - | S | S | S | S | S | S | S | S | S | S | I |
| 697 VH | 10 | Female | - | β | R | S | S | S | S | R | R | R | S | S | R |
| 458 VH | 32 | Male | + | β | S | S | S | R | R | R | S | R | S | S | R |

2.2. Chemicals and Bacteriological Media

Tobramycin was purchased from Sigma-Aldrich Chemicals (St. Louis, MO, USA). Mueller-Hinton II broth cation-adjusted (MHBCA) was from Becton Dickinson (Sparks, MD, USA). Tryptone soy agar (TSA) was purchased from Sharlau (Sentmenat, Barcelona, Spain). Precirol ATO 5 was kindly provided by Gattefossé (Madrid, Spain), and poloxamer 188 by BASF (Ludwigshafen, Rhineland-Palatinate, Germany). Polysorbate and Tween 80 were purchased from Panreac Química (Castellar del Vallès, Barcelona, Spain). Miglyol 812 was provided by Sasol (Hamburg, Germany).

2.3. Preparation of Lipid Nanoparticles

Tobramycin-loaded nanoparticles were prepared as described. Briefly, two loaded formulations were elaborated, namely solid lipid nanoparticles (SLN) and nanostructured lipid carriers (NLC) [21]. An emulsion solvent evaporation technique was chosen for the preparation of SLN. Briefly, 10 mg of antibiotic (Sigma-Aldrich, St. Louis, MO, USA) were mixed with a 5% (*w/v*) Precirol® ATO 5 (Gattefossé, Madrid, Spain) dichloromethane solution. Then, the organic phase and an aqueous surfactant containing solution (Poloxamer 188 at 1% *w/v* and Polysorbate 80 at 1% *w/v*) were mixed and emulsified by sonication at 20 W for 30 s (Branson Sonifier 250, Danbury, CT, USA). The solvent was allowed to evaporate by magnetic stirring for 2 h at room temperature. Subsequently, the resulting SLNs were washed by centrifugation in Amicon® centrifugal filtration units (100,000 MWCO, Merck Millipore, Billerica, MA, USA) at 2500 rpm for 15 min three times. For the NLC elaboration, a hot melt homogenization technique was selected. In brief, Precirol® ATO 5 and Miglyol® 812 (Sasol, Johannesburg, South Africa) were selected as the lipid core. Those lipids were mixed with the API and heated above the melting temperature of the solid lipid. The surfactant solution consisted of 1.3% (*w/v*) of Polysorbate 80 and 0.6% (*w/v*) of Poloxamer 188. The lipid and aqueous solutions were heated to the same temperature and then emulsified by sonication for 15 s at 20 W. Nanoparticles were stored at 4 °C overnight to allow lipid re-crystallization and particle formation. Then, a washing step was undergone by centrifugation at 2500 rpm in Amicon® centrifugal filtration units (100,000 MWCO) three times. All the nanoparticles prepared were freeze-dried with two different cryoprotectants, either D-mannitol or trehalose (15%). In SLN formulations, emulsifiers constituted the aqueous phase of the emulsions, stabilizing the lipid dispersion of the nanoparticles and preventing their agglomeration [22]. Thus, the influence of the emulsifier on the bioactivity of the lipid nanoparticles was examined in two different types of SLN. SLN-tobramycin nanoparticles were prepared using the emulsifiers poloxamer 188 and polysorbate 80, each at 1% *w/v*. SLN-SDS-tobramycin nanoparticles were prepared using 2% sodium dodecyl sulfate (SDS) as the co-emulsifier. NLCs loaded with tobramycin (NLC-tobramycin) were prepared using a hot melt homogenization technique, following the method described by Pastor et al. [21].

All three types of nanoparticles used in this work (SLN-tobramycin, SLN-SDS-tobramycin, and NLC-tobramycin) were stabilized by trehalose, since in previous research we determined that it was a better cryoprotectant than mannitol [20]. Solid Lipid Nanoparticles and Nanostructured lipid carriers were characterized for size, polydispersity index (PDI) and Z-potential by means of Zetaseiser Nano ZS (Malvern Instruments, Worcestershire, UK). Measurements were based on Dynamic Light Scattering (DLS). Atomic force microscopy images were obtained by using a XE-70 atomic force microscope (Park Systems, Suwon, Korea).

2.4. Drug Susceptibility Assay in Planktonic Bacteria

Susceptibility to free tobramycin and to the three formulations of nanoencapsulated tobramycin was determined using the broth microdilution method in accordance with the Clinical Laboratory Standards Institute [23]. Briefly, the isolates were grown overnight at 37 °C in MHBCA, after which 2 mL of the culture was used to inoculate 20 mL of fresh MHBCA medium. After 2 h at 37 °C and 200 rpm, the bacterial cultures were adjusted to an optical density at 625 nm (OD_{625nm}) of 0.08–0.1

and diluted 1:1000 in fresh MHBCA medium. Five μL of each diluted suspension was added to the wells (10^4 UFC/well) of 96-well microtiter plates previously filled with MHBCA and serially diluted antibiotic (free and nanoencapsulated). The plates were incubated at 37°C for 24 h, after which the minimal inhibitory concentration (MIC) was determined macroscopically, based on the visually assessed turbidity of the wells. All experiments were performed in triplicate with three technical replicates.

2.5. Effect of Free and Nanoencapsulated Tobramycin on *P. aeruginosa* Growth

Two *P. aeruginosa* CF isolates, tobramycin-susceptible strain 0565JD and tobramycin-resistant strain 362VH, were used to examine the effect of free and nanoencapsulated (SLN and NLC) tobramycin. The antimicrobials were added to exponentially growing liquid cultures (1×10^8 CFU/mL, in MHBCA) at concentrations above and below the MIC. Samples were taken aseptically at 0, 1, 2, 3, 4, and 5 h from bacterial cultures incubated at 37°C with shaking (250 rpm). Bacterial growth was measured optically to determine the $\text{OD}_{625\text{nm}}$. All measurements were carried out in triplicate.

2.6. Antimicrobial Susceptibility of Sessile Bacteria

The minimal biofilm eradication concentration (MBEC), defined in this study as the minimal antibiotic concentration required to eliminate $>90\%$ of the non-treated biofilm, was determined as described by Moskowitz et al. [24], with modifications. Briefly, the formation of bacterial biofilms was promoted as follows: the pegs of a modified polystyrene microtiter lid (catalog No. 445497; Nunc TSP system) were immersed into 96-well microtiter plates containing inoculated (10^4 UFC/well) $200 \mu\text{L}$ MHBCA/well. The modified plates were left undisturbed at 37°C for 24 h. The pegs were then gently rinsed in 0.9% NaCl and the bacterial biofilms exposed to different concentrations of free and nanoencapsulated tobramycin for 24 h at 37°C in MHBCA. The pegs were then rinsed again with 0.9% NaCl and the biofilms removed by 10 min sonication and centrifugation (2000 rpm, 10 min) in a BioSan Laboratory Centrifuge LMC-3000. Bacteria recovered from the biofilms were incubated for 24 h at 37°C . Pegs were again rinsed with 0.9% NaCl solution and biofilms removed by 10 min sonication. Recovered bacteria were incubated for 24 h at 37°C . Optical densities at 620 nm were measured in order to determine MBEC values. All experiments were performed in triplicate on at least three occasions.

2.7. Statistical Analysis

The antimicrobial susceptibilities of the tested *P. aeruginosa* strains to free and nanoencapsulated tobramycin were statistically analyzed using Cochran's Q test. A p -value < 0.05 was considered to indicate statistical significance.

3. Results and Discussion

3.1. Nanoparticle Characterization

Main characterization data of nanoparticles are shown in Table 2. AFM imaging and size measurements of particles are presented in Figure 1.

Table 2. Characteristics of nanoparticle (TB tobramycin).

| Formulation | Mean Size (nm) | PDI | Zeta-Potential (mV) | Percentage EE (Encapsulation Efficiency) |
|-------------|-------------------|------------------|---------------------|--|
| TB-SLN | 302 ± 20.5 | 0.361 ± 0.02 | -20.5 ± 6.09 | ND |
| TB-NLC | 254.05 ± 14.5 | 0.311 ± 0.01 | -23.03 ± 2.76 | 93.15 ± 0.65 |

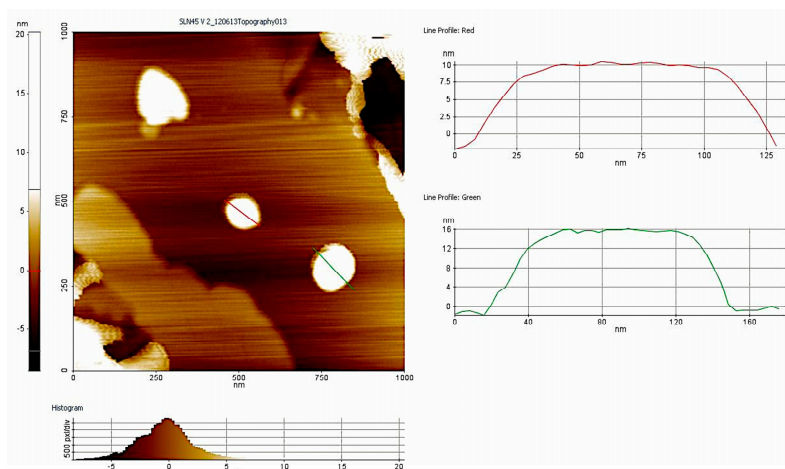


Figure 1. Size measurement performed by AFM imaging. Diameter was around 150 nm.

3.2. Antimicrobial Activity of Free and Nanoencapsulated Tobramycin

Nearly all the isolates tested in this study resulted to be susceptible ($MIC \leq 4 \mu\text{g/mL}$) to both the free and nanoencapsulated tobramycin formulations (Figure 1). The MIC of free tobramycin tested against the isolates was $0.5 \mu\text{g/mL}$, whereas that of NLC-tobramycin was slightly lower (between $0.25 \mu\text{g/mL}$ and $0.5 \mu\text{g/mL}$) and was also lower than the MICs of SLN- and SLN-SDS-tobramycin (between 1 and $4 \mu\text{g/mL}$ and $0.5 \mu\text{g/mL}$, respectively) type.

In addition, NLCs were much more active than either of the SLN preparations, as evidenced by MIC values of 0.5 and $1\text{--}4 \mu\text{g/mL}$ ($p < 0.05$), respectively. Among the two types of SLN, the formulation prepared without SDS lost antimicrobial activity (up to eight-fold higher MICs) (Figure 1). Thus, further experiments were conducted using NLC and SLN-SDS.

The efficient antibacterial activity of lipid nanoparticles loaded with tobramycin may be due to their small size and physico-chemical properties, which facilitates diffusion of the drug into the bacterial cell [25]. Similar results were reported by Ghaffari et al. [19] in their study of *P. aeruginosa* clinical isolates obtained from CF patients. The authors showed that tobramycin loaded in lipid nanoparticles had the same or higher antimicrobial activity than the free form of the drug. The slightly higher bioactivity of tobramycin-loaded NLC than SLN can be attributed to the higher drug-loading capacity of these nanoparticles and the avoidance of drug loss during storage [14,26]. As demonstrated by Moreno-Sastre et al. [27], second-generation NLC are more stable than first-generation SLN and they can be stored at a wider range of temperatures without relevant modifications of their antimicrobial activity.

The improved antibacterial activity of SLN-SDS vs. the SLN particles suggests that SDS, when used as a co-emulsifier, confers improved drug stability and release. SDS may also facilitate contact between the lipid nanoparticles and water, resulting in a better distribution equilibrium of the drug. Of relevance to our findings is the major challenge posed by ensuring drug stability in the development of colloidal drug carriers, which offer a high surface area and short diffusion pathways [28]. Figure 2b shows the data separated for mucoid and non-mucoid strains of *P. aeruginosa*.

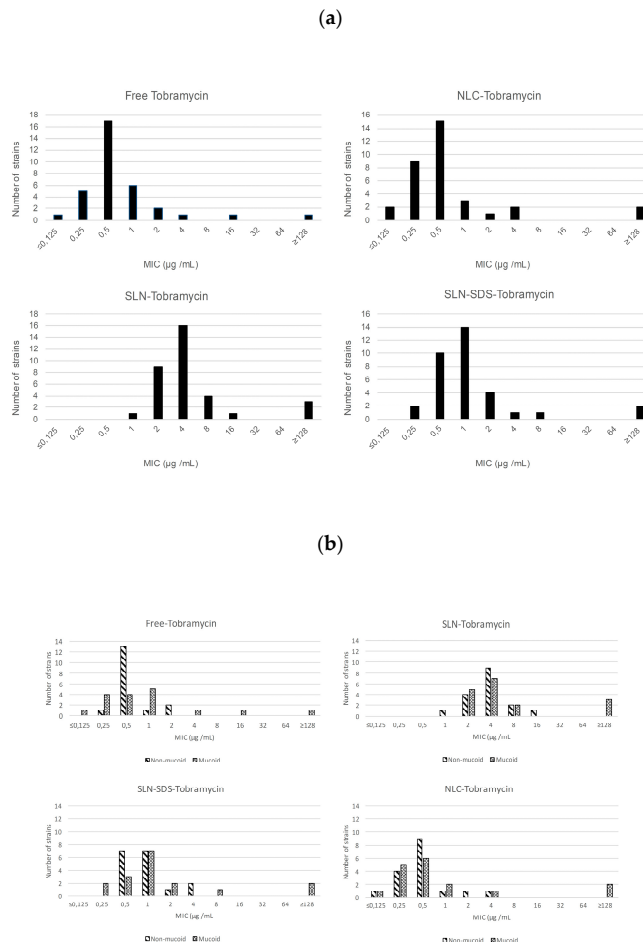


Figure 2. (a) The bioactivity (minimum inhibitory concentration, MIC) of lipid nanoparticles loaded with tobramycin in 34 strains of *Pseudomonas aeruginosa* isolated from the clinical samples of cystic fibrosis patients; (b) The same as in (a) but separated according to the 17 mucoid and 17 non-mucoid strains of the bacterium. For an explanation of the nanoparticles, see the text.

3.3. Effect of Free and Nanoencapsulated Tobramycin on Bacterial Growth

The susceptibilities of non-mucoid, susceptible (isolate 056SJD) and mucoid, resistant (isolate 362VH) *P. aeruginosa* to free and nanoencapsulated tobramycin were similar at all concentrations of the antibiotic tested (Figure 3). At sub-inhibitory concentrations ($1/2 \times \text{MIC}$), the effect of the tobramycin-loaded lipid formulations on the growth kinetics of susceptible isolate was slightly lower than that of the free drug (Figure 3a) whereas the response of the resistant isolate did not differ (Figure 3d). At the MIC, greater inhibition of the susceptible isolate was achieved, since after 5 h of antimicrobial exposure none of the formulations was able to fully inhibit the growth of the resistant isolate (Figure 3b,e). At concentrations above the MIC, the growth of the susceptible isolate was inhibited immediately after the addition of the antimicrobial (Figure 3c), but, again, none of the

formulations fully inhibited the growth of the resistant isolate (Figure 3f). Empty lipid nanoparticles had no antibacterial activity in either isolate (data not shown).

Taken together, our results demonstrate that the loading of tobramycin into lipid nanoparticles does not adversely affect the antimicrobial activity of the drug against planktonic *P. aeruginosa*. The preserved potency of lipid nanoparticles containing tobramycin may be due to their facilitated diffusion across the bacterial cell membranes. Mugabe et al. [29] showed that the effective antimicrobial activity of gentamicin loaded into liposomes involved fusion of the particles with the bacterial membrane, leading to its deformation. Further experiments are needed to better understand the interactions between the lipids in nanoformulations and the cellular membrane of microorganisms that promote drug diffusion.

The slower killing of the mucoid, resistant strain of *P. aeruginosa* than of the non-mucoid, susceptible strain by free as well as nanoencapsulated tobramycin can be explained by the additional time needed for outer membrane permeabilization by the drug, regardless of its method of preparation, and the subsequent delay in its reaching its intracellular target.

A previous study showed an immediate effect of tobramycin against most of the susceptible populations tested but not against the resistant population [30].

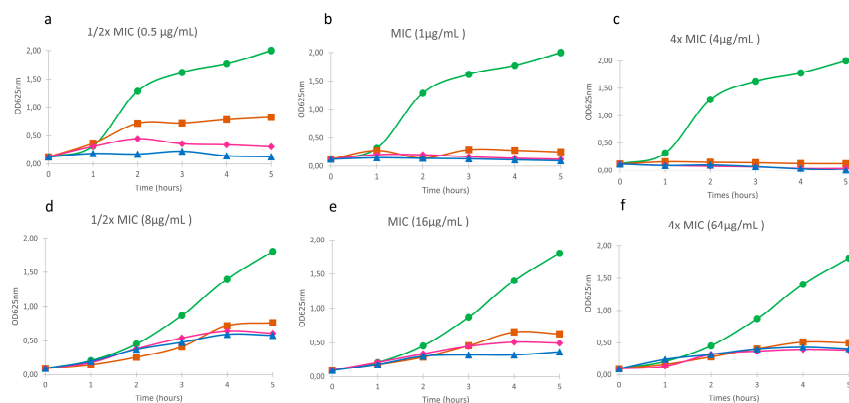


Figure 3. The effect of free and nanoencapsulated (SLN and NLC) tobramycin on the growth of *P. aeruginosa*. (a,b,c) strain 056SJD; (d,e,f) strain 362VH. Control (—●—); Free tobramycin (—■—); SLN-Tobramycin (—◆—); NLC-Tobramycin (—▲—).

3.4. Anti-Biofilm Efficacy of Free and Nanoencapsulated Tobramycin

To test the influence of the lipid nanoparticles on tobramycin's ability to kill sessile bacteria, biofilms of four *P. aeruginosa* strains were exposed to free and nanoencapsulated (SLN and NLC) tobramycin at antibiotic concentrations between 0 and 256 $\mu\text{g}/\text{mL}$. ATCC strain 27,853 and strain PAO1 were used as controls, and strains 056SJD (non-mucoid, tobramycin-susceptible) and 362VH (mucoid, tobramycin-resistant) as the *P. aeruginosa* CF isolates. All *P. aeruginosa* strains used in this experiment formed adequate biofilms (data not shown). The MIC and MBEC values of the four strains are shown in Table 3. Among the isolates susceptible to tobramycin, the MIC and MBEC values of the nanoencapsulated drug were slightly lower (1–2 logs) than those of the free drug. However, for the clinical isolate resistant to tobramycin, there were no differences in the MIC and MBEC values obtained with the nanoparticles and free tobramycin. The exception was NLC-tobramycin, in which the MBEC was slightly lower than the value obtained with the free form. The much higher MBEC vs. MIC values of both free and nanoencapsulated tobramycin likely reflected the interaction between the anionic mucopolysaccharide of the biofilm and the cationic aminoglycoside,

such that the amount of free tobramycin available to act against the resident bacteria was limited [31]. Among the two types of nanoparticles (SLN and NLC), NLC were slightly more active than SLN (1 log) for all strains tested. Specifically, the concentrations of free tobramycin needed to completely eradicate the *P. aeruginosa* biofilm were 8–16 µg/mL (tobramycin-susceptible strains) and 32 µg/mL (tobramycin-resistant strain), but the effective NLC-tobramycin concentration was lower (2–4 µg/mL and 16 µg/mL, respectively). The better results obtained with the NLC formulation of tobramycin were in agreement with our previously published results showing that colistin-loaded NLCs were highly effective in biofilm eradication [20]. A modification of MBEC assay was performed to test the efficacy of NLC-tobramycin to prevent the biofilm formation [32]. For all the isolates tested, BPC (biofilm prevention concentration) values of NLC-tobramycin were identical to values for free tobramycin. Thus, whereas NLC-tobramycin was more effective than its free form in eradicating biofilms, both free and nanoencapsulated tobramycin did not show any differences on the prevention on biofilm formation.

Table 3. Minimal biofilm eradication concentration (MBEC) and minimum inhibitory concentration (MIC) of free and NLC-encapsulated tobramycin. *P. aeruginosa* ATCC 27853 and strain PAO1 were used as controls. Strains 056SJD (non-mucoid, tobramycin-susceptible) and 362VH (mucoid, tobramycin-resistant) served as the *Pseudomonas*.

| | ATCC 27853 | | PAO1 | | 056SJD | | 362VH | |
|--------------------|-------------|--------------|-------------|--------------|-------------|--------------|-------------|--------------|
| | MIC (µg/mL) | MBEC (µg/mL) | MIC (µg/mL) | MBEC (µg/mL) | MIC (µg/mL) | MBEC (µg/mL) | MIC (µg/mL) | MBEC (µg/mL) |
| Free Tobramycin | 0.5 | 8 | 0.5 | 16 | 1 | 16 | 16 | 32 |
| SLN-SDS-Tobramycin | 0.25 | 4 | 0.25 | 8 | 0.5 | 8 | 16 | 32 |
| NLC-Tobramycin | ≤0.0625 | 2 | 0.25 | 4 | 0.25 | 4 | 16 | 16 |

Although the mechanisms underlying the efficacy of tobramycin in NLC are not fully understood, a role for charge distribution seems likely. Tobramycin loaded into NLC has a negative net charge because of the negatively charged nanoparticles, in contrast to the positive net charge of free tobramycin. The superior mucus penetration of negatively charged nanoparticles has been reported [33] and suggests the greater ability of NLC-tobramycin to penetrate the exopolysaccharide matrix surrounding the biofilm structure. Increased penetration would better allow tobramycin to reach its cellular target, in contrast to its free form. Alternatively, the fast-antimicrobial release reported by Pastor et al. [21] would ensure an initial antimicrobial concentration that is high enough to inhibit the biofilm growth of *P. aeruginosa*. Moreover, a sustained antimicrobial concentration higher than the MIC value would enable the eradication of surviving cells. However, further experiments are needed to determine which, if any, of our hypotheses is the correct one.

4. Conclusions

New antimicrobial formulations, such as lipid nanoparticles, can improve the transfer of antimicrobials to their sites of action, potentially allowing a dose reduction and therefore the avoidance of adverse side effects. Our study of planktonic cultures and biofilms of *P. aeruginosa* demonstrated that antimicrobial activity of tobramycin was not affected by nanoencapsulation. Thus, we found that nanoencapsulation of tobramycin did not improve its efficacy against planktonic *P. aeruginosa*. However, nanoencapsulation did improve its ability to eradicate *P. aeruginosa* biofilms. Given the key role of biofilms in respiratory infections of *P. aeruginosa* in CF patients, the results obtained in this study, and especially with NLC-tobramycin, may provide new options in the treatment of these infections, particularly taking into account the better distribution of antibiotics when inhaled as nanoparticles.

Acknowledgments: The bacterial strains used in this study were generously provided by the Hospital Vall d’Hebron and Hospital Sant Joan de Déu. This work was carried out under the Comprehensive Research on Effective Therapies for the Treatment of Cystic Fibrosis and Associated Diseases (TERFIQEC); IPT-2011-1402-900000 funded by the Spanish Ministry of Economy and Competitiveness. The authors gratefully acknowledge the support of University of the Basque Country UPV/EHU (UFI11/32) and the support of the Basque Government by IT 428-10 consolidated group. MV is member of the ENABLE (European Gram Negative Antibacterial Engine) European consortium (IMI-ND4BB, <http://www.imi.europa.eu/content/enable>).

Author Contributions: E.S.-S., M.J., and E.F. did the experiments; P.J.L. prepared the nanoformulations, M.V. and T.V. conceived the research and did the interpretation of data; E.S.-S. and M.V. wrote the paper.

Conflicts of Interest: The authors declare no conflict of interest

References

1. Lyczak, J.B.; Cannon, C.L.; Pier, G.B. Lung infections associated with cystic fibrosis. *Clin. Microbiol. Rev.* **2002**, *15*, 194–222. [[CrossRef](#)] [[PubMed](#)]
2. Wei, Q.; Ma, L.Z. Biofilm matrix and its regulation in *Pseudomonas aeruginosa*. *Int. J. Mol. Sci.* **2013**, *14*, 20983–21005. [[PubMed](#)]
3. Drenkard, E.; Ausubel, F.M. *Pseudomonas* biofilm formation and antibiotic resistance are linked to phenotypic variation. *Nature* **2002**, *416*, 740–743. [[PubMed](#)]
4. Li, X.Z.; Plésiat, P.; Nikaido, H. The challenge of efflux-mediated antibiotic resistance in Gram-negative bacteria. *Clin. Microbiol. Rev.* **2015**, *28*, 337–418. [[CrossRef](#)] [[PubMed](#)]
5. Fusté, E.; López-Jiménez, L.; Segura, C.; Gainza, E.; Vinuesa, T.; Viñas, M. Carbapenem-resistance mechanisms of multidrug-resistant *Pseudomonas aeruginosa*. *J. Med. Microbiol.* **2013**, *62*, 1317–1325. [[PubMed](#)]
6. Döring, G.; Flume, P.; Heijerman, H.; Elborn, J.S. Treatment of lung infection in patients with cystic fibrosis: Current and future strategies. *J. Cyst. Fibros.* **2012**, *11*, 461–479. [[CrossRef](#)] [[PubMed](#)]
7. MacLeod, D.L.; Nelson, L.E.; Shawar, R.M.; Lin, B.B.; Lockwood, L.G.; Dirk, J.E.; Miller, G.H.; Burns, J.L.; Garber, R.L. Aminoglycoside-resistance mechanisms for cystic fibrosis *Pseudomonas aeruginosa* isolates are unchanged by long-term, intermittent, inhaled tobramycin treatment. *J. Infect. Dis.* **2000**, *181*, 1180–1184. [[PubMed](#)]
8. Stehling, F.; Büscher, R.; Grosse-Onnebrink, J.; Hoyer, P.F.; Mellies, U. Glomerular and tubular renal function after repeated once-daily tobramycin courses in cystic fibrosis patients. *Pulm. Med.* **2017**, *2017*, 1–6.
9. Wargo, K.A.; Edwards, J.D. Aminoglycoside-Induced Nephrotoxicity. *J. Pharm. Pract.* **2014**, *27*, 573–577. [[CrossRef](#)] [[PubMed](#)]
10. Weintraub, R.G.; Duggin, G.G.; Horvath, J.S.; Tiller, D.J. Comparative nephrotoxicity of two aminoglycosides: Gentamicin and tobramycin. *Med. J. Aust.* **1982**, *2*, 129–132. [[PubMed](#)]
11. Cao, B.; Christophersen, L.; Kolpen, M.; Jensen, P.Ø.; Sneppen, K.; Høiby, N.; Moser, C.; Sams, T. Diffusion retardation by binding of tobramycin in an alginate biofilm model. *PLoS ONE* **2016**, *11*, e0153616. [[CrossRef](#)] [[PubMed](#)]
12. Oglesby-Sherrouse, A.G.; Djapgne, L.; Nguyen, A.T.; Vasil, A.I.; Vasil, M.L. The complex interplay of iron, biofilm formation, and mucoidy affecting antimicrobial resistance of *Pseudomonas aeruginosa*. *Pathog. Dis.* **2014**, *70*, 307–320. [[CrossRef](#)] [[PubMed](#)]
13. Das, S.; Chaudhury, A. Recent advances in lipid nanoparticle formulations with solid matrix for oral drug delivery. *AAPS Pharm. Sci. Tech.* **2011**, *12*, 62–76. [[CrossRef](#)] [[PubMed](#)]
14. Weber, S.; Zimmer, A.; Pardeike, J. Solid Lipid Nanoparticles (SLN) and Nanostructured Lipid Carriers (NLC) for pulmonary application: A review of the state of the art. *Eur. J. Pharm. Biopharm.* **2014**, *86*, 7–22. [[CrossRef](#)] [[PubMed](#)]
15. Puri, A.; Loomis, K.; Smith, B.; Lee, J.H.; Yavlovich, A.; Heldman, E.; Blumenthal, R. Lipid-based nanoparticles as pharmaceutical drug carriers: From concepts to clinic. *Crit. Rev. Ther. Drug Carr. Syst.* **2009**, *26*, 523–580. [[CrossRef](#)]
16. Hwang, T.L.; Aljuffali, I.A.; Lin, C.F.; Chang, Y.T.; Fang, J.Y. Cationic additives in nanosystems activate cytotoxicity and inflammatory response of human neutrophils: Lipid nanoparticles versus polymeric nanoparticles. *Int. J. Nanomed.* **2015**, *10*, 371–385.

17. Abdelghany, S.M.; Quinn, D.J.; Ingram, R.J.; Gilmore, B.F.; Donnelly, R.F.; Taggart, C.C.; Scott, C.J. Gentamicin-loaded nanoparticles show improved antimicrobial effects towards *Pseudomonas aeruginosa* infection. *Int. J. Nanomed.* **2012**, *7*, 4053–4063.
18. Deacon, J.; Abdelghany, S.M.; Quinn, D.J.; Schmid, D.; Megaw, J.; Donnelly, R.F.; Jones, D.S.; Kissenpfennig, A.; Elborn, J.S.; Gilmore, B.F.; et al. Antimicrobial efficacy of tobramycin polymeric nanoparticles for *Pseudomonas aeruginosa* infections in cystic fibrosis: Formulation, characterisation and functionalisation with dornase alfa (DNase). *J. Control Release* **2015**, *198*, 55–61. [[CrossRef](#)] [[PubMed](#)]
19. Ghaffari, S.; Varshosaz, J.; Saadat, A.; Atyabi, F. Stability and antimicrobial effect of amikacin-loaded solid lipid nanoparticles. *Int. J. Nanomed.* **2011**, *6*, 35–43.
20. Sans-Serramitjana, E.; Fusté, E.; Martínez-Garriga, B.; Merlos, A.; Pastor, M.; Pedraz, J.L.; Esquisabel, A.; Bachiller, D.; Vinuesa, T.; Viñas, M. Killing effect of nanoencapsulated colistin sulfate on *Pseudomonas aeruginosa* from cystic fibrosis patients. *J. Cyst. Fibros.* **2016**, *15*, 611–618. [[CrossRef](#)] [[PubMed](#)]
21. Pastor, M.; Moreno-sastre, M.; Esquisabel, A.; Sans, E.; Viñas, M.; Bachiller, D.; Asensio, V.J.; Pozo, A.D.; Gainza, E.; Pedraz, J.L. Sodium colistimethate loaded lipid nanocarriers for the treatment of *Pseudomonas aeruginosa* infections associated with cystic fibrosis. *Int. J. Pharm.* **2014**, *477*, 485–494. [[CrossRef](#)] [[PubMed](#)]
22. Attama, A.; Momoh, M.A.; Builders, P.F. Lipid Nanoparticulate Drug Delivery Systems: A Revolution in Dosage Form Design and Development. *Recent Adv. Nov. Drug Carr. Syst.* **2012**, 107–140. [[CrossRef](#)]
23. Clinical and Laboratory Standards Institute. *Performance Standards for Antimicrobial Susceptibility Testing*; 27th Informational Supplement CLSI Document M100-S27; Clinical and Laboratory Standards Institute: Wayne, PA, USA, 2017.
24. Moskowitz, S.M.; Foster, J.M.; Emerson, J.; Burns, J.L. Clinically Feasible Biofilm Susceptibility Assay for Isolates of *Pseudomonas aeruginosa* from Patients with Cystic Fibrosis. *J. Clin. Microbiol.* **2004**, *42*, 1915–1922. [[CrossRef](#)] [[PubMed](#)]
25. De Jong, W.H.; Borm, P.J. Drug delivery and nanoparticles: Applications and hazards. *Int. J. Nanomed.* **2008**, *3*, 133–149. [[CrossRef](#)]
26. Martins, S.; Sarmiento, B.; Ferreira, D.C.; Souto, E.B. Lipid-based colloidal carriers for peptide and protein delivery—Liposomes versus lipid nanoparticles. *Int. J. Nanomed.* **2007**, *2*, 595–607.
27. Moreno-Sastre, M.; Pastor, M.; Esquisabel, A.; Sans, E.; Viñas, M.; Bachiller, D.; Pedraz, J.L. Stability study of sodium colistimethate-loaded lipid nanoparticles. *J. Microencapsul.* **2016**, *33*, 636–645. [[CrossRef](#)] [[PubMed](#)]
28. Yadav, N.; Khatak, S.; Vir, U.; Sara, S. Solid lipid nanoparticles—A review. *Int. J. Appl. Pharm.* **2013**, *5*, 8–18.
29. Mugabe, C.; Azghani, A.O.; Omri, A. Liposome-mediated gentamicin delivery: Development and activity against resistant strains of *Pseudomonas aeruginosa* isolated from cystic fibrosis patients. *J. Antimicrob. Chemother.* **2005**, *55*, 269–271. [[CrossRef](#)] [[PubMed](#)]
30. Bulitta, J.B.; Ly, N.S.; Landersdorfer, C.B.; Wanigaratne, N.A.; Velkov, T.; Yadav, R.; Oliver, A.; Martin, L.; Shin, B.S.; Forrest, A.; et al. Two mechanisms of killing of *Pseudomonas aeruginosa* by tobramycin assessed at multiple inocula via mechanism-based modeling. *Antimicrob. Agents Chemother.* **2015**, *59*, 2315–2327. [[CrossRef](#)] [[PubMed](#)]
31. Khan, W.; Bernier, S.P.; Kuchma, S.L.; Hammond, J.H.; Hasan, F.; O’Toole, G.A. Aminoglycoside resistance of *Pseudomonas aeruginosa* biofilms modulated by extracellular polysaccharide. *Int. Microbiol.* **2010**, *13*, 207–212. [[PubMed](#)]
32. Fernández-Olmos, A.; García-Castillo, M.; Maiz, L.; Lamas, A.; Baquero, F.; Cantón, R. In vitro prevention of *Pseudomonas aeruginosa* early biofilm formation with antibiotics used in cystic fibrosis patients. *Int. J. Antimicrob. Agents* **2012**, *40*, 173–176. [[CrossRef](#)] [[PubMed](#)]
33. Forier, K.; Messiaen, A.S.; Raemdonck, K.; Deschout, H.; Rejman, J.; De Baets, F.; Nelis, H.; De Smedt, S.C.; Demeester, J.; Coenye, T.; et al. Transport of nanoparticles in cystic fibrosis sputum and bacterial biofilms by single-particle tracking microscopy. *Nanomedicine* **2013**, *8*, 935–949. [[CrossRef](#)] [[PubMed](#)]



© 2017 by the authors. Licensee MDPI, Basel, Switzerland. This article is an open access article distributed under the terms and conditions of the Creative Commons Attribution (CC BY) license (<http://creativecommons.org/licenses/by/4.0/>).

7.1.2. ARTICLE II

Determination of the spatiotemporal dependence of *Pseudomonas aeruginosa* biofilm viability after treatment with NLC-colistin

Eulalia Sans-Serramitjana¹
 Marta Jorba¹
 José Luis Pedraz²
 Teresa Vinuesa¹
 Miguel Viñas¹

¹Laboratory of Molecular Microbiology and Antimicrobials, Department of Pathology and Experimental Therapeutics, University of Barcelona, Barcelona, ²Laboratory of Pharmaceutics, University of the Basque Country (UPV/EHU), Centro de Investigación Biomédica en Red de Bioingeniería, Biomateriales y Nanomedicina, Vitoria, Spain

Abstract: The emergence of colistin-resistant *Pseudomonas aeruginosa* in cystic fibrosis (CF) patients, particularly after long-term inhalation treatments, has been recently reported. Nanoencapsulation may enable preparations to overcome the limitations of conventional pharmaceutical forms. We have determined the time-dependent viability of *P. aeruginosa* biofilms treated with both free and nanoencapsulated colistin. We also examined the relationship between the optimal anti-biofilm activity of nanostructured lipid carrier (NLC)-colistin and the structural organization of the biofilm itself. The results showed the more rapid killing of *P. aeruginosa* bacterial biofilms by NLC-colistin than by free colistin. However, the two formulations did not differ in terms of the final percentages of living and dead cells, which were higher in the inner than in the outer layers of the treated biofilms. The effective anti-biofilm activity of NLC-colistin and its faster killing effect recommend further studies of its use over free colistin in the treatment of *P. aeruginosa* infections in CF patients.

Keywords: cystic fibrosis, colistin sulfate, lipid nanoparticles, *P. aeruginosa*, confocal laser scanning microscopy, anti-biofilm activity

Introduction

Pseudomonas aeruginosa is a gram-negative opportunistic pathogen that frequently infects the lungs of cystic fibrosis (CF) patients in the form of chronic biofilm infections.¹ The antimicrobial resistance of bacteria assuming a biofilm mode of growth poses challenges not only to host immune clearance mechanisms but also to health care settings, in the form of an increased risk of hospital-acquired infections.² The high level of antibiotic resistance that characterizes biofilms can be attributed to their structurally heterogeneous microenvironments, some of which contain metabolically inactive cell population,^{3,4} as well as to the differential expression of multiple gene networks and extracellular matrix by the resident bacterial species.⁴

Over the last decade, increasing attention has been paid to antimicrobial peptides (AMPs) as therapeutic agents, because resistance to them is thus far rare. Moreover, these peptides are able to modulate the innate immune response.⁵⁻⁷ The AMP colistin is a cyclic cationic decapeptide that attacks negatively charged bacterial membranes, thereby disrupting both the outer and inner membranes of gram-negative species.⁷ Although the use of colistin as an antimicrobial is restricted by its high nephrotoxicity, the increasing emergence of multiresistant pathogens has renewed interest in its therapeutic potential.⁸ In fact, nowadays, colistin is administered to CF patients and to other patients with chronic respiratory diseases for the treatment of lung infections

Correspondence: Miguel Viñas
 Laboratory of Molecular Microbiology,
 University of Barcelona, Feixa Llarga
 s/n, 08907 L'Hospitalet de Llobregat,
 Barcelona, Spain
 Tel +34 93 402 4265
 Email mvinyas@ub.edu

caused by *P. aeruginosa*.⁹ However, colistin resistance, mediated by the post-translational modification of lipopolysaccharide, has emerged, perhaps driven by the increasing clinical use of this drug.^{10,11} Although resistance rates are still low in many countries, the recent identification of a plasmid-borne colistin resistance gene (*mcr-1*) in human, animal, and environmental isolates of Enterobacteriaceae may soon lead to rapid increases in resistance on a global scale.^{12,13} An awareness of this threat has catalyzed the search for less toxic antimicrobials as well as the development of synthetically modified forms enabling dose reductions, longer administration intervals, and reduced systemic toxicity. An alternative is new delivery strategies, such as the use of solid lipid nanoparticles and nanostructured lipid carriers (NLCs) to deliver colistin in CF patients with *P. aeruginosa* respiratory infections. The nebulization of antimicrobials carried in lipid nanoparticles improves drug bioavailability and allows a reduced dosing frequency.¹⁴ In principle, the administration of encapsulated drugs could overcome preexisting resistance mechanisms, including the decreased uptake and increased efflux of the drug, as well as biofilm formation.¹⁵ In a previous study, we demonstrated the higher anti-biofilm activity of NLC-colistin than of free colistin in both susceptible and resistant *P. aeruginosa* strains isolated from the sputum samples of CF patients.¹⁶ As biofilms play a key role in the natural history of *P. aeruginosa* respiratory infections in CF, the use of NLC-colistin may offer new approaches to their treatment. However, the mechanism underlying the improved efficiency of NLC-colistin in biofilm removal is unknown.¹⁶ Pamp et al¹⁷ showed that free colistin acts preferentially on bacteria with low metabolic rates; this is the case for bacteria in the deepest layers of a biofilm, as metabolic activity decreases with increasing distance from the biofilm surface. Whether the same differential response occurs with NLC-colistin has not been determined. Thus, this study explored the efficacy of NLC-colistin versus the free drug with respect to biofilm viability over time and across the different layers of the biofilm.

Materials and methods

Preparation of lipid nanoparticles

NLCs were prepared using the hot melt homogenization technique.¹⁸ The lipid core consisted of Precirol®ATO 5 (Gattefossé, Madrid, Spain) and Miglyol 812 (Sasol, Hamburg, Germany), which were mixed with colistin sulfate (Zhejiang Shenghua Biok Biology Co., Ltd., China). The temperature of the mixture was gradually increased to the melting temperature of the solid lipids. The surfactant solution was 1.3% (w/v) Polysorbate 80 (Panreac Química, Castellar del

Vallès, Barcelona, Spain) and 0.6% (w/v) Poloxamer 188 (BASF, Ludwigshafen, Rhineland-Palatinate, Germany). The mixture was emulsified by sonication for 15 s at 20 W. The nanoparticles were recrystallized by an overnight incubation at 4°C to stimulate particle formation. They were then washed three times by centrifugation at 2,500 rpm in Amicon centrifugal filtration units (100,000 MWCO). All prepared nanoparticles were freeze-dried with trehalose (15%).

Bacterial strain, culture conditions, and biofilm formation

P. aeruginosa strain PA01 in 20 mL of Mueller-Hinton II broth cation adjusted (Becton Dickinson Diagnostic Systems, Inc., Sparks, MD, USA) was grown overnight at 37°C with continuous shaking at 250 rpm. The culture was then adjusted to a concentration of $1-5 \times 10^8$ cfu/mL, and 200 μ L was used to inoculate μ -Slide 8 glass bottom wells (Ibidi, cat. num. 80827, Munich, Germany). Each well was previously coated with a 0.01% (w/v) poly-lysine hydrobromide (Sigma-Aldrich, Dorset, UK) solution to enhance bacterial cell adhesion and to prevent biofilm removal during the experiments. The slides were incubated at 37°C for 24 h to allow biofilm formation.

Confocal laser scanning microscopy imaging

Biofilms on the eight-well glass were washed once with Ringer ¼ to remove unfixed bacteria and then treated with free and NLC-colistin at a colistin concentration of 128 μ g/mL, based on previously published results.¹⁶ They were then incubated at 37°C for 20, 30, 40, 60, 80, and 100 min after which they were rinsed once with Ringer ¼. To stain the biofilms, a mixture of SYTO 9 and propidium iodide prepared at a dilution ratio of 1:2 (1.5 μ L of SYTO 9 and 3 μ L of propidium iodide in 1 mL of Ringer ¼) was applied to the entire biofilm. After 30 min of incubation in the dark at 37°C, the stained biofilms were washed once with Ringer ¼ to remove nonspecific staining. Fluorescence was observed using a Leica TCS-SL filter-free spectral confocal laser-scanning microscope (Leica Microsystems, Mannheim, Germany) equipped with a 488-nm argon laser, 543-nm and 633-nm He/Ne lasers (Scientific and Technological Centers, University of Barcelona, Bellvitge Campus, L'Hospitalet de Llobregat, Spain), and a 63 \times magnification oil immersion objective (1.4 numerical aperture). The image resolution was 1,024 \times 1,024 pixels. All experiments were performed in duplicate. Confocal laser scanning microscopy (CLSM) images were analyzed using ImageJ software (National

Institutes of health, Bethesda, MD, USA). The percentages of alive and dead bacterial cells were calculated from the total cell number.

Results and discussion

Time-dependent killing of strain PAO1 biofilms by free and NLC-colistin

Enumeration of the viable and dead bacteria for every treatment showed an increase in bacterial death over time in the strain PAO1 biofilms (Figure 1). In the control (untreated) biofilms, most of the cells were viable, with live/dead ratios of 78.2% (green) and 21.8% (red), respectively. This result was in agreement with a previous report.¹⁹ The baseline viability was taken into account in the interpretation of the experimental data. A nonlethal effect was observed in biofilms exposed for 20 min to free colistin, with the proportions of living and dead bacteria almost identical to that of the control (~80% and 20%, respectively). The killing efficiency reached a maximum of 80% after 60 min of treatment with the free formulation. By contrast, after 20 min of exposure to NLC-colistin, ~75% of the individual cells were dead (red fluorescence) and after 60 min of treatment almost 100%, thus demonstrating the rapid killing effect of the encapsulated drug.

The results shown in Figure 1 are in good agreement with the CLSM images of the untreated and treated biofilms (Figure 2). The latter mostly stained green (Figure 2), indicating a high level of bacterial viability. After 20 and 40 min of exposure to NLC-colistin (Figure 2), the red population increased over time such that very few green-staining cells were observed, consistent with the significant damage of bacteria residing in the treated biofilm. After a 60-min incubation

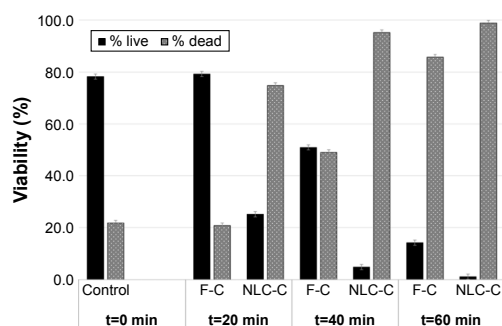
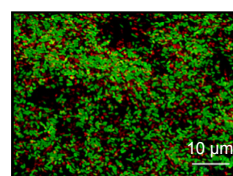


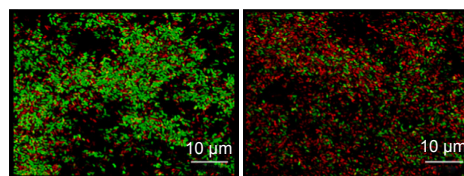
Figure 1 Graphical representation of living and dead bacteria treated or not treated with the different colistin formulations.

Note: Error bars represent the standard deviation of the mean (time: 0, 20, 40, and 60 min).

Abbreviations: F-C, free colistin; NLC-C, colistin nanoparticulated in nanostructured lipid carrier.

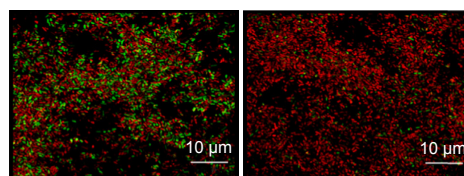


Control



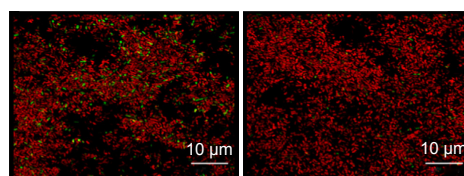
20 min free-col

20 min NLC-col



40 min free-col

40 min NLC-col



60 min free-col

60 min NLC-col

Figure 2 Confocal laser scanning microscopy images of *Pseudomonas aeruginosa* strain PAO1 biofilms.

Notes: Control: untreated biofilm. Drug exposure time: 20, 40, and 60 min. Green: viable bacteria; red: dead bacteria.

Abbreviations: free-col, free colistin; NLC-col, colistin nanoparticulated in nanostructured lipid carrier.

with NLC-colistin, all bacterial cells stained red. In the biofilms treated with free colistin (Figure 2), the percentages of the red and green populations of bacteria after 20 min were almost identical to those of the control. After 40 and 60 min (Figure 2), the red population in the free colistin treatment was always smaller than that in the NLC-colistin treatment, evidence of the faster killing of bacterial biofilms by the latter. This may reflect the ability of the lipid nanoparticles to easily penetrate the biofilm matrix, with the nanoparticulated drug then reaching the bacteria faster and more easily than free colistin.^{21,22} Islan et al²² reported similar results using levofloxacin-loaded lipid nanoparticles. In that study, rapid killing of *P. aeruginosa* biofilms by NLC-levofloxacin was achieved after 60 min of exposure.

Table 1 Percentage of the bacterial population living in the various layers and percentages of live and dead bacteria of the *Pseudomonas aeruginosa* strain PAOI biofilm after 20, 40, and 60 min of treatment with F-C and NLC-C

| Treatment | Biofilm layer | Percentage of the bacterial population (%) | | | | | | | | | | | |
|-----------|---------------|--|------|------|----------|------|------|----------|------|------|----------|------|------|
| | | t=0 min | | | t=20 min | | | t=40 min | | | t=60 min | | |
| | | Total | Live | Dead | Total | Live | Dead | Total | Live | Dead | Total | Live | Dead |
| C+ | Outer | 28.5 | 22.5 | 6.1 | | | | | | | | | |
| | Inner | 71.5 | 55.8 | 15.7 | | | | | | | | | |
| F-C | Outer | | | | 32.4 | 29.0 | 3.4 | 35.2 | 20.9 | 14.3 | 37.9 | 6.6 | 31.3 |
| | Inner | | | | 60.3 | 50.3 | 9.9 | 64.8 | 30.1 | 34.8 | 62.1 | 7.6 | 54.5 |
| NLC-C | Outer | | | | 20.8 | 5.5 | 15.3 | 17.4 | 0.9 | 16.5 | 19.6 | 0.2 | 19.5 |
| | Inner | | | | 79.2 | 19.7 | 59.6 | 82.6 | 3.9 | 78.7 | 80.4 | 0.9 | 79.5 |

Abbreviations: C+, untreated biofilm; F-C, free colistin; NLC-C, colistin nanoparticulated in nanostructured lipid carrier.

Differentiation of distinct bacterial subpopulations in the strain PAOI biofilm

Biofilms are a complex, multicellular structure that favors the generation of physiologically distinct subpopulations of bacteria that together form a community able to adapt to rapidly changing environmental conditions.²³ To explore whether free and nanoencapsulated colistin differentially act on the subpopulations residing within the biofilm, the viability of bacteria in the different layers of the biofilm was determined. As seen in Table 1, the bacterial density was much higher in the inner layers of the biofilm, consistent with the previously reported high density of cells located close to the substratum in *P. aeruginosa* biofilms.²⁴ The biofilms were investigated in greater detail by dividing them in half, which revealed that 71% of the total number of cells occupied the inner layers (Table 1). This was essentially the case in all three types of biofilms (control, free colistin, and NLC-colistin) despite the demonstrated heterogeneity among biofilms with respect to their thickness and the strength of their surface attachment.²⁵ Nonetheless, our results can be explained by the initiation of cell detachment in the upper layers of the biofilm²⁶ as well as the accumulation of high densities of smaller cells in deeper parts of the biofilm in response to external stress conditions. Also, it is likely that the washing step with buffer altered the external parts of the biofilm while leaving its deeper parts relatively undisturbed. Although weakly attached bacteria will be discarded by carefully washing the biofilms after 24 h of incubation, simultaneous disruption of the superficial layers of the biofilm is difficult to avoid.

The two colistin formulations did not differ in their effects on the various biofilm subpopulations, as the percentages of living and dead cells were higher in the inner than in the outer layers of biofilms treated with free colistin or NLC-colistin (Table 1). Our results demonstrate that both formulations are able to penetrate the deeper layers of the biofilm and thus access a dormant and anaerobically

growing subpopulation.^{27,28} A reduction of the free colistin concentration, the delayed penetration of the free drug into the deeper portions of the multilayered biofilm, and the lack of specificity of NLC-colistin in killing metabolically active bacteria versus starved cells may account for our results, as proposed in similar studies.^{17,29} Further experiments will be aimed at improving the experimental conditions to optimize the performance of NLC-colistin.

Conclusion

In our previous works,^{16,18} we demonstrated the identical antimicrobial activity of free colistin and NLC-colistin. Here we have shown that NLC-colistin was clearly more effective than its free form in eradicating biofilms of *P. aeruginosa*, the most relevant pathogen in CF patients. Thus, the use of lipid nanoparticles may be an interesting strategy to prevent the growth and development of microbial biofilms in the clinical setting. NLC-colistin was much faster than free colistin in killing *P. aeruginosa*, based on the ability of the encapsulated drug to reach both the superficial and the deep regions of the biofilm. Further experiments are needed to identify the precise mechanism underlying the efficient removal of biofilms by NLC-colistin.

Acknowledgments

We thank Wendy Ran for copy editing the English version of the manuscript. This work was carried out under the Comprehensive Research on Effective Therapies for the Treatment of Cystic Fibrosis and Associated Diseases (IPT-2011-1402-900000) funded by the Spanish Ministry of Economy and Competitiveness. The authors gratefully acknowledge the support of the Scientific and Technological Centers (University of Barcelona, Bellvitge Campus, L'Hospitalet de Llobregat, Spain) and particularly the technical assistance of Dr Benjamin Torrejón in the CLSM study. MV is a member of the ENABLE (European Gram Negative Antibacterial Engine) European consortium (IMI-ND4BB).

Disclosure

The authors report no conflicts of interest in this work.

References

- Lyczak JB, Cannon CL, Pier GB. Lung infections associated with cystic fibrosis lung infections associated with cystic fibrosis. *Clin Microbiol Rev.* 2002;15(2):194–222.
- Drenkard E, Ausubel FM. *Pseudomonas* biofilm formation and antibiotic resistance are linked to phenotypic variation. *Nature.* 2002; 416(6882):740–743.
- Machineni L, Rajapantula A, Nandamuri V, et al. Influence of nutrient availability and quorum sensing on the formation of metabolically inactive microcolonies within structurally heterogeneous bacterial biofilms: an individual-based 3D cellular automata model. *Bull Math Biol.* 2017;79(3):594–618.
- Taylor PK, Yeung AT, Hancock RE. Antibiotic resistance in *Pseudomonas aeruginosa* biofilms: towards the development of novel anti-biofilm therapies. *J Biotechnol.* 2014;191:121–130.
- Hancock REW, Sahl HG. Antimicrobial and host-defense peptides as new anti-infective therapeutic strategies. *Nat Biotechnol.* 2006; 24(12):1551–1557.
- Hancock RE. Cationic peptides: effectors in innate immunity and novel antimicrobials. *Lancet Infect Dis.* 2001;1(3):156–164.
- Haney EF, Mansour SC, Hancock RE. Antimicrobial peptides: an introduction. *Methods Mol Biol.* 2017;1548:3–22.
- Li J, Nation RL, Milne RW, et al. Evaluation of colistin as an agent against multi-resistant Gram-negative bacteria. *Int J Antimicrob Agents.* 2005;25(1):11–25.
- Döring G, Flume P, Heijerman H, Elborn JS; Consensus Study Group. Treatment of lung infection in patients with cystic fibrosis: Current and future strategies. *J Cyst Fibros.* 2012;11(6):461–479.
- Gales AC, Jones RN, Sader HS. Contemporary activity of colistin and polymyxin B against a worldwide collection of Gram-negative pathogens: Results from the SENTRY antimicrobial surveillance program (2006–2009). *J Antimicrob Chemother.* 2011;66(9):2070–2074.
- Carmeli Y, Troillet N, Eliopoulos GM, Samore MH. Emergence of antibiotic-resistant *Pseudomonas aeruginosa*: comparison of risks associated with different antipseudomonal agents. *Antimicrob Agents Chemother.* 1999;43(6):1379–1382.
- Liu YY, Wang Y, Walsh TR, et al. Emergence of plasmid-mediated colistin resistance mechanism MCR-1 in animals and human beings in China: a microbiological and molecular biological study. *Lancet Infect Dis.* 2016;16(2):161–168.
- Jeannot K, Bolard A, Plésiat P. Resistance to polymyxins in Gram-negative organisms. *Int J Antimicrob Agents.* 2017;49(5): 526–535.
- Cipolla D, Shekunov B, Blanchard J, Hickey A. Lipid-based carriers for pulmonary products: Preclinical development and case studies in humans. *Adv Drug Deliv Rev.* 2014;75:53–80.
- Pelgrift RY, Friedman AJ. Nanotechnology as a therapeutic tool to combat microbial resistance. *Adv Drug Deliv Rev.* 2013;65(13–14): 1803–1815.
- Sans-Serramitjana E, Fusté E, Martínez-Garriga B, et al. Killing effect of nanoencapsulated colistin sulfate on *Pseudomonas aeruginosa* from cystic fibrosis patients. *J Cyst Fibros.* 2016;15(5):611–618.
- Pamp SJ, Gjermansen M, Johansen HK, Tolker-Nielsen T. Tolerance to the antimicrobial peptide colistin in *Pseudomonas aeruginosa* biofilms is linked to metabolically active cells, and depends on the *pmr* and *mexAB-oprM* genes. *Mol Microbiol.* 2008;68(1):223–240.
- Pastor M, Moreno-sastre M, Esquisabel A, et al. Sodium colistimethate loaded lipid nanocarriers for the treatment of *Pseudomonas aeruginosa* infections associated with cystic fibrosis. *Int J Pharm.* 2014; 477(1–2):485–494.
- Singh R, Monnappa AK, Hong S, Mitchell RJ, Jang J. Effects of carbon dioxide aerosols on the viability of *Escherichia coli* during biofilm dispersal. *Sci Rep.* 2015;5:13766.
- Klodzińska SN, Priemel PA, Rades T, et al. Inhalable antimicrobials for treatment of bacterial biofilm-associated sinusitis in cystic fibrosis patients: challenges and drug delivery approaches. *Int J Mol Sci.* 2016; 17(10). pii: E1688.
- Nafee N, Husari A, Maurer CK, et al. Antibiotic-free nanotherapeutics: ultra-small, mucus-penetrating solid lipid nanoparticles enhance the pulmonary delivery and anti-virulence efficacy of novel quorum sensing inhibitors. *J Control Release.* 2014;192:131–140.
- Islan GA, Tornello PC, Abraham GA, et al. Smart lipid nanoparticles containing levofloxacin and DNase for lung delivery. Design and characterization. *Colloids Surfaces B Biointerfaces.* 2016;143:168–176.
- Moormeier DE, Bayles KW. *Staphylococcus aureus* biofilm: a complex developmental organism. *Mol Microbiol.* 2017;104(3):365–376.
- Yang L, Nilsson M, Gjermansen M, Givskov M, Tolker-Nielsen T. Pyoverdine and PQS mediated subpopulation interactions involved in *Pseudomonas aeruginosa* biofilm formation. *Mol Microbiol.* 2009; 74(6):1380–1392.
- Flemming HC, Wingender J, Szewzyk U, Steinberg P, Rice SA, Kjelleberg S. Biofilms: an emergent form of bacterial life. *Nat Rev Microbiol.* 2016;14(9):563–575.
- Rollet C, Gal L, Guzzo J. Biofilm-detached cells, a transition from a sessile to a planktonic phenotype: a comparative study of adhesion and physiological characteristics in *Pseudomonas aeruginosa*. *FEMS Microbiol Lett.* 2009;290(2):135–142.
- Kim J, Hahn JS, Franklin MJ, Stewart PS, Yoon J. Tolerance of dormant and active cells in *Pseudomonas aeruginosa* PA01 biofilm to antimicrobial agents. *J Antimicrob Chemother.* 2009;63(1):129–135.
- Bjarnsholt T, Ciofu O, Molin S, Givskov M, Hoiby N. Applying insights from biofilm biology to drug development – can a new approach be developed? *Nat Rev Drug Discov.* 2013;12(10):791–808.
- Haagensen JAJ, Klausen M, Ernst RK, et al. Differentiation and distribution of colistin- and sodium dodecyl sulfate-tolerant cells in *Pseudomonas aeruginosa* biofilms. *J Bacteriol.* 2007;189(1):28–37.

International Journal of Nanomedicine

Publish your work in this journal

The International Journal of Nanomedicine is an international, peer-reviewed journal focusing on the application of nanotechnology in diagnostics, therapeutics, and drug delivery systems throughout the biomedical field. This journal is indexed on PubMed Central, MedLine, CAS, SciSearch®, Current Contents®/Clinical Medicine,

Submit your manuscript here: <http://www.dovepress.com/international-journal-of-nanomedicine-journal>

Dovepress

Journal Citation Reports/Science Edition, EMBASE, Scopus and the Elsevier Bibliographic databases. The manuscript management system is completely online and includes a very quick and fair peer-review system, which is all easy to use. Visit <http://www.dovepress.com/testimonials.php> to read real quotes from published authors.

7.2. ANNEX II

During the realization of this doctorate, I have participated in some studies not directly related to the topic of the PhD. I have collaborated in the exploration of the eventual survival of microorganisms on clinical sterilized healing abutments with the aim to determine whether their reuse is safe or not (Article iii).

7.2.2. ARTICLE III

Journal section: Oral Medicine and Pathology
Publication Types: Research

doi:10.4317/medoral.22967
http://dx.doi.org/doi:10.4317/medoral.22967

Is the re-use of sterilized implant abutments safe enough? (Implant abutment safety)

M^a Angeles Sánchez-Garcés ¹, Marta Jorba ², Joan Ciurana ³, Miguel Vinas ⁴, M^a Teresa Vinuesa ⁵

¹ PhD, MD. Aggregate Professor Department of Dentistry. Faculty of Medicine and Health Sciences IDIBELL. University of Barcelona, Campus Bellvitge, Barcelona. Spain

² Ms in Microbiology. Department of Pathology & Experimental Therapeutics, Faculty of Medicine and Health Sciences. University of Barcelona and IDIBELL. Campus Bellvitge, Barcelona. Spain

³ Ms Student. Department of Dentistry. Faculty of Medicine and Health Sciences IDIBELL. University of Barcelona, Campus Bellvitge, Barcelona. Spain

⁴ PhD. Chairman in Microbiology. Department of Pathology & Experimental Therapeutics, Faculty of Medicine and Health Sciences. University of Barcelona and IDIBELL. Campus Bellvitge, Barcelona. Spain

⁵ PhD, MD. Associate Professor. Department of Pathology & Experimental Therapeutics, Faculty of Medicine and Health Sciences. University of Barcelona and IDIBELL. Campus Bellvitge, Barcelona. Spain

Correspondence:

Department of Pathology and experimental Therapeutics
Feixa Llarga s/n. Pavelló de Govern, 5^a planta
08907 L'Hospitalet de Llobregat. Barcelona. Spain
tvinuesa@ub.edu

Received: 08/01/2019
Accepted: 04/02/2019

Sánchez-Garcés MA, Jorba M, Ciurana J, Vinas M, Vinuesa MT. Is the re-use of sterilized implant abutments safe enough? (Implant abutment safety). Med Oral Patol Oral Cir Bucal. 2019 Sep 1;24 (5):e583-7. <http://www.medicinaoral.com/medoralfree01/v24i5/medoralv24i5p583.pdf>

Article Number: 22967 <http://www.medicinaoral.com/>
© Medicina Oral S. L. C.I.F. B 96689336 - pISSN 1698-4447 - eISSN: 1698-6946
eMail: medicina@medicinaoral.com
Indexed in:
Science Citation Index Expanded
Journal Citation Reports
Index Medicus, MEDLINE, PubMed
Scopus, Embase and Emcare
Indice Médico Español

Abstract

Background: The reuse of implant healing abutments is common in dental practice. Effective elimination of bacteria and viruses is accomplished by conventional sterilization.

The aim of this work was to explore the eventual survival of microorganisms on sterilized healing abutments and to rule out the presence of transmissible organic material after standard procedures.

Material and Methods: A total of 55 healing abutments previously used in patients will be washed and sterilized in a steam autoclave at 121°C for 15 min. Each healing abutment will be cultured in Brain Heart Infusion broth (BHI) under strict aseptic conditions. Besides, two control groups will be included: one of 3 unused healing abutments, and the other of just medium. After 10 days at 37°C under a 5% CO₂ 100 µl of the broth will be plated on solid media (Brain Infusion Agar, BHIA) and Columbia Blood agar to test for sterility. The remaining volume will be centrifuged, the sediment fixed, and a Gram stain performed to discard the presence of non-cultivable microorganisms. Moreover, to determine the presence of remaining organic material after the cleaning and sterilizing treatments, the bioburden will be determined by measuring total organic carbon (TOC) in another 10 previously used healing abutments, cleaned and sterilized, that will be submerged in Milli-Q water and sonicated.

Outer membrane: a key obstacle for new antimicrobial agents

Results: No bacterial growth was detected on any of the 58 cultured abutments, indicating that the sterilization was completely satisfactory in terms of removal of live bacteria or spores. Nevertheless, significant amounts of organic carbon may still be recovered (up to 125,31 µg/abutment) after they have been sterilized.

Conclusions: Significant amounts of the bio burden remained adhered to the surfaces in spite of the cleaning and sterilization procedures. Taking into account our results and data from other authors, the presence of infectious particles on the reused healing abutments such as prions cannot be ruled out.

Key words: *Healing abutment, abutment surface, peri-implantitis, mucositis, sterilization.*

Introduction

The reuse of implant abutments is common practice, as it reduces costs for both patients and dentists. Since abutments are mostly made of titanium, it has been assumed that autoclave sterilization guarantees the safety of such reuse, although it can alter the composition of the surface due to atmospheric pollutants, especially when the sterilization process is repeated several times (1).

Abutments should favor the maturation of peri-implant tissues during osseointegration, favouring the modeling of soft tissues surrounding the implant. Moreover, the attachment of soft tissue around the implant abutments takes place through the establishment of a hemidesmosomal junction involving inflammatory cells (about 3 mm thickness) that contributes to osseointegration.

Prevention of the presence of bacteria in the region together with the use of sterile instruments and components to avoid cross-infection between patients are primary goals of implantology. Thus, despite the common practice of reutilization, most manufacturers recommend just a single use (2). Several authors have concluded that the use of sterilization procedures alone for the treatment of reused abutments might not be sufficient, and recommend previous cleaning protocols to detach incrustated material before a re-sterilization step (3).

Different strategies have been assayed to minimize the consequences of reutilization, including the use of cheaper materials, such as glass-fiber (4,5), and different cleaning processes (6-8).

The aim of this work was to explore the eventual survival of microorganisms on sterilized abutments, as well as to explore to what extent bacteria found on abutments could be the direct cause of implant failures. There is a high proportion of initial implant success, and later failure is normally attributed to biomechanical or microbiological causes (2-9). Thus, our aim can be extended to answer a new question: To what extent does biological detritus on reused abutments contribute to implant failure?

Material and Methods

A total of 55 healing abutments previously used in one or more patients during the passive osseointegration pe-

riod of three to six months were provided by eight different dental clinics of Barcelona, Spain. Once retired, the healing abutments were processed for cleaning and disinfection by immersion in enzymatic detergent for 2-5 minutes, followed by an ultrasound bath at 40-45°C for 10-15' and finally dried. They were placed in heat-sealed sterilization bags (3M Steri-Dual ECO, Ref: 8652). The sterilization was carried out with a Class B autoclave in a program for metals (134°C, 12 minutes, 2.1 bar pressure).

-Sample culture

Each healing abutment was removed from the sterilization bag and submerged in a rich microbiological medium (10 mL of Brain Heart Infusion broth (BHI) Sharlau, Sentmenat, Spain) in 18x180 mm test tubes under strict aseptic conditions. Two control groups were prepared: the first consisted of three new (unused) healing abutments (Nobel Biocare, Sweden; Ref: 33445 BmK Syst RP; Sterilized using irradiation); and the second, of just the bacteriological medium (lacking an abutment). The tubes were incubated for 10 days, at 37°C under a 5% CO₂ atmosphere and examined visually daily for turbidity. At the end of the experiment, the tubes were examined again and Petri dishes containing BHI agar (BHIA) and Columbia Blood agar (Sharlau, Sentmenat, Spain) were inoculated with 100 µl of the medium from each tube to test for sterility. The contents of each tube were centrifuged at 2.500 rpm and sediment was Gram stained and observed at 1000 x' to discard the presence of non-cultivable microorganisms (Fig. 1).

-Determination of Total Organic Carbon (TOC)

Moreover, to determine the presence of remaining organic material after the cleaning and sterilizing treatments, the bio burden present in the used abutments was determined by measuring total organic carbon (TOC) present.

A different stock of 10 previously used healing abutments, cleaned and sterilized, were submerged in 10 Eppendorf flasks with 1.5 ml Milli-Q water and sonicated in an ultrasonic bath for 1 hour.

A volume of 15 ml Milli-Q water was used as blank control.

TOC was measured using a multi N/C® 3100 analyzer (Analytic Jena, Jena, Germany).

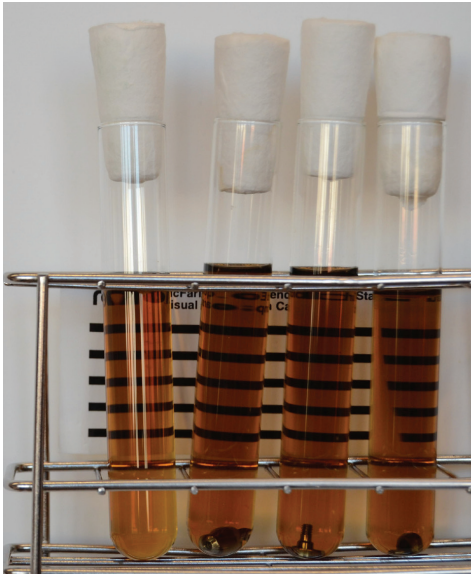


Fig. 1: Microbiological cultures. 4 tubes containing 10 ml of Brain Heartth broth, the left one been the negative control with only medium and the other ones with 3 healing abutments, after incubation at 37°C for 10 days under 5% CO₂ atmosphere. No differences in turbidity were observed.

Results

-Sample culture

None of the 55 used abutments processed in the microbiological experiments produced obvious visible turbidity in the medium, although in some cases microparticulated material appeared after 24 hours of incubation (first examination) and remained throughout the incubation period. However, it should be stated that in none of these samples did the turbidity increase over this period. Moreover, after 10 days of incubation and the subsequent inoculation of aliquots of the liquid medium onto BHIA and Columbia Blood agar plates, no bacterial growth was detected on any of them, indicating that the sterilization of the used abutments was completely satisfactory in terms of removal of live bacteria or

spores. In some cases, the Gram stain examination of the smear was difficult to interpret because of the presence of abundant debris stained with a pink color.

-Determination of Total Organic Carbon (TOC)

The TOC determinations of the abutments were much higher than expected (Table 1). It is worth noting that a significant amount of organic material was recovered from the used abutments, indicating that it had remained adhered to the surfaces of the abutments. Since there is a huge difference between the organic carbon content of the abutments and the Milli-Q water used for submerging the abutments prior to sonication, our results demonstrate that significant amounts of the bioburden remained adhered to the surfaces.

Discussion

Although no living cells survive the autoclaving, it is well known that many molecules as well as epithelial and blood cells and bacterial fractions may retain certain properties after the sterilization procedure. The organic material found on the reused abutments would come from the patient in which the abutment was connected to. Subsequently, it may either affect cell adhesion and the effective spreading and attachment of epithelium and connective tissue(2,10), or promote inflammatory processes in a hypothetical re-receptor. The proteins and amino acids that can remain adhered to titanium are extremely difficult to remove.

Sterilization of previously used or intentionally contaminated healing abutments is a safe procedure to eliminate bacteria, virus and fungi as different studies had demonstrated previously (1) .

Given that recent studies suggest that the sterilization of the healing abutments does not eliminate all the biological debris, the placement of contaminated abutments could be associated with the development of peri-implant disease allowing a good place to adhere and grow (11-13).

All this represents different kinds of health risk for the second user. One of these risks may be illustrated by considering prions. Biological debris could act as an effective vector for the transmission of prions. These infectious proteinaceous agents can cause neurodegenerative diseases that in humans include Kuru, Creutzfeldt-Ja-

Table 1: Values of Carbon adhered to used abutments. TOC: Total Organic Carbon, IC: Inorganic Carbon , TC: Total Carbon (TC = IC+TOC).

| Parameter | Blank | | Abutments | |
|-----------|------------------|---------------|--------------------|---------------|
| | Value | Sd. Deviation | Value | Sd. Deviation |
| TOC | 4,09 µg/abutment | | 125,31 µg/abutment | |
| IC | 0,81 µg/abutment | 0,1 | 1,07 µg/abutment | 0,69 |
| TC | 4,90 µg/abutment | 0,05 | 126,39 µg/abutment | 108,45 |

kob disease, Gerstmann-Straussler-Scheinker disease, and Fatal Familial Insomnia. In principle, the measurement of “viability” when considering prions should be regarded as the measurement of the maintenance of infectivity. Despite only a few laboratories in the world are undertaking experimental work with prions, notably that of Stanley B. Prusiner (Nobel Prize in Physiology or Medicine, 1997), the work has led to several major concerns (14). The first and most relevant in the current context is that prions need to be completely inactivated using harsher conditions than those used against bacteria and viruses. To ensure prion inactivation, the thermal sterilization should be combined with chemical treatment. It would appear that procedures used for routine sterilization of surgical instruments cannot inactivate prions (15,16), which already led to the development of new and more stringent recommendations for reprocessing instruments and these should eventually be applied to abutments (17). This has been reinforced by the discovery that prions that are responsible for bovine spongiform encephalitis (BSE) can be up to 1 million times more difficult to inactivate than the most commonly used hamster prions; thus, one cannot exclude the possibility that human prions are also much more resistant than the laboratory prions (10). These recommendations are based on conventional autoclaving (121°C) combined with chemical attack; this may be achieved by autoclaving in the presence of 1 M sodium hydroxide, or by soaking in 2% bleach for 1 h. Such treatments are extremely corrosive and may cause irreversible damage to the surface of abutments (18).

Prevalence of asymptomatic Creutzfeldt-Jakob disease (CJD) in UK population in people born from 1941 to 1985 is 1:2000 and prion iatrogenic transmission (blood transfusions, organ transplants and surgical instrumentation) is therefore possible. Another source of prions could be bovine bone substitutes used widely for bone regeneration after or simultaneously to the dental implant placement. These materials keep some proteins, their manufacturing processes are not guaranty to the inactivation of the prion, and in consequence, Kim *et al.* (19) suggest abolishing the use of bovine bone.

The presence of organic carbon reported in our study means that organic material originating in the patient is adhered to the surface and, subsequently, the presence of prions cannot be ruled out. In conclusion, we believe that, despite costs, the practice of reusing implant abutments should be abandoned, since it cannot be demonstrated to be safe enough.

Further studies trying to identify the source of the organic carbon adhered in the abutments are needed. In addition, it is worth elucidating if there could be any safe procedure to effectively remove all the organic material present in the titanium surfaces of the reused healing abutments.

References

1. Vezeau PJ, Keller JC, Wightman JP. Reuse of healing abutments: an in vitro model of plasma cleaning and common sterilization techniques. *Implant Dent.* 2000;9:236-46.
2. Wadhvani C, Schonnenbaum T, Audia F, Chung K. In vitro Study of the Contamination Remaining on Used Healing Abutments after Cleaning and Sterilizing in Dental Practice. *Clin Implant Dent Relat Res.* 2016;18:1069-74.
3. Cakan U, Delilbasi C, Er S, Kivanc M. Is it safe to reuse dental implant healing abutments sterilized and serviced by dealers of dental implant manufacturers? An in vitro sterility analysis. *Implant Dent.* 2015;24:174-9.
4. Etxeberria M, Abdulmajeed AA, Escuin T, Vinas M, Lassila LV, Närhi TO. Load-Bearing Capacity of Fiber-Reinforced Composite Abutments and One-Piece Implants. *Eur J Prosthodont Restor Dent.* 2015;23:62-9.
5. Etxeberria M, López-Jiménez L, Merlos A, Escuin T, Viñas M. Bacterial adhesion efficiency on implant abutments: a comparative study. *Int Microbiol.* 2013;16:235-42.
6. Etxeberria M, Escuin T, Vinas M, Ascaso C. Useful surface parameters for biomaterial discrimination. *Scanning.* 2015;37:429-37.
7. Canullo L, Micarelli C, Ianello G. Microscopical and chemical Surface characterization of the gingival portion and connection of an internal hexagon abutment before and after different technical stages of preparation. *Clin Oral Impl Res.* 2013; 24:606-611.
8. Canullo L, Micarelli C, Lembo-Facio L, Ianello G, Clementini M. Microscopical and microbiologic characterization of customized titanium abutments after different cleaning procedures. *Clin Oral Impl Res.* 2014; 25:328-336.
9. Hämmerle CHF, Tarnow D. The etiology of hard- and soft-tissue deficiencies at dental implants: A narrative review. *J Periodontol.* 2018;89 Suppl 1:S291-S303.
10. Stacchi C, Berton F, Porrelli D, Lombardi T. Reuse of Implant Healing Abutments : Comparative Evaluation of the Efficacy of two Cleaning Procedures. *Int J Prosthodont.* 2018;31:161-2.
11. Mombelli A, Decaillet F. The characteristics of biofilms in peri-implant disease. *J Clin Periodontol.* 2011;38:203-213.
12. Flanagan D. Enterococcus faecalis and Dental Implants. *J Oral Implantol.* 2017;43:8-11.
13. Pérez-Chaparro PJ y cols. The Current Weight of Evidence of the Microbiologic Profile Associated With Peri-Implantitis: A Systematic Review. *J Periodontol.* 2016;87:1295-1304.
14. Giles K, Glidden DV, Beckwith R, et al. Resistance of bovine spongiform encephalopathy (BSE) prions to inactivation. *PLoS Pathog.* 2008 ;4:e1000206.
15. Fernie K, Hamilton S, Somerville RA. Limited efficacy of steam sterilization to inactivate vCJD infectivity. *J Hosp Infect.* 2012;80:46-51.
16. Sushma B, Gugwad S, Pavaskar R, Malik SA. Prions in dentistry: A need to be concerned and known. *J Oral Maxillofac Pathol.* 2016;20: 111-14.
17. World Health Organization WHO infection control guidelines for transmissible spongiform encephalopathies. Report of WHO consultation, Geneva, Switzerland, 23-26 March 1999. P 38. Available in: <http://www.who.int/csr/resources/publications/bse/whocdses-graph2003.pdf?ua=1>.
18. Sonntag D, Peters OA Effect of prion decontamination protocols on nickel-titanium rotary surfaces. *J Endod.* 2007;33:442-446.
19. Kim Y, Rodriguez AE, Nowzari H. The risk of prion infection through bovine grafting materials. *Clin Impl Dent Rel Res.* 2016;18:1095-102.

Financial support

The laboratory research was financed by own resources and did not receive any financial support neither from private companies nor from public agencies. The clinician dentists who provided the abutments used were rewarded with the same number of new pillars by Nobel Biocare Ibérica for its contribution (Supported by Novel Biocare with research grant 2016-1443).

Authors' contribution

MV, TV and MA S-G performed the research design, MA S-G and JJC did the literature review, MA S-G and TV did Data collection, MJ, MV and TV did Data analysis/interpretation, MV and TV did the draft of the article and its critical revision.

Conflicts of interest

All authors disclaim any conflict of interest.

